Theoretical and experimental studies of neuronal network dynamics: Relating topology to function

by

Xiaojing Wang

A dissertation submitted in partial fulfillment
of the requirements for the degree of
Doctor of Philosophy
(Applied Physics)
in The University of Michigan
2010

Doctoral Committee:

Associate Professor Michal R. Żochowski, Chair
Professor Mark E. Newman
Professor Leonard M. Sander
Associate Professor Jennifer P. Ogilvie
Assistant Professor Victoria Booth

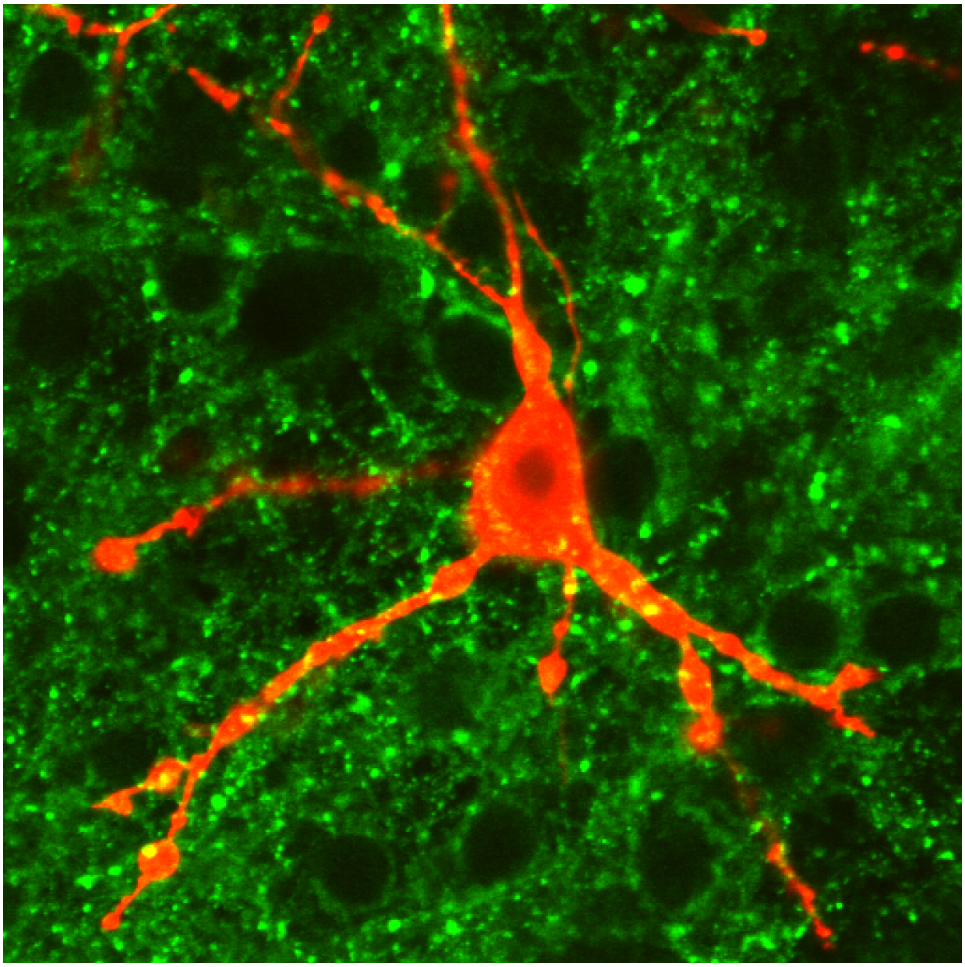

To my mom, who was with me every step of the way.

ACKNOWLEDGEMENTS

The last five years have been among the most formative of my life, and I truly would not have been able to get through them or to take these last few steps on the path to my doctoral degree without the help of a lot of important people. First, I would like to thank my mom for being one of the few constants in my life, and for always being there to listen through the various rough spots that graduate school entails. My dad also deserves acknowledgement for reminding me that there is life after graduate school, after all.

I was fortunate to meet a group of great friends, who made this challenging path a whole lot more fun – in particular Niki, Ed, Jeannie, Vanessa, Brieta, Andres, and Andre. You made it all worth it. And a special thanks to Dave, who always knew how to make me laugh, even when I didn't necessarily feel like it.

I would also like to thank my research group, and in particular my advisor Michal Żochowski for his guidance and invaluable support. You made me the scientist I am today. And thank you to my fellow lab members Troy Lau, Tony Smith, Liz Shtrahman, and Chris Fink for great discussions.

My research involved collaborations with and contributions from many other scientists, and I'd like to briefly acknowledge their help here. Chapter II is from a paper written with Michal Żochowski and Gina Poe, who provided the experimental data and some analysis. It was published in Physical Review E in 2008 [183]. Chapters II and III involve analyses done with the help of computing resources from the Center for the Study of Complex Systems and the Center for Advanced Computing at the

University of Michigan.

Chapter IV contains images taken at the Microscopy and Image-analysis Laboratory (MIL) at the University of Michigan, Department of Cell & Developmental Biology, and in particular I would like to acknowledge the assistance of Chris Edwards for his help in the use of these microscopes. This chapter was also a collaboration between myself and a previous graduate student of the lab, Sarah Feldt, who conducted the electrical recordings and functional clustering analyses.

Funding for my research was generously provided through the Applied Physics Rackham Regents' Fellowship (2005-2007), the NIH Molecular Biophysics Training Grant (2007-2009), and the Rackham Pre-doctoral Fellowship (2009-2010).

TABLE OF CONTENTS

LIST OF FIGURES

Figure

LIST OF ABBREVIATIONS

DIV days *in vitro*

EEG electroencephalogram

FCA functional clustering algorithm

fMRI functional magnetic resonance imaging

GFAP glial fibrillary acidic protein

ISI interspike interval

LTD long-term depression

LTP long-term potentiation

MEA multi-electrode array

PBS phosphate buffered saline

REM rapid eye movement

STDP spike timing-dependent plasticity

SWN small-world network

SWS slow-wave sleep

CHAPTER I

Introduction

The brain is simultaneously one of the most familiar and yet the least understood entities known. Sensory processing, consciousness, and planning comprise the bedrock of our everyday existence, and yet the functional mechanisms of almost all aspects of cognition continue to resist elucidation. Perhaps one of the major reasons for this difficulty lies in the brain's sheer complexity, both in numbers and in structure. With the human brain containing roughly 10^{11} neurons each making thousands of connections to other cells, any tractable method of study necessitates vast amounts of approximation to the system. As a result, there exists a multitude of scales of study and corresponding observational methods, ranging from full brain imaging to probing single proteins or molecules of a neuron. Additionally, these different scales are not independent of each other, but rather interact in complex and unpredictable ways characteristic of a complex network, in contrast to systems in which internal dynamics either average out (as with statistical mechanical systems) or completely correlate (as with rigid bodies). Such network effects can be seen as due to the internal dynamics between constituent units manifesting on multiple scales and are widely believed to be the functional bases for cognition and information processing [31, 23, 107].

Networks exist at virtually every scale in the study of neuroscience. At the cellular

level, differences in local potential due to the spiking activities of separate neurons converging at different points of the dendritic branch of a postsynaptic neuron interact within the cell to determine if an action potential is generated. Single neurons in turn form complicated circuits, the connectivity pattern of which heavily influence their spiking patterns. It is also possible to examine the interactions between entire brain regions, as it has been shown through neuroimaging processes such as functional magnetic resonance imaging (fMRI) that different cognitive functions are correlated with activation of localized areas of the brain [24, 28]. Each component acts as a dynamical unit which behaves as a function of the way it's connected within the network. Although the physiological details differ at each scale, the mathematics and analyses used to examine the networks of interactions remain the same. By focusing on the networks rather than details of the components, we can elucidate mechanisms of interaction which can be true at every scale and which are not observed when studying single isolated components.

The tools we can use in this endeavor have been developed for centuries, beginning with the mathematics of graph theory introduced by Leonhard Euler in 1736. However, with the advent of the computer, recent decades have witnessed a resurgence in the science of network phenomena. Network science in general focuses on the interactions between constituent elements when representing, characterizing, or analyzing a system and draws considerably from the mathematics of graph theory. A network is a representation of a given system highlighting the interactions between its constituent elements. In the language of network science, the interactions are called "connections" or "links," and the elements are called "nodes." For a more complicated system, there may be more than one network representation because multiple interactions can exist between elements. For instance, in a social network in which people are the nodes, a variety of networks can be created depending on the types of interactions studied, such as how often people speak on the phone, who they consider

to be friends, and so on. Ecological food webs are another type of network which have been extensively studied, in which the nodes are the animals and a directed connection exists if one eats the other. The details of network science are beyond the scope of this dissertation; for a good review please refer to [121].

These studies have typically focused on characterizing the structure of the network at one or discrete points in time, especially if information about the network is not continuously available or time-stamped. The growth of citation networks, in which connections form if one journal article cites another, can be readily studied because articles are dated, but in general it's difficult to characterize changes in links over time. Additionally, network elements do not usually display dynamics, or a temporally evolving internal state, and thus they are considered "static networks."

Brain systems can be represented as both a static and a dynamic network. A static network representation only takes into account anatomical connectivity, such as the existence of a synapse between two neurons. A neuron which is synaptically connected to another neuron would thus exhibit a link to the other neuron, and the strength of the synapse would define the weight of the link. A dynamic network representation of the brain takes into account the time-varying internal states of the neuron, such as action potentials or membrane voltages. Connections between two neurons then can be characterized by rates of firing and temporal similarities or other correlational relationships between their evolving states. The dynamic network specified in this fashion can also be considered "functional" structure or connectivity because it is the dynamics of the brain which underlies its function.

An important distinction between anatomical structure and functional structure is that the former is relatively stable over time, even as the connections are able to undergo experience-dependent plasticity. Functional structure, on the other hand, can rapidly fluctuate due to transient changes in dynamics, possibly as a result of external perturbation or task-driven information processing. The effects of anatomical

structure on functional structure are far from clear, because the same anatomical substrate can give rise to different functional connectivities depending on various factors such as neuromodulatory factors or sensory input. Extensive research to determine both types of networks – as well as how the two are related – is ongoing and vital to making further progress in decoding the language of the brain.

One of the main drives of this dissertation is to relate anatomical connectivity to functional structure and spatiotemporal patterns of neuronal dynamics in order to understand cognitive functions such as memory, attention, and even consciousness, which represent interactions across multiple temporal and spatial scales. Often it is observed that how functional connectivity arises from anatomical structure is dependent on instantaneous states of the system due to local and global modulatory mechanisms which define different modes of function. In addition, correlated activity is able to affect anatomical structure through plasticity and learning, completing a feedback loop of information processing and interaction with external environments.

Utilizing theoretical, modeling, and experimental methods, I focus on exploring the roles of these modulatory and plasticity systems in addressing the relation between functional and anatomical networks of learning and memory. In Chapter II, I examine how global modulation of excitability can give rise to functional structure reflecting underlying heterogeneous connectivity associated with stored memory. This mechanism, coupled with two different timescales of plasticity and inhibitory feedback, can mediate information transfer and memory consolidation. These dynamics are matched with experimental data observed during behavioral learning. This work has been published in Physical Review E with Gina Poe and Michal Zochowski [183].

In Chapter III, I further characterize how spatially varying topologies affect memory activation and retrieval. In particular, I focus on the importance of heterogeneous inhibitory connectivity in increasing competition between linked memories as well as the role of global modulation in optimizing memory retrieval. Such findings point to

the importance of inhibitory-excitatory current balance on both a local and global scale to information processing in neuronal networks. This was work done under the advisement of Michal Zochowski and is currently under review for publication.

Having examined the theoretical underpinnings of network interactions, I sought to explore how anatomical connectivity relates to functional structure in a real biological network. Chapter IV presents an investigation into the morphological and dynamical characteristics of cultured networks of hippocampal cells. I relate the growth of anatomical neuronal networks as well as the modulatory effects of a confluent glial network to changes in spiking activity, and find that all three are non-trivially connected. This work is in review for publication with Sarah Feldt, Liz Shtrahman, Rhonda Dzakpasu, Eva Olariu, and Michal Zochowski.

The rest of this introduction provides general background of neurobiology, learning and memory, and the methodological tools utilized in this research.

1.1 Neurophysiology

Neurons are electrically excitable cells which act as the functional core components of the brain and are the basis for information processing. Though they all share the same basic structure, there exist hundreds of types of neurons, which can be connected in any of a number of ways, allowing them to form anatomical circuits of endless complexity. They are in general composed of a soma (cell body) and extruding processes which can be categorized into dendrites (signal inputs) and one axon (signal output) (see Figure 1.1). While neuron bodies usually range in the tens of microns in diameter, the processes which extend from them vary greatly in size, especially axons, of which the longest are meters in length. Neurons usually exhibit many dendrites branching off the main body, forming a complex dendritic arbor which can extend in many directions, but they only have one axon which extrudes directly from the soma, although it can branch multiple times before synapsing onto other cells. Their unique

cellular physiology allows neurons to both spatially and temporally integrate input signal from other cells and then, based on numerous intrinsic and extrinsic factors, transduct their own output signal to other neurons.

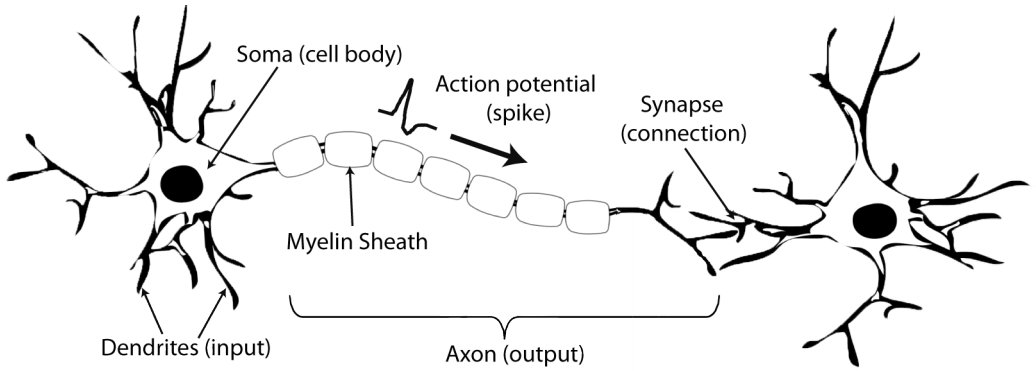

Figure 1.1: Diagram of a neuron. Soma are the cell bodies of neurons, and their processes include dendrites, which receive signals from other cells and therefore function as input, and axons, which are capable of generating and carrying action potentials. The propagation speed of action potentials can be considerably increased if axons are further encased in dielectric membranes called myelin sheaths. The connections between neurons are called synapses, and they are the primary sites of neuromodulatory and plasticity processes.

Neurons maintain a resting potential, or voltage, of around -65 mV with respect to the extracellular environment. Ion channels allow for the passive and active transport of various ions, the most prominent being sodium (Na^+), potassium (K^+), chloride (Cl^-), and calcium (Ca^{2+}). Passive channels work to maintain the potential at the baseline level, while active channels are gated and open in response to certain voltage ranges (voltage-gated) or binding events (ligand-gated). Influx of sodium ions across the cellular membrane causes depolarization, or an increase in the intracellular potential. If this depolarization is larger than a specific threshold value, roughly -45 mV, a series of chain reaction events occur involving opening of additional voltage-dependent sodium as well as calcium and potassium channels, which results in the generation of an action potential [86].

Action potentials have a very distinct time trace, with a fast rising and falling

phase followed by a short duration of roughly 5-10 ms, called the refractory period, of hyperpolarization in which the voltage is lower than the resting potential and the neuron is not excitable (Figure 1.2). They are typically generated in the axon hillock, or the portion of the axon closest to the cell body, and are actively propagated via the opening of additional ion channels (mainly Na^+ and K^+) down the length of the axon to communicate with connected cells. Action potentials, which are also known as spikes, tend to be stereotyped (similar in form) and all-or-nothing (boolean), and thus they act as the primary mode of information coding, processing, and transmission. One of the major drives in neuroscience is to understand this neural code and how it translates raw sensory information into internal representations and further is able to manipulate those representations in the act of thinking.

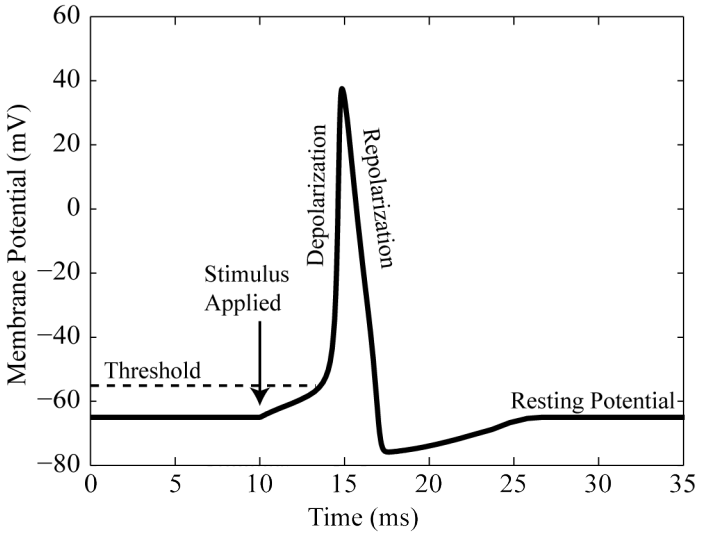

Figure 1.2: Plot of a typical action potential. Neurons typically have an intracellular resting potential of around -65 to -70 mV. Depolarization, or an increase in this potential, occurs due to flow of charged ions into or out of the cell. If this depolarization crosses a threshold value, roughly -45mV, a positive feedback process is initiated resulting in the rapid increase (due to the influx of Na^+ across Na^+ voltage-gated channels) and then rapid decrease (due to the efflux of K^+ across K^+ voltage-gated channels) of the membrane potential by about 100 mV and lasting for 1-2 ms. Action potentials are actively propagated down the length of the axon to cause the release of neurotransmitters into the synaptic cleft, or a small region of space adjacent to another neuron's input processes, typically its dendrites.

Action potentials are transmitted from one neuron to the next via connections or junctions called synapses, defined as a small region of space in which the one neuron is in close proximity and can communicate information to the dendrite (or in some cases the soma) of another neuron. Synapses can be either chemical or electrical. Chemical synapses are defined as the small (20-40 nm) cleft of space between two neurons within which neurotransmitters, or chemical messengers, can be released by one neuron and bound to specific receptors located within the cellular membrane of the other neuron. The receptors mediate the opening of ligand-gated ion channels which affect the neuronal intracellular potential and can trigger a dendritic signal, which is propagated to the cell body and integrated with other signals. If the net effect of this input causes the soma membrane potential to rise above the threshold level, an action potential is generated. Because of the leak current due to passive channels, generation of an action potential is sensitive to the timing between dendritic inputs; coincident inputs tend to result in a higher probability of postsynaptic firing.

Chemical synapses are by definition unidirectional since one only cell can release neurotransmitters (presynaptic neuron) and only one can receive (postsynaptic neuron), meaning that impulses can only be transmitted one way. However, in the case of electrical synapses, also called "gap junctions," connections are bidirectional since neurons can directly affect each others' intracellular potentials because they are electrically connected through gap junction channels spanning the membranes of both cells [86]. For the purposes of this dissertation, I will focus on chemical synapses since they are much more numerous and involved in memory and plasticity processes; therefore, from here on "synapse" will be understood to refer to only a "chemical synapse."

1.2 Plasticity and neuromodulation

Synapses can be either excitatory, meaning that presynaptic firing causes depolarization of the postsynaptic neuron's membrane potential and thus increases its chance of firing, or they can be inhibitory, meaning that postsynaptic neurons are hyperpolarized and less likely to fire as a result of a presynaptic signal. Excitatory synapses are in general mediated by the neurotransmitter glutamate, while inhibitory synapses are primarily mediated by γ-aminobutyric acid (GABA). Neurons can and do receive a mixture of both excitatory and inhibitory input signals depending on the types of receptors they exhibit, but their outputs are purely excitatory or purely inhibitory. We can thus refer to "excitatory neurons," also known as principle neurons, or "inhibitory neurons," also known as interneurons.

An important aspect of synapses is that they are not constant, but instead are able to be strengthened or weakened through activity-dependent or other processes, a phenomenon known as "synaptic plasticity." The strength of a synapse can be measured as the amount of postsynaptic response to a presynaptic signal, typically an action potential. The idea of activity-dependent plasticity was first explored by Donald Hebb, who theorized that simultaneous activation of neurons tended to strengthen their connection [77]. Since then, much experimental work has focused on the mechanisms of plasticity, the most notable being long-term potentiation (LTP), or synaptic strengthening, and the closely associated long-term depression (LTD), or synaptic weakening. This form of plasticity involves long-lasting changes to synaptic strength as a result of paired activation of synaptically connected neurons [20, 19, 17], and experimental evidence exists which point to it as the physiological basis for some forms of learning and memory, especially within the hippocampus and amygdala [108, 26, 127].

Further investigations have shown that temporal ordering and precise timing relationships of pre- and postsynaptic activity impact ensuing plasticity, a concept termed spike timing-dependent plasticity (STDP) [101, 13, 52, 153]. In STDP, firing

of the presynaptic neuron before the postsynaptic neuron leads to strengthening of the synapse, while the reverse ordering leads to weakening. Additionally, the extent of the change increases as the timings of the two spikes decreases, so that there is an effective window within which plasticity can occur [1]. An important aspect of STDP is that it allows for stabilization of firing rates by instituting a balance between LTD and LTP, thereby preventing a runaway positive feedback loop between activity and synaptic potentiation. Another form of plasticity which addresses this issue is homeostatic plasticity, in which neurons are able to regulate their synapses in response to sustained changes in activity in order to maintain firing rates within an optimal range [125, 169, 170]. This is achieved through processes such as synaptic scaling [172, 140, 29], where all synapses convergent on a postsynaptic neuron are scaled by a constant factor which is dependent on neuronal activity.

In addition to local modification of synapses, neuronal responses can also be altered or modulated on a more global level by neuromodulators, acting in contrast to neurotransmitters which directly mediate neuronal signaling. Neuromodulators are a class of chemicals defined by their mode of influence on dynamics, and thus many neurotransmitters are also considered neuromodulators, such as acetylcholine, norepinephrine, serotonin, and dopamine. They are able to regulate spiking activity of neurons by either altering synaptic efficacy or modulating excitability and intrinsic membrane properties, in both a more spatially diffuse as well as longer lasting fashion than neurotransmitters [70, 100]. This allows for far more complex network interactions than would exist with neurotransmitters alone. More importantly, due to neuromodulators' spatially and temporally extended range of action, they are ideally suited for controlling transitions between different brain region states, since identical anatomical circuitry can yield vastly different dynamics depending on the strength and combination of different neuromodulators. For this reason, they have been linked to various cognitive functions such as attention [193], cortical reorganization of sensory

fields [110, 87], and – most relevant to this dissertation – memory in the hippocampus and neocortex [71, 72, 27].

Neuronal signaling can additionally be modulated by other types of cells within the brain, because they are intimately surrounded by a host of satellite cells called glial cells, which outnumber neurons by at least 10 to 1. Glial cells act to support neuronal growth and survival in a variety of ways, including providing nutrients, structural support, neuronal repair, and axonal guidance during development [122]. More recently, it's been shown that astrocytes, the most common type of macroglial cells, also interact extensively with neurons to modulate synaptic transmission and signaling [15, 16, 175]. Due to their close proximity with neurons, they are able to uptake or release neurotransmitters within chemical synapses, thereby modulating signal transmission between two neurons. Although they can't generate action potentials, astrocytes are capable of displaying sustained intracellular calcium oscillations which propagate via gap junctions and are sometimes invoked by neuronal activity. These oscillations can in turn elicit calcium changes in neurons, indicating a bidirectional mode of communication with possible repercussions on information processing [128, 119].

1.3 Network mechanisms of learning and memory consolidation

Neuronal dynamics are clearly highly dependent on both global states as well as local synaptic properties. Further, in attempting to understand the neural code underlying behavior and cognition, it's necessary to quantify relationships in activity between neurons as a function of their placement within a complex network of interactions. Because of the intricate nature and highly complex structure of the brain, network analysis utilizing math and concepts from the field of graph theory seems

particularly appropriate in the exploration of the functional bases of behavior. This framework is especially suitable in examining learning and memory, which have been shown to be particularly difficult to localize to specific and isolated brain regions and are thus likely to be primarily network phenomena.

Memory and the act of remembering form the basis for our everyday life and even our sense of self, as memory is the cumulative effect of the external environment interacting with our internal states throughout our entire lives. We routinely engage in multiple acts of remembering in even the simplest of tasks, such as dialing a phone number, retelling a story, or even driving. Although no one clear classification scheme exists, memory can be most intuitively divided up based on time of retention.

The shortest retention time belongs to sensory memory, which lasts hundreds of milliseconds for visual stimuli and up to a second for auditory stimuli. An example of sensory memory might be hearing a particular sound and maintaining it in sensory memory for several seconds. It is by definition not contextual or processed, and is unable to be rehearsed [37].

Short-term memory lasts on the order of minutes to hours, and is often used interchangeably or in close association with working memory, although the two concepts emphasize different cognitive aspects – the former highlights retention capabilities while the latter highlights attentional faculties. Short-term memory is limited in capacity as well as duration, as was famously observed by Miller in his 1956 psychological study which showed that humans can retain "seven plus or minus two" distinct items or concepts at a time in working memory [112].

Long-term memory refers to both facts and events we can actively recall, termed "explicit" or "declarative" memory, and learned skills and reflexes which are not consciously remembered, termed "implicit" or "procedural" memory. Explicit long-term memory can further be divided into episodic, or memory of specific events located in time and place, and semantic memory, which is knowledge of general facts and events.

Episodic memories involve temporally coincident knowledge gleaned from many senses so that it's contextual, whereas semantic memories are context-free, general knowledge gradually created over time from many different integrated experiences [167]. Long-term memory can persist indefinitely, and it's capacity for storage is unknown.

Although the psychological aspects of memory have been explored since the 19^{th} century, it wasn't until the landmark case of Henry Molaison, better known as Patient H.M., in the 1950s that the field saw extensive progress on the neurological underpinnings of memory and the functional processes involved. Henry Molaison had suffered from intractable epilepsy due to brain trauma suffered as a child; his condition was so serious as to be life-threatening. Not responding to standard medication or treatment, his doctors proceeded to surgically remove extensive brain tissue from both of his temporal lobes, including most of the hippocampus, the entorhinal cortex, portions of the associational neocortex, and the amygdala [150] (see Figures 1.3 and 1.4).

Afterwards, though his epilepsy was significantly contained, he was left with severe amnesia of two kinds: 1) retrograde amnesia, in which he lost significant portions of his memory from the most recent years before his surgery, and 2) anterograde amnesia, in which he was unable to form new long-term memories. Although he still maintained the same general level of intelligence and had the ability to form short-term memories lasting on the order of minutes, he was unable to retain anything beyond that. For the last 5 decades of his life, he was unable to remember anything new. Further, H.M.'s memory loss was different for different types of memory. For instance, he was able to gain new skills and improve at solving puzzles at the same rate as controls, even though he didn't remember actually doing any of these tasks. This suggested that the removed brain structures were important to the management of declarative memories, especially in turning short-term memory into long-term memory, a process known as "consolidation" [4].

In order to understand this process, some general neurobiological background must be given. On a cellular level, short-term memory has been linked to two separate processes: 1) transient spatiotemporal dynamics such as persistent self-sustained reverberating activity [185] or synchronization of oscillations among and between various neurologically significant frequency bands [166, 9], and 2) temporary changes in synaptic efficacy due to facilitation and depression processes [59] or early phase protein synthesis-independent LTP [174]. The former is more closely associated with the idea of "working memory," or memory lasting on the order of minutes which is being actively kept in consciousness, while the latter refers to reflex habituation or the very first stages of long-term potentiation which involve synaptically "tagging" neural circuits for later consolidation and can last for hours [58]. The primary brain regions associated with short-term memory are the hippocampus, amygdala, entorhinal cortex, and the prefrontal cortex. Because of the transient nature of short-term memories, they're quickly forgotten unless encoded into long-term memory stores via gene expression, protein synthesis, and possibly axonal or dendritic growth in the process of consolidation. The final storage site for long-term memory is the neocortex, which is also the same region that first processes incoming stimuli.

This is no coincidence, because as H.M.'s case clearly shows, the hippocampus and entorhinal cortex are vital to stabilizing and transferring short-term memory to long-term memory and are therefore intimately connected to the neocortex. The neocortex is the outermost layer of the cerebrum and is linked to higher cognitive functions such as language, sensory perception, reasoning, and even consciousness (see Figure 1.3).

The hippocampus is a seahorse-shaped structure located deep in the medial temporal lobe which supports spatial mapping and declarative, contextual memory. It displays a very layered organization and as a result its connectivity pattern is one of the most studied and well-known. The hippocampus consists of the dentate gyrus, the cornu ammonis (CA) subregions, and subiculum. Its primary inputs are from

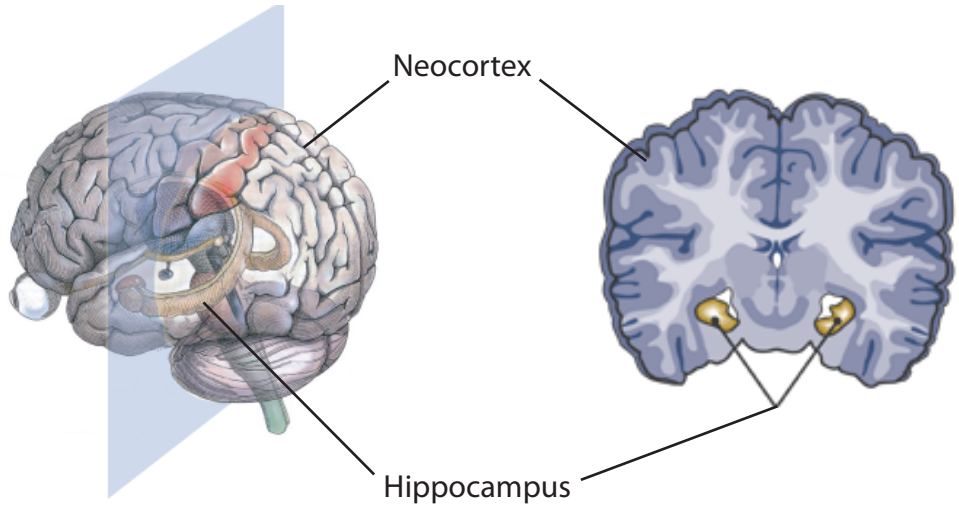

Figure 1.3: Anatomy of hippocampus and neocortex. Adapted from www.macalester.edu/psychology/whathap/UBNRP/ltp04 (left) and pubs.niaaa.nih.gov/publications/arh284 (right).

the entorhinal cortex, which receives sensory information from the parahippocampal and perirhinal cortices as well as the olfactory bulb. The entorhinal cortex projects via the perforant path to the dentate gyrus and region 3 of the CA, or CA3, and to CA1 via the temporoammonic path. The dentate gyrus passes signals to CA3, via mossy fibers and is believed to be responsible for orthogonalizing and separating pattern representation within that region [103, 92, 117]. CA3 is notable for containing many recurrent connections, making it an attractive candidate for an autoassociative content-addressable memory store. It projects to area CA1 via a pathway called Schaffer collaterals, which itself feeds into the subiculum. From there, the information leaves the hippocampus and re-enters the entorhinal cortex, to be passed back to the higher associational cortices of the neocortex.

Sensory information therefore converges and travels in a bidirectional feedback loop from the neocortex to the hippocampus for processing and encoding and back again via the entorhinal cortex, which gates both pathways (see Figure 1.4) [49, 89].

It's believed that the hippocampus and neocortex function in a highly interactive

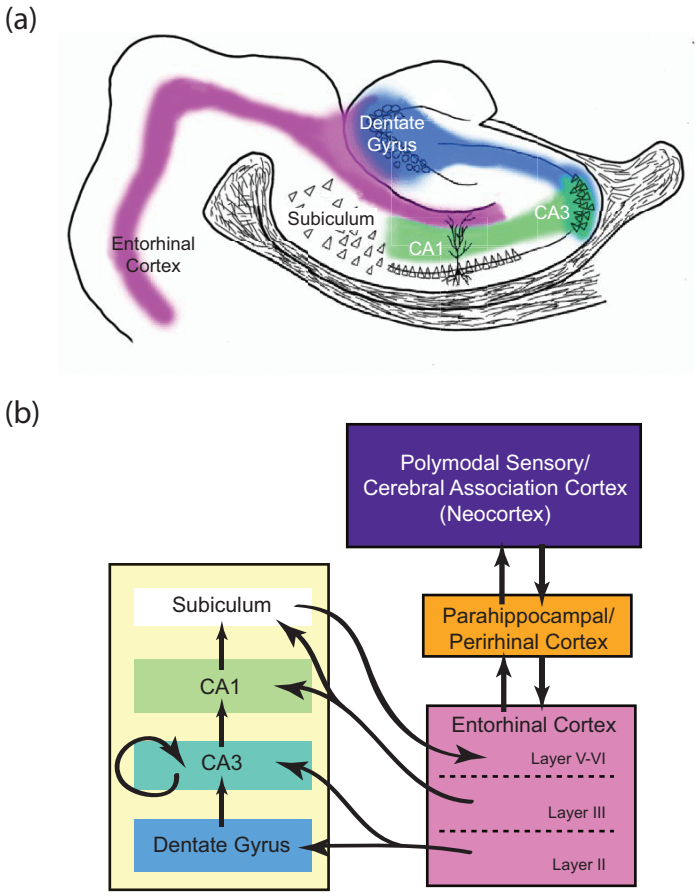

Figure 1.4: Circuit organization of hippocampal-neocortical memory pathway. a) Depiction of a coronal, cross-sectional slice of the hippocampus. Image adapted from groups.northwestern/edu/pruston. b) Sensory input is initially processed by various regions of the neocortex associated with the different senses, which then transfers information to the entorhinal cortex via the parahippocampal and perirhinal cortices. From there, the entorhinal cortex communicates with the dentate gyrus and the CA3 of the hippocampus via the perforant path from its superficial layers, and also projects into CA1 via the temporoammonic path. The dentate gyrus also synapses into the CA3 via mossy fibers, which itself projects into the CA1 via Schaffer collaterals but also has extensive recurrent connections with itself. CA1 feeds into the subiculum which subsequently feeds back into the deep layers of the entorhinal cortex, which then relays information back to the neocortex again. There is therefore a bidirectional feedback loop between the neocortex and hippocampus via the entorhinal cortex.

manner to both quickly encode declarative memory traces within the former and slowly transferring these traces to associational long-term stores in the latter [106]. This mechanism is not well understood, but there is strong evidence to support that it depends highly on sleep. Specifically, the type of memory which is consolidation depends on the amount of time spent in each stage of sleep. The typical sleeping person will cycle fully through all the stages in about 90 minutes, starting in non-REM stages 1 and 2 and rapidly descending into slow-wave sleep (SWS), also known as non-REM stages 3 and 4, before rising back through the stages. Instead of waking, however, the sleeper begins rapid eye movement (REM) sleep, which is when most of us tend to experience dreams (see Figure 1.5).

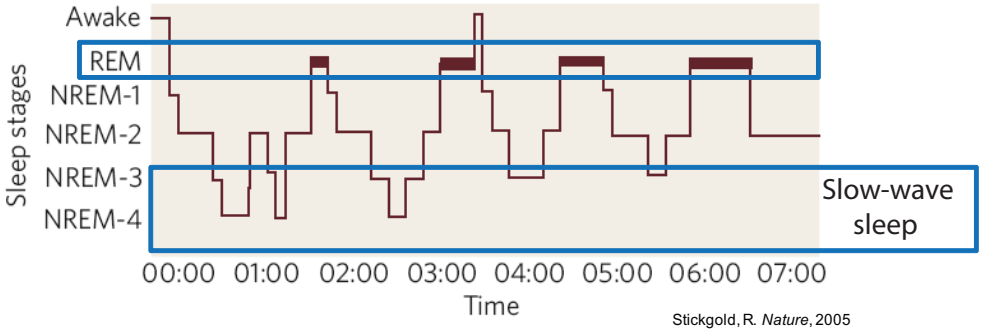

Figure 1.5: The stages of sleep. The typical full night's sleep for a human involves roughly 5 90-minute cycles of non-REM sleep stages 1-4 followed by REM sleep. Throughout the course of the night, the sleeper spends progressively more time in REM and less in non-REM. Non-REM sleep stages 3-4 are also known as SWS, characterized by large, slow (0.5-4 Hz) oscillations seen during EEG recording. REM sleep is characterized by rapid eye movement, theta oscillations (4-10 Hz), and dreams. Adapted from [161].

In declarative memory tasks, subjects generally experience enhanced memory recall as the amount of SWS increases, while procedural tasks are benefited from increased REM sleep [42, 63, 161]. Consolidation has been shown to occur over the span of hours, days, and even up to years [88, 106, 155]. There is still much controversy over the neurobiological underpinnings of consolidation and the role of sleep;

see [182] for a good review. Nevertheless, the general consensus is that sleep, and particularly memory reactivation, are important to the stabilization of new memory. Memory reactivation is the replay during sleep of previously activated neuronal cell assemblies seen during awake learning. In declarative memory experiments with rats, certain hippocampal cells which mark specific places with selectively high levels of firing ("place cells") are capable of firing in the same sequential order during REM as during previous novel learning tasks [96, 191]. It is hypothesized that sleep plays an important role in consolidation by allowing the memory traces to reactivate long after the initial sensory stimuli to give enough time for long-term potentiation processes to stabilize and encode the new memory into the neocortex [162].

Studies examining the time course of consolidation have shown experience-dependent reactivation of hippocampal cells and, in particular, that the reactivation of a given experience during sleep is greatest when the experience is novel and diminishes with repeated exposure [129, 134]. They have also indicated a progressive shift of the phase of place cell firing in CA1 during REM sleep as memories become gradually more familiar [134, 22]. This phase is relative to an overall hippocampal theta rhythm (4-10 Hz) in the population activity often observed during sleep and activity exploration and which is thought to be crucial to mnemonic coding [40, 10]. Such a phase shift could be due to a change in input driving from being dominated by intrahippocampal CA3 excitation to extrahippocampal driving from the entorhinal cortex, resulting in CA1 neurons switching from firing at the peak of hippocampal theta to firing at the peak of cortical theta, which is 180° out of phase [22]. Firing at the hippocampal trough could provide a possible mechanism for the erasure of old memories from the hippocampus which have been consolidated into long-term neocortical stores.

In a later chapter, I examine the dynamical underpinnings of time-dependent memory transfer from the hippocampus to the neocortex and classify how this dynamics is modulated by stimulus novelty and especially inhibitory feedback from the neo-

cortical input pathway which signals progressive familiarity. I hypothesize that network structural heterogeneities are capable of mediating this novelty detection and the eventual consolidation of memories, rendering them hippocampus-independent. Specific patterns of neural activation can also modify the network connectivity through plasticity mechanisms to allow this pattern to be retrieved at a later time, completing a feedback cycle between spatiotemporal dynamics and network architecture.

1.4 Memory storage and retrieval

As discussed in Section 1.2, synaptic plasticity and LTP are believed to be the neurophysiological substrates of learning and memory. Therefore memory representations can be encoded through the patterns of synaptic weights within a network which result in the increasingly associative activation of a subpopulation of neurons as learning progresses. Recall of distinct memories consists of activation of distinct patterns of neuronal activity which is in turn based on underlying connectivity.

Whether memories are encoded within the firing rates (rate coding) or the precise temporal timings (temporal coding) of neuronal spikes is still unknown, as evidence exists for both. Working memory in particular is thought to function through persistent activity of subpopulations of neurons which are either topographically or functionally associated with each other [45, 184]. The hippocampal CA3 subregion is known to be highly recurrent and is therefore thought to be an associative memory store, capable of completing activity patterns when presented with an incomplete input cue [102, 167, 118]. However, more recently, it's been proposed that temporal sequences of events making up episodic memory are encoded in the precise ordering of neuronal spikes [48, 74].

In general, it seems reasonable to assume that a subset of neurons which are more highly connected to each other would result in the stable persistent firing of the entire ensemble, corresponding to the activation of a memory concept which cannot be

temporally decomposed. In this way, memories and information are encoded through inducing local variations in the densities of synapses and synaptic strengths, resulting in a heterogeneous network topology which can exhibit subcommunity and hierarchical structure [43]. Such heterogeneities introduce spatially varying yet temporally stable patterns of firing reflecting the underlying connectivity and which represent attractor states of the network [167].

The entorhinal cortex receives input (either directly or indirectly, via the parahippocampal and perirhinal cortices) from widely distributed higher sensory cortices and projects back to nearly the same areas, leading to the idea that long-term memories are encoded in the same areas they are first processed [4]. This is most likely so that different aspects of a memory are associated with similar previously encoded concepts, promoting a gradual integration of new knowledge with the old as well as hierarchically organized experience and memory. Various models of the consolidation process have theorized that memory encoding within the hippocampus serves to bind together these disparate neocortical areas until they have formed strong enough synaptic connections through LTP processes that they can activate independently of the hippocampus [113, 105, 104].

It's not too difficult to see how the progressive storage of experiential episodic memory can lead to the formation of semantic memory (knowledge) because as various experiences are encoded, overlapping concepts and commonalities eventually become independent of their temporal and associated context as they become linked with so many episodic experiences that they cease to offer information about the context. Experimental evidence has linked episodic and semantic memory activation to the same memory system and underlying anatomical circuitry [136, 30], with the two representing different modes of functioning. Theoretical models have also been posed suggesting that the hippocampus is responsible for relating distinct episodic memory sequences and extracting common features for semantic representation [48].

More complex concepts or memories will tend to share common features, which would be encoded by the same sets of cell assemblies. For example, "green ball" and "red ball" share the concept "ball," while green ball and green grass share "green." With standard autoassociative memory models such as those of Hopfield [80] or Hebb [77], this poses a problem because activation of one representation also activates all associated representations simultaneously, resulting in the retrieval of an amalgam of many memories instead of only one. Recurrent networks also frequently suffer runaway synaptic modification as well as (and as a consequence of) uncontrolled activity because novel inputs tend to also activate old memories and become encoded as a part of them. Therefore additional inhibitory or competitive feedback drives must be in place to facilitate single memory recall or completion.

Experimental evidence exists which shows that excitation is frequently balanced on both a global and local level by inhibition, such as in the local dendritic branches of hippocampal neurons [95] and in neocortical dynamics [68]. Theoretical models have implemented inhibitory feedback as a mechanism of threshold control and stabilization of activity [75], and have shown detailed excitatory-inhibitory current balance to be vital to signal gating [177]. Inhibitory feedback therefore increases the dynamic range of the responsiveness of the network and allows for optimal information processing under a variety of sensory input levels.

Uniformly global inhibitory feedback does not, however, address the issues of runaway activity or learning in recurrent networks. Neuromodulation has been suggested as a method of preventing runaway learning by separating the encoding phase from the retrieval phase during consolidation [71]. Theoretical and experimental investigations have supported the notion of differential input drives throughout consolidation [22, 134]. In the encoding phase, the hippocampus must encode new memory rapidly, and thus its activity should be dominated by extra-regional input from the entorhinal cortex. However, in the reactivation phase, the hippocampus must replay this

previously stored activity and thus must be primarily governed by internal dynamics. This neuromodulation is thought to be mediated by differential levels of acetylcholine present during different sleep stages and wake-vs-sleep behavior [76, 72].

Physiologically, lateral inhibition in the visual [116, 18] and auditory [190] cortices allows for selective tuning of receptor cells. It's also been shown that pattern separation within the CA3 can be achieved through inhibitory input or suppression of excitatory input from the dentate gyrus (DG) [103, 92, 117]. However, little is known about the actual pattern of this feedback inhibition, although it is clearly not uniform.

In Chapter III, I focus on how overlapping concepts or semantic memories can be optimally stored within a neural network and examine the role of topologically structured inhibition in mediating competitive memory retrieval and activation. I also investigate the role of a global excitability level corresponding to neuromodulatory effects on the performance of the model in retrieving and replaying stored memories.

1.5 Methodological tools: Networks, modeling, and reduced experimental systems

1.5.1 Network dynamics underlie information processing

Multiple statistical properties can be defined and calculated given a specific network. For nodes distributed in a Euclidean space, such as with neuronal networks, we can define a physical distance between two elements in addition to the link distance, or the shortest route between any two elements in the graph counted in terms of how many links separate them. Within the brain, there exist both short-range (spatially close in a Euclidean sense) connections between neurons as well as long-distance connections, where two neurons are connected synaptically despite being separated by large distances. Networks with both short-range and long-range connections were

first introduced as "small-world networks" (SWN) by Watts and Strogatz, who characterized them as having both high clustering, or likelihood that the spatial neighbors of a vertex are connected to each other, as well as a short path length, or average number of links it takes to travel from any one element to another [188].

The dynamics of a network is heavily determined by its network properties because these properties govern the effects which elements have on each other. A random network exhibits connections between random pairs of elements regardless of their physical separation and therefore shows the shortest path length; this allows for maximum transmission of information across a neuronal network, but a weak ability to form dynamically coherent clusters of neurons. A completely regular network, where elements are only connected to their k nearest neighbors would display slow information transfer but a high propensity for coherent cluster formation.

A small-world network is one in which random connections are added to or replace links in a local network with a probability p, and varying this value allows for careful tuning between the two extremes as well as quantitative representation of the network topology, as shown in Figure 1.6. It has been shown that in small-world networks, addition of relatively few shortcuts allows formation of coherent dynamics from local synchronized clusters [56, 159]. Scale-free networks are another type of topology which have been identified as having real-world relevance and practical importance. These networks are characterized by a power law distribution in the number of connections each node is likely to have. That is, the probability of a node having k connections is given by $P(k) \propto k^{-\gamma}$, where γ usually ranges from 2 to 3. Such a structure necessarily entails the existence of "hub nodes," or nodes with very large numbers of connections, alongside the vast majority of nodes which have few connections [11, 21].

Both small-world and scale-free networks have been identified in the brain. Small-world networks have been discovered in the anatomical networks of *in vitro* neuronal cultures [151] as well as in functional networks between entire brain regions using

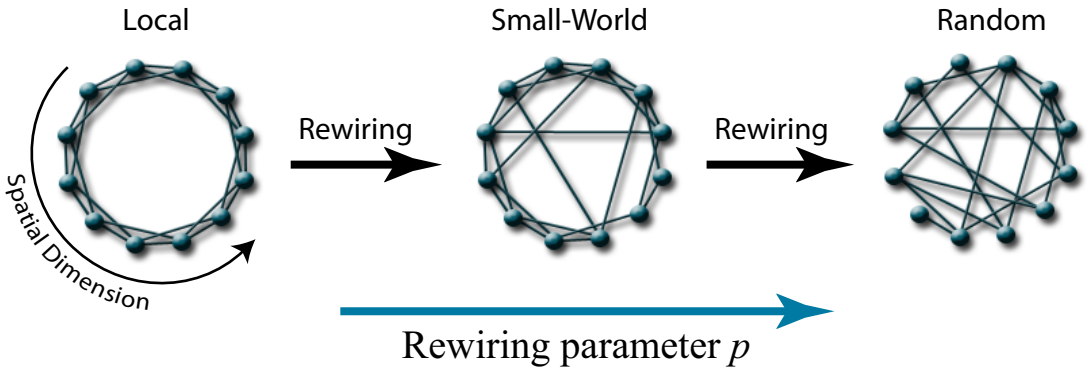

Figure 1.6: Creation of a small-world network. Left-most graph shows a fully local, regular 1-D lattice with periodic boundary conditions and $k = 4$ nearest neighbor connections per neuron. By breaking a few of these local connections and then randomly rewiring them, we've introduced some long-range connections which link spatially distant portions of the network. As the fraction of links rewired increases, denoted by the rewiring parameter p, the network becomes increasingly random.

fMRI [149] and EEG [111] data. This could be an attempt by the brain to maximize information flow across distances while minimizing the energetic costs of building and maintaining connections [28]. FMRI has also been able to identify scale-free correlations between different brain areas during task performance [47].

Small-world networks of oscillators are found to synchronize more easily than random or local networks [12], while a largely heterogeneous distribution in number of connections of each node tends to desynchronize systems [123]. Synchronization is a uniquely network effect, defined by the existence of functional temporal correlations in trajectory between two or more dynamic elements. Within the brain, synchronization is theorized to serve as a mechanism of integrating distributed neural activity to form coherent thought and organized cognitive processes [173]. Small-world networks of integrate-and-fire neurons (a simplistic neuronal model with built-in refractory behavior, described in Chapters II and III) can exhibit bistable dynamic behavior which switches between a quiescent state and persistent self-sustained activity depending on the stimulation [148]. Persistence is due to re-injection of activity into distant

and recovered (i.e. no longer in a refractory period) areas of the network via a few long-range connections, while most activity propagates locally via short-range connections. This allows for the formation of reverberating loops and sustained high activity levels. As the network moves closer to random topology, a higher probability of failure occurs due to inability of the neurons to recover before being re-injected. This self-sustained persistent elevation of selective neural firing is widely accepted to be a neural correlate of working memory [184, 35, 36]. It has been theorized that neurons and networks within memory structures form dynamical systems that can exhibit bistable (or multi-stable) states of activity where high activation states correspond to activation of a specific memory [44].

1.5.2 The role of modeling

Large-scale dynamics of the brain are not generally obvious or deducible from the micro-interactions, so that they are emergent properties of the system. This behavior is characteristic of a complex system, a relatively new term which has come to (vaguely) define any collection of elements which interact in a nonlinear way to result in macroscopic properties which can be self-organized or unpredictable. It is this unpredictability which has necessitated exploration of new ways of thinking and investigation.

For centuries, immense advances in our understanding of nature have come from combining inspired theories with carefully conducted experiments. If measurements matched with those predicted, then confidence in our mentally constructed concept of the system grows. However, when a system grows complex enough, it becomes necessary to augment natural human intuition with computational modeling power in constructing sensible theories. This is true for two reasons: 1) The interrelated nature of complex dynamic networks such as those in the brain make it difficult to isolate, control for, and sometimes even identify single parameters in experiment and

analysis, and 2) These networks often behave in counterintuitive and unexpected ways due to the existence of multiple interacting forces and features, necessitating the use of reduced models in comprehending distinct driving forces.

The bulk of experimental work in the sciences have operated under what is now considered "reductionist" principles, or the practice of breaking a system up into smaller and smaller components in order to understand its function. In some cases, such as with high energy physics, characterization of the smallest components such as quarks and gluons is the end goal. However, with the more applied sciences which target function on the macroscale, implicit in this reductionist method is the idea that properties of the constituent elements manifest on the macroscopic scale in a mostly linear, superpositional way. This has brought forth great advances as it's often the case that interaction forces are either negligible in comparison to bulk behavior or can be averaged in some manner to yield statistical information. Neither of these apply to complex dynamic networks, in which multiple spatial and temporal scales interact to create highly nonlinear interactions so that neither pure randomness nor pure order is able to dominate. This makes it quite difficult to identify or experimentally alter one physical feature of the system which would not affect others.

To be sure, this same weakness can exist in models of complex dynamic networks as well. If a model of a system were designed which incorporated all the complexities and nonlinear interactions of the real-life system, it's unclear what can be learned about its function by adjusting various parameters, despite immensely better control over conditions and rules of interaction. Therefore the real power of creating a network model lies in its ability to reduce and condense complex systems into something already understood with the exception of one added component which we are interested in exploring. This can be seen as a different but analogous type of reduction as compared to classical reductionism; instead of eliminating interaction effects between components, we eliminate various layers of detail in the components themselves. The

general strategy is then to elucidate and test individual theories of function which can be incomprehensible if present all at once within a system.

Modeling can also offer insight into network effects gleaned through the process of thinking through its construction. Along with the ability to examine the data in arbitrarily close detail, constructing networks from the ground up instills and to an extent requires intuition into workings of networks. Similar to how thermodynamics can be understood most palpably if one has an intuition of how microscopic properties of single molecules affect macroscopic properties of bulk matter, it's important to form an intuition of how complex micro-interactions at the single unit level affect large-scale dynamics.

Of course, the major drawback of models is that they're inherently decoupled from reality. Therefore it's vital to choose and construct models carefully and interpret the results within the proper scope. Paired with data analysis and experiment, this can yield great insight into the complex workings of neural coding and network interactions underlying brain functions. It is within this framework that I explore the neural correlates of learning and memory, making meaningfully chosen simplifications in order to probe network functioning.

1.5.3 Neuronal models

The advent of the computer has allowed us to pose theories of much more complexity than before. With models, we can test hypotheses of function with ease. However, it is critical to determine the optimum amount of detail to incorporate into a model, as this decision can drastically affect the way the results should be interpreted. Models range from the abstractly simple to the realistically detailed. Simplicity tends to promote understanding, and thus the simpler models are useful for elucidating principles of function. Complex and detailed models risk inheriting the complications and ambiguity of the objects they're modeled after, but are useful for testing parameters

and ranges of function. There is thus a trade-off between understanding and realism, and the aim is always to maximize the amount of understanding given the sacrifice in realism.

The simplest models of neural functioning are mathematical abstractions which approximate the internal voltage of a neuron as a direct function of its summed inputs, which is then usually thresholded to yield boolean values representing active or nonactive states. The most famous memory model which made use of these artificial neurons was implemented by Hopfield who connected them into a recurrent network with weights that with proper training allowed the recovery of low-energy attractor states as the units evolved over many iterative steps [80].

Biological neuronal models account for the explicit time dependence of input currents and membrane potentials. The simplest model incorporating these features is known as the integrate-and-fire neuron, which evolves according to a single linear differential equation linking the rate of change of the membrane voltage to input current. There are several artificialities generally incorporated into this model to account for the nonlinear nature of real neurons which cannot be captured by a single equation, such as a refractory period and the synaptic output current. The advantages of integrate-and-fire neurons include their light computational requirements as well as the ease of linking them into very large networks.

The most famous biological model explicitly accounting for voltage-gated ion channels is the Hodgkin-Huxley neuron, which is a set of four nonlinear differential equations describing the membrane potential, a voltage-gated Na^+ channel conductance, a voltage-gated K^+ channel conductance, and a passive leak conductance [79]. The biological realism of the Hodgkin-Huxley neuron allows for the exploration of a wide range of complex ion channel-dependent neuronal dynamics, but its many coupled equations make it difficult to implement into large-scale networks. Several simplifications to this model have been developed which take advantage of the different

timescales of the various ion channels and reduce the number of differential equations to three [78] and two [54].

The most realistic neuronal models are concerned with the propagation of electrical current across the spatial extent of a neuron, and incorporate features such as dendritic branching or cross-sectional area and the active propagation of action potentials down the length of the axon. Such systems are usually referred to as cable theory or multi-compartmental neurons and are useful for examining the electrophysiological properties of single neuron functioning.

The more detailed a model is, the more difficult it is to model neurons within a network since the computational requirements increase exponentially as interactions between neurons are incorporated. Since learning and memory are primarily functions of the network interactions between neurons, the networks involved can be quite large. Therefore, I implement the leaky integrate-and-fire model to highlight the effects of network properties and topologies on the neuronal activity and to limit the number of free parameters to manageable levels.

1.5.4 Experimental networks: *in vitro* cell cultures

As mentioned previously, complex networks are difficult to experimentally test due to their interdependent nature, but a few biologically reduced systems can be tractably studied to gain insight into the networks of the brain. One of these which we study in our lab is the dissociated hippocampal cell culture, composed of neurons and glial cells. These cultures are created by plating and growing rat hippocampal cells which have been dissociated from each other to break all synaptic connections. After plating, they are able to regrow processes and thus form biological networks as well as exhibit spiking dynamics.

Dissociated cultures offer the advantage of clear unobstructed imaging, relatively easy pharmacological and mechanical manipulation, and the ability to be grown on

MEAs which allows for spatially extended electrical recording. Thus, anatomical connectivity can be connected to firing dynamics to assess for the relationship between network structure and dynamics.

Cultures are analyzed over various days of growth and in two conditions: high glial and low glial growth levels. Glial cells are known to be vital to neuronal growth and survival [122] in addition to modulating neurotransmission [15, 16, 175]. Glial cells are connected to each other via gap junctions and can directly connect to neurons via either gap junctions or chemical synapses [16]. However, they much more commonly indirectly modulate neuronal activity. Morphological investigations show that astrocytes tend to surround the synapses of neurons, forming a "tripartite synapse" [7] in which they engage in bidirectional interaction with pre- and postsynaptic neurons via Ca^{2+}-dependent release of gliotransmitters such as glutamate and ATP. This allows them to function as an active third partner in neuronal communication [131, 120].

I closely characterize various aspects of the anatomical structure with immunocytochemistry and fluorescence labeling, including the density of synapses along the neuronal processes, the extent of neuronal process growth, the extent of glial cell growth, and the length and complexity of the processes of individual neurons. Immunocytochemistry involves the use of antibodies and antigens to label for specific proteins in a cell. I utilize an indirect two-step labeling process which involves first labeling with a primary antibody which binds to the target protein, followed by a secondary antibody which binds to the primary antibody and is conjugated with a fluorescence marker. Such a procedure allows for increased sensitivity over direct labeling methods. I also use a diffusive carbocyanine membrane dye to individually stain neurons so that entire processes can be visualized. Carbocyanine dyes are useful because they are extremely bright and stable with low photobleaching. They are lipophilic and so are able to diffuse through the entire cell membrane, staining all processes while avoiding staining surrounding neurons, even synaptically connected

ones.

These results are compared with analyses of their functional structure derived from spiking dynamics, provided by Sarah Feldt. It is found that changes in the anatomical structure of the neuronal network is linked to changes in functional connectivity, and, further, the morphological characteristics of the glial network impacts the range of neuronal signaling.

CHAPTER II

Memory consolidation

2.1 Introduction

The memory formation process is founded upon synaptic reorganization and modification regulated by neural activity. When associative memories are first formed, cortical sensory areas which project to the hippocampal associative network activate the hippocampus and rapidly (within seconds) form a new network of synaptic weights encoding that memory. Over the span of days and weeks, rapidly formed novel memory networks in the hippocampus are consolidated to the cortex in a time- and activity-dependent fashion [88, 134, 22], eventually allowing memories to be independent of the hippocampus altogether [106]. Recent studies [168] have shown that storage and recall of spatial memory can occur independently of the hippocampus once schemas have been formed. Moreover, studies investigating brain metabolism and activity-related genes in mice suggest the decreasing importance of the hippocampus as time passes after learning and the increasing importance of several cortical regions [57]. These and other findings [158] suggest that the hippocampus is a general-purpose learner of new facts and events, both spatial and non-spatial [157], but that the cortex handles long-term storage of memory. Electrophysiological [191, 135, 134, 139] and genetic [142] studies have combined with behavioral and neurological case studies [156, 181] to build a coherent cellular and behavioral theory of how the consolida-

tion process occurs off-line (e.g. during sleep) through the reactivation of patterns of neuronal activity observed during awake learning [96, 22, 55, 141].

From a dynamical perspective it is generally assumed that an enhanced spiking activity in the form of persistent reverberation for several seconds is the neural correlate of working memory [60, 61, 66]. The formation of these persistent activity patterns has been studied extensively [64, 163, 164]. Some of this work concentrated on investigating what intrinsic neuronal properties can support such activity patterns [114, 178], while others focused on defining the exact activity matrix that would support attractors exhibiting localized, memory-specific, persistent activity [147, 34]. We have shown recently that selective persistent activity during reactivation is an intrinsic property of an inhomogeneous dynamic memory structure [83] and is due to recurrent excitation supported by the networks with Small-World (SW) topology [148]. Biologically, such heterogeneities are shown to exist [187]. Moreover, we showed the network can regulate the stability of the persistent activity regime through change of global parameter, namely excitation. This allows the networks to undergo a seamless transition between activity regimes.

It remains unclear, however, what the dynamical underpinnings of time-dependent memory transfer from the hippocampus to the cortex are and how this dynamics is modulated by stimulus novelty. Experimental work has shown that the reactivation of a given experience during sleep is greatest when the experience is novel and diminishes with increased exposure [129, 134]. Moreover, hippocampal recordings indicate that there is a significant phase shift of neural activity with respect to the hippocampal theta rhythm during the consolidation process [134], which could indicate a difference in input drives through the two hippocampal excitatory input pathways as consolidation progresses [22], as the firing of neurons in the hippocampal subfield CA1 switches from being aligned with the peaks of hippocampal theta oscillation to being aligned with the peaks of cortical theta rhythm. However, basic questions remain

concerning 1) how the stimulus novelty is assessed from changes in localized activity patterns, 2) how these changes are related to structural network modifications, 3) how the hippocampal-cortical interaction regulates memory storage and erasure within hippocampus, and finally 4) how all these processes come together to generate the experimentally observed, complex and novelty dependent memory management scheme.

Here we show that this phenomenon can be easily explained through generic modifications of network structure which in turn evokes dynamical changes in network response. Namely, our results indicate that the dynamic formation of localized network inhomogeneities, coupled with basic anatomy of hippocampal-cortical structure, can underlie both novelty detection within hippocampal and cortical networks, as well as memory management processes based on this novelty assessment. To be able to concentrate solely on the structural network underpinnings of the observed dynamics, we use integrate-and-fire neurons; however the results apply to biologically detailed neuronal models.

In order to more closely examine the network structural and dynamical underpinnings of these phenomena, we present each component of our model separately and discuss their implications on the novelty detection and the memory management. Both the hippocampus and the cortex were each modeled as a reduced assembly of excitatory and inhibitory networks [Figure 2.1b] having periodic Small-World topology per the Watts-Strogatz formulation [189]. This general topology was found to be present in local and global brain networks [2, 154]. Dynamic Small-World topology allows for simultaneous local propagation of activity as well as long-range re-injection of current, promoting formation of "on" states of persistent activity [148].

First, we show that a relatively small increase of connectivity in a discrete (i.e. well-defined) network region can play two distinctly different roles, depending on the network dynamical regime. When the network is in the low excitation regime, the

changes of local network response to incoming sensory stimuli can act as familiarity/novelty detection mechanism. However when the global network excitation is increased, the same region will exhibit a persistent self-activation in the absence of external input. Our results indicate that the evolution of these two dynamical states correspond to observed neurobiological responses to a presentation of increasingly familiar stimulus during animal wake state and to memory reactivation experienced during sleep, respectively.

Further, we show that structural network inhomogeneities provide at the same time a dynamical mechanism of intra-network novelty detection and inter-network signaling of the level of discrete memory consolidation within the cortical network. This last mechanism subsequently provides a self-regulated means for the hippocampus to clear already consolidated memory traces. When implemented in conjunction with a simple learning rule, as well as the assumption of fast plasticity in the hippocampus coupled with slow plasticity in the cortex, we can reproduce complex memory management processes similar to that observed in behavioral data.

2.2 Model Structure and Methods

2.2.1 Intra-hippocampal/cortical network

The two brain structures were composed of a population of 500 excitatory neurons coupled with a smaller population of 100 inhibitory neurons. The network size ratios and connection densities used were chosen to grossly reflect biological distributions and connectivity patterns in the hippocampus (Figure 2.1a); however, these parameters are easily modifiable without loss of observed dynamical response.

We used leaky-integrate-and-fire neurons given by

$$\tau_m \frac{dV_{i/e}^j}{dt} = -\alpha_j V_{i/e}^j + I_{i/e} + \sum_k w_{jk} I_{syn}^k \tag{2.1}$$

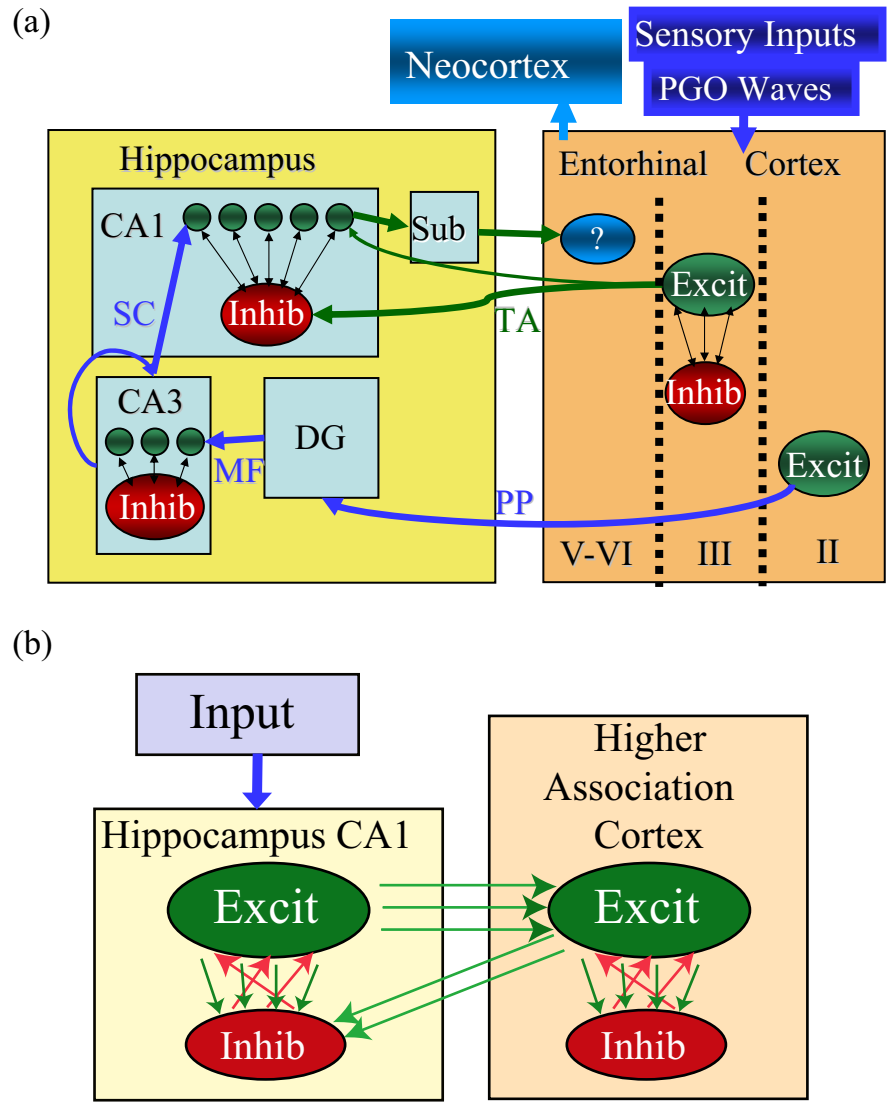

Figure 2.1: Diagrams of network structure. (a) Circuit diagram of anatomical connectivity between hippocampal and cortical structures. Entorhinal cortex layers II, III and IV-VI project through the perforant path (PP) to the Dentate Gyrus (DG) and CA3, through the temporoammonic (TA) path to the Subiculum (Sub) and CA1, and from the CA1 and Sub to the deeper layers of the entorhinal cortex, respectively. MF=Mossy Fibers and SC=Shaffer's Collaterals. (b) Diagram of model used in simulations. Single network (Hippocampus or Cortex): the network is composed of a larger population of excitatory neurons and a smaller population of inhibitory neurons. Both inhibitory and excitatory networks comprise Small World network having periodic boundary conditions. Feedback between hippocampus and cortex: the excitatory hippocampal neurons locally innervate the excitatory cortical network (e.g. the entorhinal cortex). The cortical excitatory network suppresses the hippocampal excitatory network through random inhibitory pathways.

to represent the reduced dynamics of the network elements. The i/e denotes either an inhibitory or excitatory neuron; $V_{i/e}^{j}$ is the membrane voltage of the j'th neuron; α_j is the membrane leak rate constant randomly distributed such that $\alpha_j \in [1, 1.3]$; $\tau_m = 30ms$ is the membrane time constant; I_{syn}^{k} is the incoming current to the j'th neuron from the k'th neuron; and w^{jk} is the connection strength between neurons j and k. For the global excitatory network the local connections are established between cells such that the relative distance from one to another lies within the radius $R_e = 5$, $p_g^e = 0.15$ is the rewiring parameter defining the fraction of the number of local connections to the number of random, long-range ones, and the connections are of strength $w_{ex} = 2$. Similarly, the global inhibitory interneuron subnetwork has $R_i = 1$, $p_g^i = 1$, and $w_{in} = 10$, forming a random graph network. Every inhibitory cell receives input from $n_{ei} = 5$ neighboring excitatory neurons with strength $w_{ei} = 4$, and every excitatory neuron receives input from $n_{ie} = 10$ random inhibitory ones with strength $w_{ie} = 2$. Locality and relative distance were determined by considering a one-dimensional lattice with periodic boundary conditions, done for graph visualization purposes. Synaptic strengths were chosen to balance number of incoming connections so that total possible input to all cells remains the same. The external current $I_{i/e}$ is uniform over the entire inhibitory/excitatory network and functions as a global modulatory mechanism (control parameter) that mediates response transitions from low-frequency random activity, to spontaneous activation of discrete network regions, and finally to global bursting. This network architecture promotes global inhibition driven by focal excitation that creates selective, persistent reactivation patterns. For a detailed description, refer to [83].

When the membrane potential of a given cell assumes a maximum value of $V_{reset} = 1$, the neuron emits an action potential, its membrane potential is reset to $V_{rest} = 0$, and the neuron enters a refractory period for $\tau_{refr} = 10ms$. The synaptic current

emitted by spiking neuron (k) is of the form

$$I^k_{syn}(t) = exp(\frac{-(t - t^k_{spike})}{\tau_s}) - exp(\frac{-(t - t^k_{spike})}{\tau_f}), \tag{2.2}$$

where $(t - t^k_{spike})$ is the time since neuron k last spiked, $\tau_s = 1.5ms$ is the slow time constant, and $\tau_f = 0.15ms$ is the fast time constant. Aside from the deterministic input drive received from other cells, all neurons have a $p_{fire} = 10^{-3}$ probability of firing spontaneously at any time step, defined as $0.5ms$.

In this reduced model, the network heterogeneities are built into the excitatory subnetworks of both the hippocampal network and the cortical network by adding random connections to distinct non-overlapping subgroups of excitatory neurons, i.e. neuron IDs 1-100, 101-200, 201-300, 301-400, and 401-500. The additional connections increase the density of interconnectivity within these regions beyond the average global connectivity density, allowing subgroups of neurons to recurrently innervate and effectively increasing regional excitability. These subgroups can be thought of as memory structures formed through long term potentiation (LTP) processes which are known to occur readily during exploration of a novel environment [109, 50, 39, 124].

2.2.2 Inter-hippocampal-cortical feedback

In the brain, the cortex and hippocampus are connected via two main input pathways: 1) the perforant path (PP) from layer II of the entorhinal cortex to the dentate gyrus, to CA3, and then to CA1 (Figure 2.1a and modeled as "input" in Figure 2.1b); and 2) the TA pathway directly from layer III of the entorhinal cortex to the inhibitory interneurons in the lacunosum-moleculare layer of the CA1 region and on to the subiculum (represented as Higher Association Cortex excitatory to Hippocampus inhibitory cell connections in Figure 2.1b) [6]. These two PP and TA input pathways function separately to encode novel memories and serve as a con-

solidation index for familiar memories, respectively [176]. It is the slowly building familiarity index of the TA pathway that is the first step in memory consolidation which is modeled herein. To model this neurophysiology, the model network hippocampus and cortex were coupled through localized excitatory connections from the hippocampus to the cortex, and also with diffuse feedback inhibition from the cortex to the hippocampus (Figure 2.1b). This connectivity grossly reproduces the anatomic connectivity (Figure 2.1a) between the two structures [6]. The one-to-one excitatory mapping from the hippocampus to the cortex is instituted for visualization purposes only; the qualitative results of this model would remain the same as long as the cortical structures, representing the long-term consolidated memories, can effectively and selectively affect hippocampal memory reactivation.

2.2.3 Activity-dependent synaptic modifications

In the last stage of our modeling, we introduce self-regulated formation of new connections within the excitatory networks to show the progression of sequential memory management: rapid memory formation in the hippocampus, its reactivation in hippocampus and consolidation in the cortex, and subsequent erasure in the hippocampus. Hippocampal and cortical excitatory subnetworks are allowed to undergo synaptic modification based on spiking activity of these cells. Subnetworks are of Small-World topology, with a local radius of $R_e = 10$ and a rewiring parameter $p_g^e = 0.15$, and are composed of 50% non-modifiable, homogeneous, active connections with weight $w_{ex} = 2$ as well as 50% of modifiable, initially silent synapses, which are connections initially with weight 0 but can modulate their strength between 0 and $w_{ex} = 2$ as a function of neuronal activity [82].

The changes in synaptic strength are implemented based on a simplified neurobiological rule of spike-timing dependent plasticity [13, 101, 17, 91]. The synapse strength is incrementally increased when the pre and postsynaptic neurons fire together within

a set interspike interval (ISI) of $T_L = 7.5ms$, and, conversely, synaptic efficacy in the modifiable group is decreased when the two cells do not activate congruously and their ISI is above the set threshold $T_F = 15ms$:

$$\Delta w^*_{jk} = \begin{cases} \frac{w_{ex}}{\tau^{h/c}_{learn}} & \text{if } t_j - t_k < T_L \ ; \\ -\frac{w_{ex}}{\tau^{h/c}_{forget}} & \text{if } t_j - t_k > T_F \ ; \\ 0 & \text{if } T_L < t_j - t_k < T_F. \end{cases} \tag{2.3}$$

The w^*_{jk} indicates the weight of modifiable synapses between neurons j and k, $w_{ex} = 2$ is the strength of non-silent synapses in the excitatory network, $t_j - t_k$ is the ISI between neurons j and k, and $\tau^{h/c}_{learn}$ and $\tau^{h/c}_{forget}$ are the time constants of learning and forgetting in the networks, where h/c denotes the hippocampal/cortical network, respectively. The time constants of learning and forgetting are much larger in the cortical network, reflecting slower learning (LTP) in the cortex [46, 137, 138]. We have used $\tau^h_{learn} = 7.5ms$, $\tau^h_{forget} = 10ms$, $\tau^c_{learn} = 25ms$, and $\tau^c_{forget} = 200ms$.

In this simplified model we concentrate on memory formation only within hippocampal and cortical structures. In the brain, LTP occurs both within the hippocampus, within the cortex, and between the two structures during learning. LTP occurs readily in the trisynaptic pathway from layer II of the entorhinal cortex (EC) to the dentate gyrus (DG). LTP is also easily produced in the Schaffer collateral (SC) fibers from CA3 to CA1 as noted *in vitro* and *in vivo* [176, 81]. LTP in the direct temporoammonic (TA) inputs to CA1 have not been well described, indeed it is only recently that attention has been paid to this input pathway in models of hippocampal function, mostly in reference to memory consolidation as we are considering here. As was noted earlier, LTP in the TA pathway is more difficult to induce and would therefore probably occur more slowly than LTP in the trisynaptic pathway [46, 138].

2.2.4 Experimental procedures for biological recording and data analysis

The experimental procedures are thoroughly described in [134]. Briefly, rats were anesthetized and implanted with a 14-tetrode drive above the hippocampus CA1 region in the brain. After surgical recovery, rats were food restricted to maintain 80-95% of their free feeding weight, and were trained to run on a raised rectangular track for food morsel rewards placed in food cups around the edges of the track. Rats ran laps on this same track for 45 min each day to familiarize them with the environment, procedure, and recording setup.

REM sleep was characterized by lack of movement and sustained large theta (5-10 Hz) frequencies in the field potential following at least 3 min of non-REM sleep. Cell spike, field potential and position data were recorded while the rat traversed the familiar training track for 20 min, then traversed a similar track located in a previously hidden area of the room for another 20 min, then returned for a final 20 min run on the familiar track. The same procedure of Familiar-Novel-Familiar maze running followed by sleep recording was followed every day for a week while the initially novel maze became familiar to the animal.

The relative amplitude of the spike peak and trough, and other waveform characteristics were used to identify nearly 100 recorded pyramidal cells and interneurons from the CA1 cell body layer. The spike times of each cell were then listed and compared with the position of the animal at the time of firing, the state of the animal, and the phase of the field potential filtered for theta. Thirty-one of the recorded CA1 pyramidal cells were selected for further analysis because they showed consistent place-specific firing (place fields) on either the familiar maze only (n=12), or formed a stable new place field on the novel maze (n=19). The firing rate of the familiar and novel place cells during the exploration phase and during the subsequent 4 h sleep period was calculated. The reactivation rate and theta pattern of cell firing during REM sleep was compared with the activity rates and patterns of the same cells during

the prior exploration period.

Theta phase and firing rate changes during running and REM sleep were first reported in Poe *et al* [133].

2.3 Results

We show below that formation of structural network heterogeneities defined as local variations of synaptic density can lead to dramatic changes in network dynamics which may underlie stimulus novelty detection and regulate memory management between the hippocampus and the neocortex. We ultimately show that this simple mechanism modulating hippocampal activation through cortical feedback reproduces the experimental data presented and, further, replicates the full process of hippocampal memory management (i.e. hippocampal storage $\rightarrow$ hippocampal reactivation $\rightarrow$ cortical storage $\rightarrow$ hippocampal deactivation). For clarity, in the sections below, we discuss each dynamical component of the phenomena separately.

2.3.1 Single network mechanism can underlie novelty detection and memory reactivation

We have shown earlier [83] that network heterogeneity may underlie selective network reactivation. Here we want to show that the structural network modifications may play a twofold role during network dynamics. Random addition of relatively few synapses (1-2% of total possible connections) to a selected network region can dramatically change activity response of this region to stimulation when the network is in its low global excitation state (i.e. low I_e), and at the same time it can lead to formation of persistent activity state within the same region when the network is in its high global excitation state (i.e. high I_e).

To illustrate these effects we first measured network responses to a focal external drive (Figures 2.2a-c). The network shows preferential activation of the region with

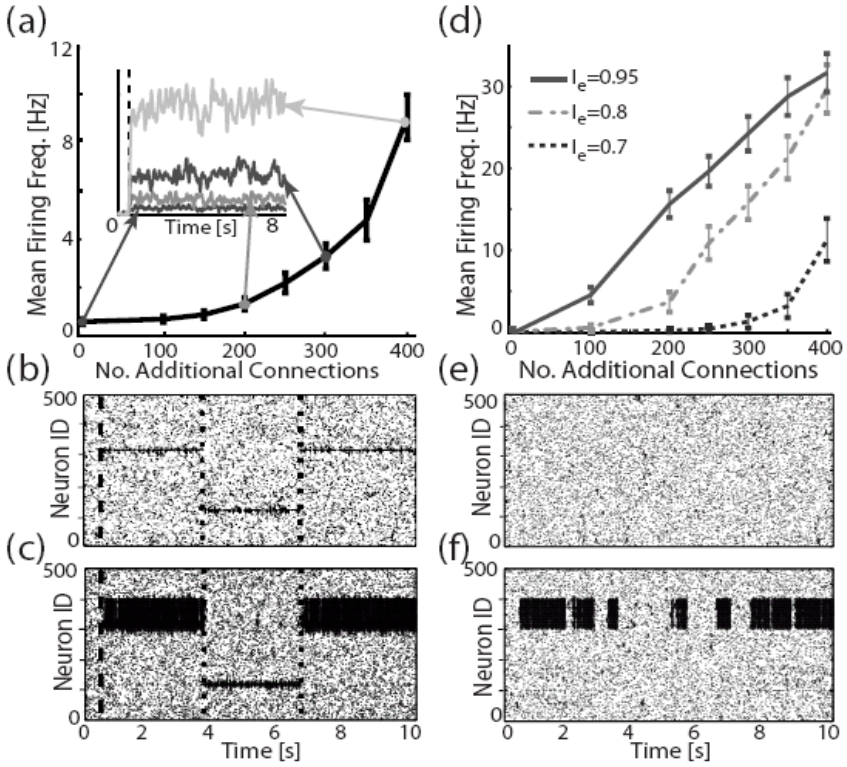

Figure 2.2: Network response modulated by localized increases in connectivity density. (a) Activation of a network region, measured as a mean firing frequency of neurons in the subnetwork (neuron IDs 300-400), in response to stimulation of 6 cells (neuron IDs 315-320; global excitation $I_e = 0.6$; stimulation current $I_{stim} = 0.7$) as a function of number of added connections to the subnetwork. Activation is averaged over 20 runs and over time. Inset: sample time course of activation for 4 different connectivity densities (dashed line denotes onset of the stimulation). (b), (c) Sample raster plots of the network response during alternating stimulation to illustrate locality of response; neurons 315-320 are stimulated between the dashed line and first dotted line, neurons 115-120 between the first dotted and second dotted lines, and neurons 315-320 are finally stimulated between second dotted line and end of run. (b) No heterogeneities are present. (c) $N = 400$ connections are added to the neuron IDs 300-400 region of the network. (d)-(f) Reactivation as a function of local connectivity density. (d) Mean firing frequency as a function of added connections for different values of global excitation . (e),(f) Sample raster plots depicting network reactivation when (e) no heterogeneities are present, and f) N=400 connections are added to the region encompassing neuron IDs 300-400.

added connections directly related to the magnitude of the structural network heterogeneity. Since the formation of the heterogeneity is the outcome of LTP processes incurred during learning [109, 50, 39, 124], the changes in the intrinsic response of the network to the stimulation can be directly linked to the novelty/familiarity of the presented stimulus.

Furthermore, as we have shown before, these regions of network inhomogeneities can be spontaneously activated when network's global excitation level (I_e) is increased. Figures 2.2d-f depict examples of spontaneous reactivation as a function of connectivity density within the heterogeneous region. One can observe clear reactivation exemplified in the persistent activation of the neurons within the heterogeneous network region. The reactivation itself is due to reciprocal feedback activity which is mediated by the fact that SW topology provides a structurally random yet stable re-injection mechanism supporting prolonged activation of neurons in spite of their refractory time [148]. The discrete localization of the reactivating region is, on the other hand, due to lowered threshold within the inhomogeneity for such dynamics to occur as well as increased inhibition spreading randomly to other network regions.

Thus, we show that network structural inhomogeneity provides a dynamical mechanism mediating and modulating local, discrete network responses to stimulation, while also able to self-activate under conditions of increased global excitation of the network. Here, the network dynamics can be viewed during wake behavior as an unstable attractor that becomes activated only by stimuli of appropriate characteristics, and yet during off-line consolidation becomes a stable attractor which can activate spontaneously.

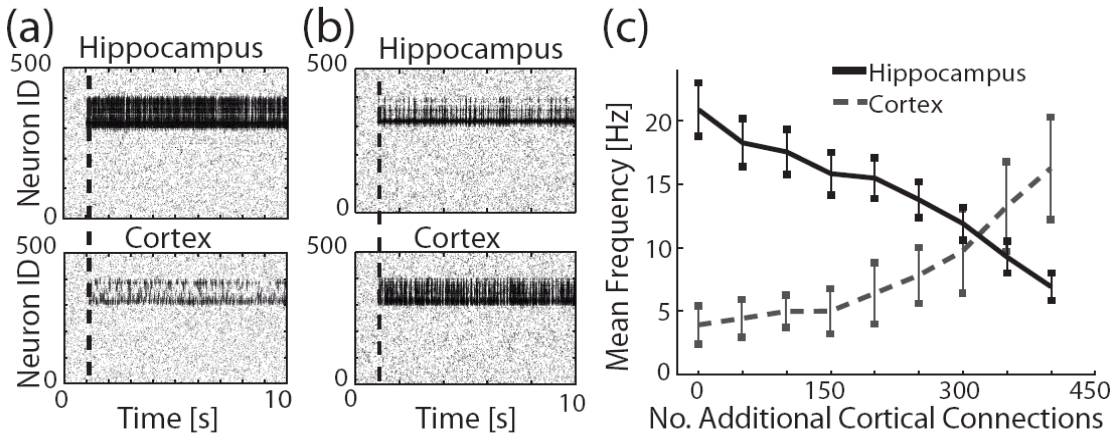

Figure 2.3: Changes of the hippocampal response as a function of structural properties of cortical network. The hippocampus has one stored memory (neuron IDs 300-400), in the form of 400 additional network connections. (a) Cortex is a homogenous network (i.e. no stored memory). Six neurons in the hippocampus, IDs 315-320, are stimulated with input $I_{stim} = 4$ and show strong activation, whereas the activation of the homogeneous cortex due to input from hippocampus is limited. (b) The cortex has a single network heterogeneity (memory) stored in the form of 400 additional connections. The hippocampus, with the same memory stored, is stimulated by the same input current, and subsequently triggers the cortical memory, which activates strongly and depresses activation of the hippocampus. (c) Mean activation of hippocampal and cortical networks as a function of added connections. As the memory is progressively stored in the cortex (i.e. becomes more familiar), cortical activation increases while hippocampal activation is depressed.

2.3.2 Modulation of hippocampal activation and reactivation by cortical feedback

Having established a common mechanism modulating both network response to stimulus based on its novelty as well as spontaneous reactivation during off-line processing, we will proceed to apply this concept within an experimentally established framework of hippocampal and cortical interactions. The underlying assumption that we are making is that progressive storage (i.e. memory formation) of the presented stimulus is achieved by the formation of network inhomogeneity first in the hippocampus (i.e., fast, short-term storage) and then in the cortex (i.e., slower, long-term storage). In order to highlight the effects that cortical storage has on hippocampal activation and eliminate transient effects, we disallow synaptic modifications (i.e. learning) and examine the network dynamics at various static points of cortical memory storage.

We investigated the changes in cortical and hippocampal activation patterns as a function of the degree of regional inhomogeneity in the cortex (representing long-term memory storage) when the external stimulus is present. The hippocampal network (Figure 2.3) had a single structural heterogeneity, located at neuron IDs 300-400 and created by the addition of 400 random connections within this region, and was driven by focal external stimulation applied as an additional input current ($I_{stim} = 4$) driving 6 cells (IDs 315-320). One can observe that when the cortex was homogeneous, with no added connections, the stimulated region in the hippocampus was highly activated (Figure 2.3a). However, in the presence of cortical structural inhomogeneity, hippocampal activation was attenuated through diffuse inhibitory feedback stemming from cortical feedback excitation of hippocampal interneurons (Figures 2.1a, 2.1b and 2.3b). In general, we see that hippocampal activation systematically decreased as additional connections were added to the cortex, while cortical activity increased at the same time (Figure 2.3c). Therefore, the level of long-term memory consolidation

in the cortex is able to control activation of the same memory in the hippocampus, serving as a novelty detection mechanism which can be utilized by the hippocampus in the consolidation process.

2.3.3 Cortical modulation of hippocampal memory replay

As noted before, it is thought that memory reactivation observed during sleep plays an important role in long-term memory storage as a possible memory replay mechanism mediating memory consolidation into the cortex. In such a system, it is important that consolidation, and thus reactivation, is regulated by stimulus novelty (i.e. over-consolidation of a given memory may lead to disruption of other memories, while lack of consolidation of novel memory will inhibit its storage). We postulate that, toward this end, the cortex has a novelty-dependent and memory-specific regulation of memory reactivation. We will show below that this mechanism becomes an intrinsic property within the modeled cortical-hippocampal interactions.

2.3.3.1 Simulation Results

We demonstrate this mechanism in our hippocampal-cortical network, again in the absence of learning in order to eliminate transient, time-dependent effects. Three network regional inhomogeneities (neuron IDs 0-100, 200-300, 400-500) representing memory structures were created in the hippocampal network and kept unchanged during the simulation. At the same time, the cortical network was initially set to be homogeneous, and then new connections were progressively added to a region matching one of the hippocampal network heterogeneities (neuron IDs 200-300), to represent the progressive consolidation of that cortical memory. Figure 2.4a depicts the regional hippocampal activity in the three network regions of interest, normalized to their activity when there are no additional connections present in the cortex. One can observe a significant decrease of reactivation of the hippocampal network region (Figure 2.4a;

"familiar" line), linked to the cortical region where structural inhomogeneity was progressively formed. The reactivation ratios of the other two hippocampal regions remained virtually unchanged (Figure 2.4a; "novel 1" and "novel 2"). This indicates that, the cortex can selectively deactivate reactivation of a particular network region, representing a single familiar memory, within the hippocampus while keeping the reactivation of others virtually unchanged. Figures 2.4b-c depict an example of localized hippocampal deactivation by the cortex. As soon as the "familiar" hippocampal region (IDs 200-300) started to reactivate, the linked cortical region immediately activated, during which activity of the whole hippocampus was inhibited. After the reactivation in the "familiar memory" region was abolished in the hippocampus, the cortex subsequently deactivated and other hippocampal regions (representing novel, as yet cortically unconsolidated memory) were able to again reactivate.

2.3.3.2 Experimental Confirmation

To validate our results, we compared them with experimental findings [134]. Here we concentrate on two basic aspects: the progressive cortical involvement in hippocampal processing during memory consolidation, and changes in the off-line, autonomous (i.e. not stimulus driven) hippocampal processing (i.e. reactivation).

We measure the progressive cortical involvement in hippocampal processing by monitoring the phase shift in hippocampal neurons firing in relation to field potential theta oscillation phase. The phases of theta oscillations in the hippocampus and in the cortex are shifted with respect to each other by 180 degrees [22, 85]. In addition, according to previous research [134, 22, 133], the firing pattern will be aligned with the field potential theta oscillation phase of the dominant input structure (i.e. hippocampal or cortical). The activity of hippocampal neurons in relation to field potential theta oscillation phase over the time course of memory consolidation is shown in Figure 2.4d. The strong progressive shift in the activity of hippocampal

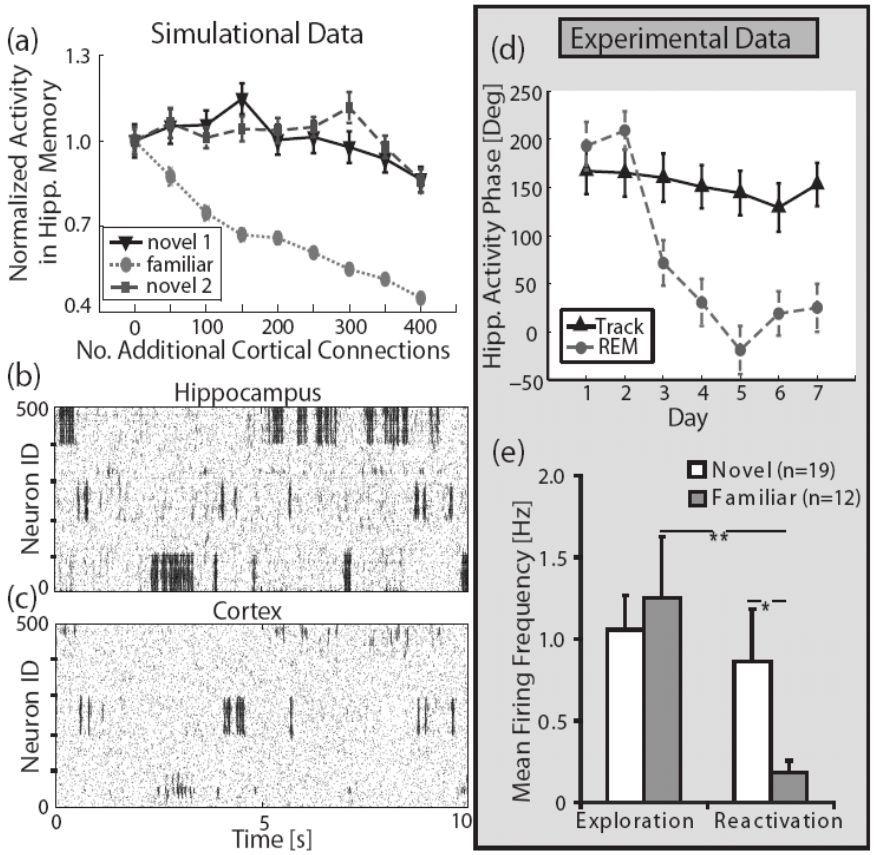

Figure 2.4: Selective autonomous memory reactivation in the hippocampal-cortical structure – simulations and experimental data. The hippocampus has 3 regions of network heterogeneities (IDs 1-100, 200-300, 400-500). One memory structure (IDs 200-300) is stored in the corresponding region in the cortex. (a) Average reactivation activity of familiar (neuron IDs 200-300) versus novel (neuron IDs 1-100 and 400-500) memories as a function of additional cortical connections. Activity was measured by normalizing total spike counts within a memory region for the total duration of the run to total spike counts for the homogenous cortex run. Sample raster plots for (b) hippocampus and (c) cortex. (d), (e) Experimental data: (d) Phase locking of hippocampal neurons activity to local theta oscillations as a function of days of exposure to the stimulus (i.e., stimulus novelty). Solid black line ("Track") denotes phase locking to CA1 layer theta peaks during active exploration; dashed gray line denotes the same phase relation observed during REM sleep reactivation ("REM"). (e) Frequency of hippocampal activity in novel and familiar environments during exploration (left) and sleep reactivation (right).

neurons to fire in the trough of the hippocampal theta cycle, i.e. in phase with theta at the site of direct cortical inputs through the TA pathway, indicates that as the reactivated memory becomes increasing familiar, the cortex plays a progressively larger role in the hippocampal reactivation pattern. This supports directly our results which show that as familiarity is increased, the cortical involvement in hippocampal firing dynamics also increases.

We measure the progressive change in hippocampal off-line processing by monitoring the spiking frequency of the reactivating place cells. Once the consolidated cortical TA pathway began to directly drive hippocampal reactivation (Figure 2.4d), the spiking frequency of neurons encoding the (cortically) familiar environment decreased significantly (Figure 2.4e, right), just as predicted by the simulations. The switch in both theta phase and frequency of firing during reactivation can be explained by the consolidated cortical memory network effectively suppressing hippocampal CA1 reactivation, possibly through projections to the opioid-sensitive inhibitory neurons [46, 98, 180], just as we observed in our simulations.

2.3.4 Cortical-hippocampal memory management sequence

The hippocampus, being a short-term memory storage location [88], is thought to perform three primary memory management tasks: store novel memory traces, reactivate these traces during quiet waking and sleep for consolidation to the cortex, and lastly erase them from itself to prevent saturation. We posit that these complex memory management processes are autonomously controlled on the basis of their familiarity. As the last part of this paper, we present the full model, with synaptic plasticity (i.e. learning dynamics) and show that localized cortical activation together with the modeled hippocampal-cortical feedback can act as a dynamical, autonomous hippocampal memory management mechanism. Self-regulation of this process within the hippocampal-cortical structure has the required and experimentally established

phases (i.e., initial hippocampal learning during stimulus exposure, reactivation when the stimulus is not present, inhibition of reactivation when cortical heterogeneity is formed, and subsequent deactivation of the memory through deconstruction of the hippocampal heterogeneity). To do so, we introduce self-regulating synaptic modifications (as described in the methods section).

During the simulation, a subset of neurons (IDs 200-300) in the hippocampal excitatory network were injected with external current at times denoted as the shaded time segments on the hippocampus raster plot on Figure 2.5a) to simulate a new sensory experience, and both hippocampal and cortical networks were allowed to modify their silent synapses starting at 1.5 s (dashed vertical line). The external stimulation coupled with synaptic plasticity allowed for rapid formation of network inhomogeneity in the hippocampus, while synaptic modifications happened on a much slower timescale in the cortex (Figure 2.5c). When the external stimulation was stopped, the local structural changes created in the hippocampus drove its continued reactivation, allowing for further activation and structural modifications in the cortex. At a critical point, the cortical heterogeneity became large enough that its activity blocked the reactivation in the hippocampus through the interneuronal feedback (Figures 2.5a-b). As the hippocampus shut down, its inhomogeneity started to clear out due to its ability to quickly depotentiate the synapses, while the cortex maintained its memory structure even in the absence of stimulation or activation.

Anatomically, this depotentiation occurs through TA inputs to interneurons which have spike-blocking activity [46] and release depotentiation-enhancing peptides [180]. Concurrently, the hippocampus increases its sensitivity to the direct TA cortical inputs [98]. Upon repeated stimulation to the same hippocampal area (second shaded blue region in Figure 2.5a), we see that reactivation in the hippocampal network became shorter as the memory became progressively more familiar to the cortex and direct cortical inputs to the hippocampus through the TA pathway became more

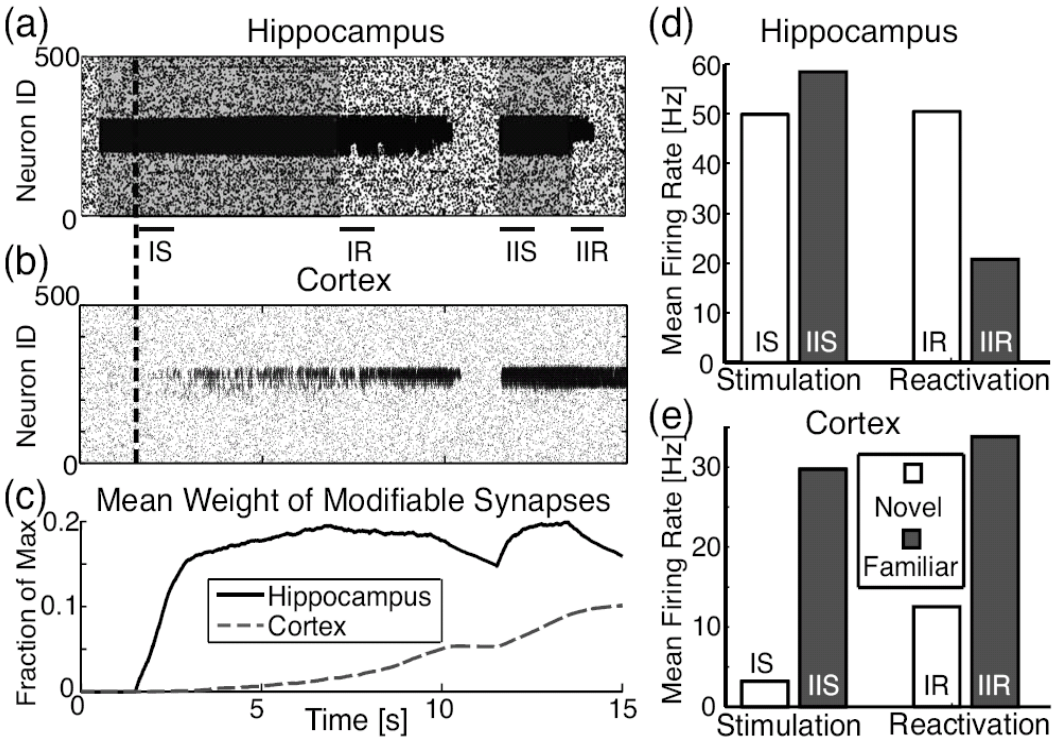

Figure 2.5: Memory management through hippocampal/cortical feedback. Raster plots of activity in (a) hippocampus and (b) cortex. The hippocampus is presented with the stimulus (represented by shaded region) in neurons 200-300, immediately undergoing fast, local synaptic formation in the stimulated region. Concurrently, cortical activity driven by the hippocampus induces slower synaptic modifications in the cortex. Dashed vertical line denotes start of learning for both networks. Formation of local connections in the hippocampus allows spontaneous reactivation of the network even when the external stimulation is terminated. Activation of the cortex eventually inhibits reactivation in the hippocampus which promotes forgetting. Upon subsequent stimulation of this same region in the hippocampus (second shaded portion, starting at 11.5 s), the cortex immediately activates and further learns, strengthening its inhibitory feedback to the hippocampus. (c) Average synaptic weight of silent synapses, normalized to maximum possible value, $w_{ex} = 2$. (d), (e) Histograms of spiking frequency obtained from different time regions of the simulation (denoted by the labeled black bars IS, IIS, IR, IIR) for (d) hippocampus and (e) cortex. IS labels the first stimulation time window, corresponding to novel exploration (Figure 2.4e); IIS labels the second stimulation (familiar exploration); IR labels the first reactivation time window (novel reactivation); IIR labels the second (familiar reactivation). The changes in frequency response in the hippocampus accurately reproduce the experimental data (Figure 2.4e).

active. Figures 2.5d and 2.5e compare observed spike frequencies from the behavioral time points corresponding to the experimental data (Figure 2.4d). Here, one can observe a slight increase of the hippocampal spike frequency during the second stimulation period (labeled "IIS"). This is due to the fact that the inhomogeneity was not completely cleared from the hippocampus, and therefore the hippocampal network activation due to the formation of network heterogeneity corresponding to this memory was stronger than the simultaneous inhibition received from the cortical network. At the same time the cortical feedback mediated dramatic shortening or abolition of reactivation when the external stimulation ceased.

2.4 Discussion

In this paper we show that distributed network dynamics modulated by local modifications in network structure can play a pivotal role in complex processes of memory management. Specifically, we have demonstrated that structural network heterogeneities created through local modifications of network connectivity can act in two ways depending on the dynamical regime: they effect differential activation of the network in response to the external stimulus, and they can mediate autonomous reactivation of selective network regions. The former phase represents associative memory processes during active exploration of the environment. We have shown that differential activation during stimulation may serve as a novelty/familiarity assessment of the incoming stimulus in the cortical network, which in turn may facilitate self-controlled memory management in the hippocampal-cortical interaction. The latter phase indicates memory reactivation observed during various stages of quiet waking and sleep [88, 134, 22]. The transition from one phase to the other can be self-regulated through adjustment of the global network excitation. In the brain, such regulation is known to exist and is controlled through neuromodulatory processes [62, 76, 160].

By utilizing the structural network underpinnings of the dynamical network response together with cortical feedback we can reproduce the sequential memory management stages that have been observed in the hippocampus. This mechanism is built on several phenomena supported by experimental findings, which we have explored in this paper: discrete activation and reactivation of heterogeneous structures within hippocampal and cortical networks, cortical regulation of linked hippocampal memory structures based on familiarity level, which acts as the basis for novelty discrimination among parallel and concurrent memories, and finally spike-timing dependent plasticity of the hippocampus and cortex which occur on different timescales. We simulate hippocampal and cortical response to both novel and increasingly familiar stimuli and show that, upon repeated exposure, hippocampal reactivation of the memory is lessened due to increased feedback from the cortical memory region.

We have compared the obtained results with the available experimental data. Experimental findings show that the frequency of reactivating neurons in the hippocampus coding familiar stimuli is significantly lower than the reactivation frequency while encoding novel stimuli. Furthermore, the observed progressive theta phase shift in activation of hippocampal CA1 neurons as a function of memory novelty (from in-phase with the hippocampal theta rhythm to in-phase with the theta peaks at the cortical input pathway) indicates a progressive increase in cortical driving, which is observed in our model. This is also consistent with recent research which shows a temporal correlation between cortical and hippocampal replay of consolidated memories, indicating a strong interaction between the two structures during sleep [84]. Neocortical up-down states have been shown to be phase-locked to hippocampal interneurons [67], indicating that this temporal correlation is at least partly due to their excitatory cortical drive, also in support of our model.

The increase in cortical firing rate after consolidation that is predicted in our model (Figure 2.5e) could also be manifested as an increase in the functional connectivity

between the cortex and hippocampus via a strengthening of the TA inputs to CA1. This synaptic weight modification would have additional effect on the dynamics of hippocampal-cortical interactions and the increase in firing rates during reverberation. Thus, whether slow increases in cortical firing increases the TA inputs or LTP of the TA inputs occurs slowly, the net effect on the network activity pattern is the same; increased input strength to the hippocampal inhibitory cells would effectively shut down hippocampal activity after consolidation, probably due to increased activation of the opioid sensitive interneurons in the distal SLM layers [46, 98, 180]. Indeed, the firing rate of hippocampal reactivation is reduced in familiar memory networks (Figure 2.4e), and that shutdown occurs primarily at the phase of theta when the CA1 cells are most depolarized and CA3 inputs should be most capable of causing CA1 cells to fire.

The reduced model presented here is not meant to faithfully reproduce every structural and dynamical aspect observed experimentally but to act as a tool to elucidate the link between structural network modifications and its dynamics during associative network storage processes — in essence, to highlight the role of network processes and dynamics in memory formation. For the sake of visual simplicity, and as a test of proof of principle, we implemented several artificial aspects into our model, such as non-overlapping, localized memory structures. Further preliminary work shows, however, that the qualitative results presented in this paper do not change by implementing distributed, overlapping memories.

We have also not implemented any underlying oscillatory rhythms within our model cortex and hippocampus. The comparison of our results with the phase locking observed in the experimental data is only to highlight the increased role of cortical input during progressing memory consolidation. Furthermore, it is important to note that the cortical feedback itself is excitatory but that, in our model, it targets only inhibitory interneurons of the hippocampal structure. Anatomically it is known that

this excitatory feedback also targets the pyramidal cells [6] and could consequently mediate the phase locking observed in the data.

Clearly, our model makes simplifying assumptions which do not wholly represent the complexity of hipoccampal-cortical processing, but it nonetheless elucidates a possible network dynamical mechanism mediating memory management and opens interesting avenues of further research.

CHAPTER III

Memory storage and recall

3.1 Introduction

The hippocampus is thought to be both the initial store and regulator of episodic memory, with the CA3 region in particular computationally functioning as a content-addressable memory with an ability to both store and complete patterns [102, 144]. Replay during sleep of activity patterns that were experienced during active exploration within the hippocampus plays an important role in memory consolidation, the process of forming hippocampus-independent memory schemas within the cortex [96, 63]. Certain studies have shown that recurrent networks underlying working and short-term memory models allow for focal persistent discharges, representing remembered information, as a result of the network being bistable between a resting state and a persistent memory activation state [5, 148]. This process can be mediated by either slow-changing presynaptic buffer currents [114] or NMDA receptors coupled with inhibition [35].

We've explored previously the interaction of heterogeneous structure in the anatomical connectivity with global top-down signaling to produce three distinct functional states: regime 1 – low-frequency, noisy firing, regime 2 – selective activation of single population subsets reflecting the underlying structural heterogeneities, and regime 3 – global, synchronized bursting behavior [83, 183]. Heterogeneity in the anatomical

structure is created through the addition of random connections to a discrete portion of the network coupled with global inhibition. Additionally, patterns of activity within cortical regions have been shown to exist as functionally discrete circuits [65]. In dealing with complex episodic memories which can comprise many hierarchies of substructure and modular organization of concepts, an important issue in the storage and retrieval process concerns how to deal with representations which are overlapped. Correlation or overlap between patterns tends to degrade the selective retrieval of single memories. As memories share an increasing fraction of neurons, the network quickly loses the ability to activate and selectively replay single memories without also coactivating linked memories. It has been suggested that inhibitory input from the dentate gyrus (DG) via the mossy fiber recruitment of inhibitory interneurons [103] serves as a mechanism for pattern separation within the CA3 [92, 117]. Loss of inhibitory interneurons has been linked to brain disorders such as epilepsy [51] and schizophrenia [14], and inhibitory cells hold significance in spatiotemporal organization involved in binding or memory tasks [31]. Structured inhibition in the form of layer-specific lateral inhibition has been shown to be important to cortical organization [3], and heterogeneity in pyramidal cell inhibition has been demonstrated in the primary olfactory cortex [97]. However, little is known about how specifically different connectivity topologies affect pattern retrieval in various brain states.

Here we examine the network mechanisms controlling both awake activation and sleep reactivation of stored memory patterns and determine processes which promote the quick pattern separation evident in episodic memory retrieval associated with the hippocampus and long-term neocortical memory stores [126]. We have modeled a memory storage and retrieval system loosely based on the functions of the hippocampal CA3 region and associated neocortical memory stores [145]. We focus only on retrieval dynamics in the absence of learning, as a first step in understanding the complex role network topology plays in system dynamics. Memory retrieval was mod-

eled as increased spiking frequency of regional subpopulations of excitatory neurons, akin to attractor states, and storage of memories is denoted by increased density in connectivity patterns between subpopulations of neurons, creating heterogeneities in the network topology. We first examine how memory distribution as well as increased overlap between two memories embedded within an excitatory-inhibitory network degrades single pattern retrieval in the cases of sleep reactivation and awake recall. Then we characterize the abilities of different inhibitory-to-excitatory connection topologies in counteracting this degradation, highlighting the role of inhibitory interneurons in being able to regulate discrete and selective activations of stored memories. Through simple rules of targeted inhibition, networks are able to achieve selective memory replay even when memories are highly associated with each other.

Finally we show that by coupling network excitability to network activity, the network is able to self-regulate its behavioral state and enhance single memory recovery. We explore the role of global excitability self-modulation to bring the network into the memory retrieval state, because as memories become increasing correlated, higher densities of recurrent connections are created which increases the effective excitability of the network and necessitates modulatory mechanisms to bring the network back to optimal working states. This study is not meant to mimic the detailed biological neural correlates of memory recall, but rather is an examination of the capacity of a neural network to regulate its storage and activation capabilities through topological changes and global network monitoring.

3.2 Methods

3.2.1 Network structure and dynamics

The network is composed of two subpopulations, an excitatory subnetwork and an inhibitory subnetwork each composed of a single one-dimensional periodic lattice

of neuronal units, both containing highly recurrent connections (Figure 3.1). The excitatory network is a population of $N_e = 1500$ excitatory neurons with a uniform 0.5% chance of being randomly connected to each other. Excitatory neurons are embedded with two memory structures, each of which are composed of C clusters of size $g = N_M/C$, where N_M is the number of neurons per memory structure to be stored in the network. Neuronal clusters are derived from the concept of cell assemblies [69], which are subpopulations of neurons which can enervate and display persistent coordinated activity (i.e. reverberation) without direct stimulation due to highly recurrent connections within the assembly.

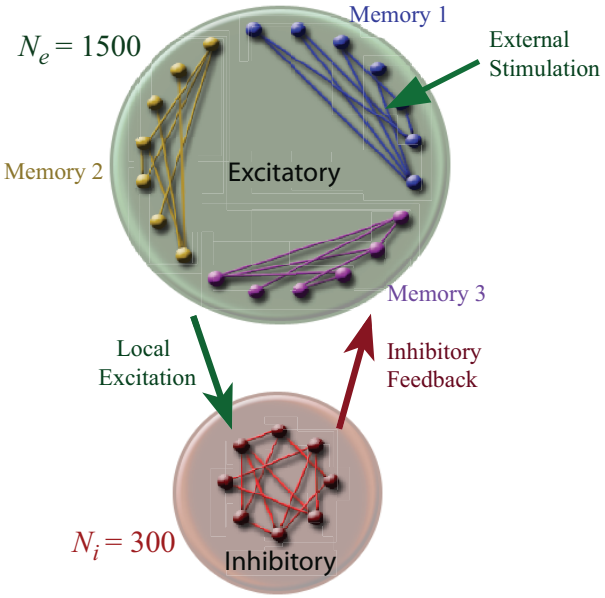

Figure 3.1: Schematic of excitatory-inhibitory network. The network is composed of an excitatory subpopulation and a smaller inhibitory subpopulation enervated locally by the excitatory network, which is itself inhibited with connections from the inhibitory layer. The excitatory network layer is embedded with multiple memory structures in the form of localized increases in connectivity density.

As memory structures become more distributed, the number of neurons in each cluster, g, decreases so that a single memory is stored throughout the network in smaller contiguous clusters rather than being localized. Within each cluster neurons

are coupled in small-world fashion consistent with the Watts-Stogatz model [189], with $p_{ex} = 0.1$, at 8% of maximum connectivity. Clusters are grouped into two subpopulations (memories) composed of N_M neurons by adding additional connections randomly to these subpopulations at 4% of maximum connectivity, $N_M * (N_M - 1)$. These subgroups can be thought of as memory structures formed through long term potentiation (LTP) processes which are known to occur readily during exploration of a novel environment [109, 50, 39, 124]. These additional connections increase the density of interconnectivity within these regions beyond the average global connectivity degree, allowing subgroups of neurons to recurrently innervate and effectively increasing regional excitability. Memory structures are allowed to be both overlapped and distributed (see Figures 3.2 and 3.4b), and assignment of clusters to memories is done in a stochastic fashion. Overlapped memories share neuronal clusters, and the amount of overlap L is defined as the percentage of total number of neurons in a memory structure N_M which are also shared with another memory.

The inhibitory neuronal subnetwork is composed of $N_i = 300$ neurons connected randomly to each other so that each neuron is connected to 30 other neurons ($S_i =$ 10% of maximum connectivity). The excitatory subnetwork is connected to the inhibitory subnetwork in a local fashion, so that each inhibitory neuron receives connections from 15 nearest excitatory neurons ($S_{ei} = 1\%$ of total possible). Three conditions of inhibitory-to-excitatory layer connections were tested to determine effects of inhibitory topology on replay performance (described in Section 3.2.2). The network size ratios and connection densities used were chosen to grossly reflect biological distributions and connectivity patterns in the hippocampus; however, these parameters are easily modifiable without loss of observed dynamical response.

We used leaky-integrate-and-fire neurons given by

$$\tau_m \frac{dV_{i/e}^j}{dt} = -\alpha_j V_{i/e}^j + I_{i/e} + \sum_k w_{jk} I_{syn}^k \tag{3.1}$$

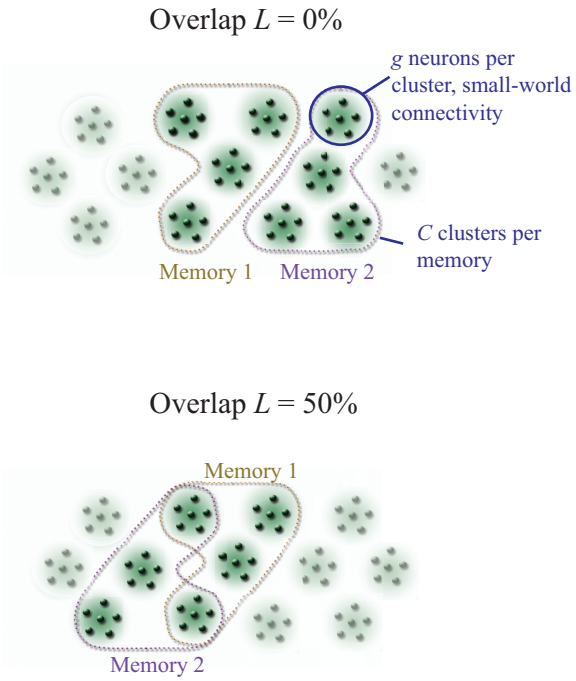

Figure 3.2: Depiction of overlapped memory structures. Example network topologies with 2 memory structures are shown with no overlap (top) and L=50% overlap (bottom). Memory structures are composed of C clusters, which are of size g and connected in small-world fashion with $p = 0.1$ and 8% connectivity density. Neurons within a memory are randomly connected to each other with a 4% probability. Increased overlap between memories occurs when they share increased numbers of clusters.

to represent the reduced dynamics of the network elements. The i/e denotes either an inhibitory or excitatory neuron; $V_{i/e}^{j}$ is the membrane voltage of the j-th neuron; α_j is the membrane leak rate constant randomly distributed such that $\alpha_j \in [1, 1.3]$; $\tau_m = 30$ ms is the membrane time constant; I_{syn}^{k} is the incoming current to the j-th neuron from the k-th neuron; and w^{jk} is the connection strength between neurons j and k. The excitatory subnetwork is connected with connection strengths of $w_e = 2$ and the inhibitory subnetwork with $w_i = 2$; the excitatory-to-inhibitory network connections are of strength $w_{ei} = 4$ and inhibitory-to-excitatory network connections $w_{ie} = 3$. Synaptic strengths were chosen to inversely scale with the number of incoming connections so that total inhibitory current was roughly balanced with excitatory current. The external current $I_{i/e}$ is uniform over the entire inhibitory/excitatory

network. I_i is held constant at 5; I_e is allowed to vary in the range 0-10 and functions as a global modulatory mechanism (control parameter) that controls response transitions from low-frequency random activity, to spontaneous activation of discrete network regions, and finally to global bursting. Biologically, excitability represents the responsiveness of neurons within the network to both recurrent activity and external input. Within a certain range of excitability, regions with high local density of connections activate selectively while suppressing the rest of the network. This is due to the fact that heterogeneities allow for additional synaptic transmission within a localized region, amounting to higher effective excitability. This network architecture promotes regional inhibition driven by focal excitation that creates selective, persistent reactivation patterns. For a detailed description, refer to [83, 183].

When the membrane potential of a given cell assumes a maximum value of $V_t = 1$, the neuron emits an action potential, its membrane potential is reset to $V_{rest} = 0$, and the neuron enters a refractory period for $\tau_{refr} = 10ms$. The synaptic current emitted by spiking neuron k is of the form

$$I^k_{syn}(t) = exp(\frac{-(t - t^k_{spike})}{\tau_s}) - exp(\frac{-(t - t^k_{spike})}{\tau_f}), \tag{3.2}$$

where $(t - t^k_{spike})$ is the time since neuron k last spiked, $\tau_s = 3$ ms is the slow time constant, and $\tau_f = 0.3$ ms is the fast time constant. Aside from the deterministic input drive received from other cells, all neurons have a $p_{fire} = 10^{-3}$ probability of firing spontaneously per millisecond.

To represent input from other cortical regions or external sensory information, neurons within one memory is stimulated with a current I_d. Because memory patterns are already stored, this driving input may represent encountering a familiar object or memory which recalls specific patterns while suppressing others.

3.2.2 Topology of inhibitory-to-excitatory connectivity

The inhibitory network is connected to the excitatory network using one of four connectivity conditions: 1) purely random with connectivity denoted by S_r, 2) purely local with connectivity denoted by S_{ie}, 3) part local and part random inhibition, and 4) local inhibition coupled with additional targeted connections with connectivity denoted by S_a. Connectivities S_{ie} and S_r are calculated as a percentage of the total possible number of inhibitory-to-excitatory connections $N_e * N_i$. Local inhibition consists of lateral suppression of nearby clusters similar to Mexican hat inhibition in visual [116] and other cortical network models [186]. The g excitatory neurons closest to the inhibitory neurons remain active (are not inhibited) while nearby clusters of excitatory neurons which are most likely associated with other memory structures are suppressed. The connection probability between an inhibitory and excitatory cell is represented by a Gaussian of standard deviation $\sigma = g$ excitatory neurons, modified with the center g neurons taken out (see Figure 3.3a), where g is the number of neurons per cluster. Fully random connectivity assigns connections randomly between inhibitory and excitatory cells according to a uniform probability.

Mixed connectivity topologies consist of both local and nonlocal connections. On top of a baseline level of local connectivity $S_{ie} = 10\%$, networks also include either additional random inhibitory-excitatory synapses (at connectivity S_r) or additional targeted synapses (at connectivity S_a) to test for the effect of selective inhibition between memory structures. This feedback inhibition effectively counteracts increased association which exists when two memories are overlapped and thus share neurons. Inhibitory connections are added such that inhibitory neurons associated with each memory structure (locally enervated by excitatory neurons within these memory structures) will synapse randomly onto all other areas of the excitatory network (see Figure 3.3b), so that activation of a single memory will globally suppress the rest of the network and other memories. Reciprocally, excitatory cells of each

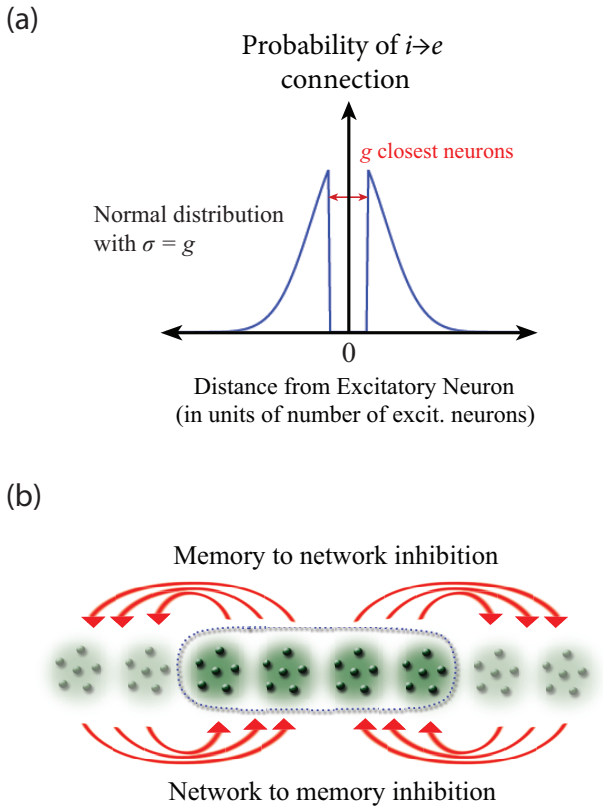

Figure 3.3: Local and targeted inhibitory feedback. A) Formation of inhibitory synaptic connections onto excitatory neurons are determined by a Gaussian probability function with the center g excitatory neurons taken out so that surrounding clusters are suppressed. B) Targeted, additional inhibitory connections are created in the form of random connections from inhibitory neurons associated with (enervated by) a memory structure to the rest of the network as well as connections from inhibitory cells associated with the rest of the network back to the memory structure itself. Amount of targeted inhibition is tuned by the parameter S_a which is the fraction of total inhibitory connections possible between the memory structure and the rest of the network.

memory structure receive the same number of (but not identical) inhibitory connections from non-associated areas of the inhibitory network. This inhibitory pathway aids in the suppression of linked memories when a single memory is more strongly activated than the rest of the network. We test various amounts of added inhibitory connections, $S_a = 0\%$, 2%, 4%, and 6%, where S_a is the percentage of total possible connections between a single memory structure and the rest of the network, where the total number of possible connections is given by $N_M * (N_e - N_M)$.

Comparisons are made between runs which have the same total amount of inhibitory connections, the only difference being the topology of the connections.

3.2.3 Self-modulated excitability

Because the external current $I_{i/e}$ acts as a global modulatory mechanism controlling network activity states ranging from low-frequency noisy firing, to discrete regional activation, and finally to global bursting, we examined if the network could control this parameter to self-tune its state as a response to monitored global activity. The importance of excitatory-to-inhibitory current balance has been shown before in the generation of gamma frequencies [8], neocortical dynamics [68], and signal gating [177]. Biological agents of global modulation could include acetylcholine; the importance of acetylcholine to memory and consolidation has been suggested in numerous studies [73, 132, 72] and evidence exists for diffuse, volume transmission of acetylcholine [41]. In addition, self-regulatory mechanisms, such as homeostatic plasticity, have been shown to be important to memory storage and the stability of recurrent as well as feedforward neural networks [170]. We present a mechanism whereby the number of neurons over threshold is maintained at a set level, determined by the average size of all stored memories. The network determines total number of excitatory neurons N_a with an integrated average activity above a set threshold of activation (8 times noise level), where activity is integrated over the last $w = 20$ ms. The network then dynamically adjusts I_e by either incrementing or decrementing by an amount depending on N_a, so that the excitability I_e at time t is determined by the following equations:

$$I_e(t+1) = \begin{cases} I_e(t) + \alpha * D, & |D| > \xi \\ I_e(t), & \text{otherwise} \end{cases}, \tag{3.3}$$

where $\alpha = 3$ and $D = (N_M - N_a)/N_M$ is the relative difference between the number of neurons per memory and the total number of active neurons N_a, defined as the number of excitatory cells at time t with spiking activity within the last 20 ms greater than 8 times that expected from noise. Formally, $N_a(t) = \sum_n R_n(t)$, where $R_n(t)$ is 1 if $\sum_{i=t-20}^{t} S_{n,i} > 8 * \sum_{i=t-20}^{t} p_{fire}$ and 0 otherwise, where $S_{n,i}$ is 1 if neuron n spikes at time i. $\xi = 0.067$ sets a tolerance for this relative difference so that small differences due to noise do not cause adjustment of excitability. All simulations are run with a time step of 0.1 ms.

3.2.4 Measures

Activity overlap. For a pair of memories u and v, we can define a memory activation overlap $A_{u,v}$ from the activity traces $S_{u/v}(i)$ of the nonoverlapped neurons (belonging to only one memory) in u and v. In other words, $S_{u/v}(i)$ is the summed and binned activity time trace of each memory less the activity contributed by neurons which are common to both memories as well as the baseline noise:

$$A_{u,v} = 2 * (1 - \frac{1}{T} \sum_{i}^{T} \frac{\max_t\{S_u(i), S_v(i)\}}{S_u(i) + S_v(i)}), \text{where} \tag{3.4}$$

$$S_x(i) = \sum_{n \in x, n \notin y}^{N} (s(n,i) - b * p_{fire}), \tag{3.5}$$

for $x, y \in \{u, v\}$. The total number of spikes $s(n,i)$ fired by neuron n at time bin i is calculated with a sliding window of b =20 ms with 50% overlap between successive time bins, and T is the total number of time bins for the simulation.

$A_{u,v}$ has been normalized to a range of [0,1], where 0 denotes minimal overlap between two memories. $A = 0$ would signify that the network activity is entirely due to the activity of one memory, while $A = 1$ denotes that all memories are activating simultaneously at the same amplitude. Activity overlap measure gives us an idea of how exclusively the network is within one attractor state, as it is a measure of the

degree of coactivation of embedded memories. Figure 3.5 presents five simulation runs and depicts how the value A relates to memory co-activation as excitability is increased. The dip in activity overlap is due to the network being in a noise regime at low excitability, giving an activity overlap of 0.4, a value dependent on the noise level p_{fire} and the size of the window used to calculate activity levels. As excitability increases, activity overlap dips drastically for the driven network, and less so for the reactivation cases, until reaching full network bursting in which all memories are co-activated and thus give an A of 1.

Table 3.1: List of key parameters and measures.

Parameter	**Variable**	**Value range**	**Default**
Number of excitatory neurons	N_e	$200 - 2000$	1500
Number of neurons per memory	N_M	$100 - 1000$	750
Number of clusters	C	$5 - 50$	5
Number of neurons per cluster	g	$15 - 150$	150
Ratio of memory size to excitatory network size	f	$0.05 - 0.5$	0.5
Memory overlap	L	$0 - 40\%$	0%
Excitability	I_e	$0 - 10$	n/a
Driving current to one memory	I_d	$0 - 5$	$0, 2$
Local inhibitory-to-excitatory connectivity	S_{ie}	$0 - 16\%$	10%
Random inhibitory-to-excitatory connectivity	S_r	$0 - 16\%$	0%
Targeted inhibitory-to-excitatory connectivity	S_a	$0 - 6\%$	0%
Measure	**Variable**	**Value range**	
Activity overlap	A	$0 - 1$	
Integrated activity overlap	μ	n/a	

Integrated activity overlap. While the overall minimum value of A obtained over the various excitabilities may not drastically change as parameters are varied, the range of excitabilities for which reactivation dynamics is achieved is indicative of the robustness of this state, or the ease with which the network can either enter

or maintain single memory dynamics. Therefore in order to quantify the extent of regime 2 dynamics, we define a measure μ which represents the area of the A versus excitability curve under 0.4, illustrated in Figure 3.6. The higher μ is, the more robust selective memory reactivation is for a particular network configuration. Excitability ranges are chosen so that the network displays both regime 1 and regime 3 dynamics at either end of this range.

3.3 Results

Previous work has highlighted the role of recurrent synaptic connections on reverberating patterns of activity [148], as well as the effect of global neuronal excitability on network states. A recurrent network with regional heterogeneities, or localized increases in connectivity densities, displays three regimes of behavior depending on a global control parameter: excitability I_e [83]. Figure 3.4a illustrates three regimes of behavior as excitability changes from low to high: regime 1 – low-frequency, noisy firing, regime 2 – discrete activation of population subsets, and regime 3 – globally synchronous bursting behavior. We associate regime 2 with memory reactivation during REM, slow-wave sleep, or quiet waking. In the absence of driving, stored memory traces activate spontaneously offline, as has been observed experimentally to happen within the hippocampus during sleep or quiet waking states after previous awake learning [96]. Similar dynamics are observed within the model network; in the absence of external stimulation, activity patterns are able to spontaneously emerge as the population falls into a single attractor state. During active exploration, it's possible to encounter familiar stimuli and preferentially activate the relevant memory pattern in a process of recognition.

As overlapped memories share more and more neurons in common, it becomes increasingly difficult to have one memory activate without causing coactivation of correlated or overlapped memories. At high degrees of pattern overlap, two memories

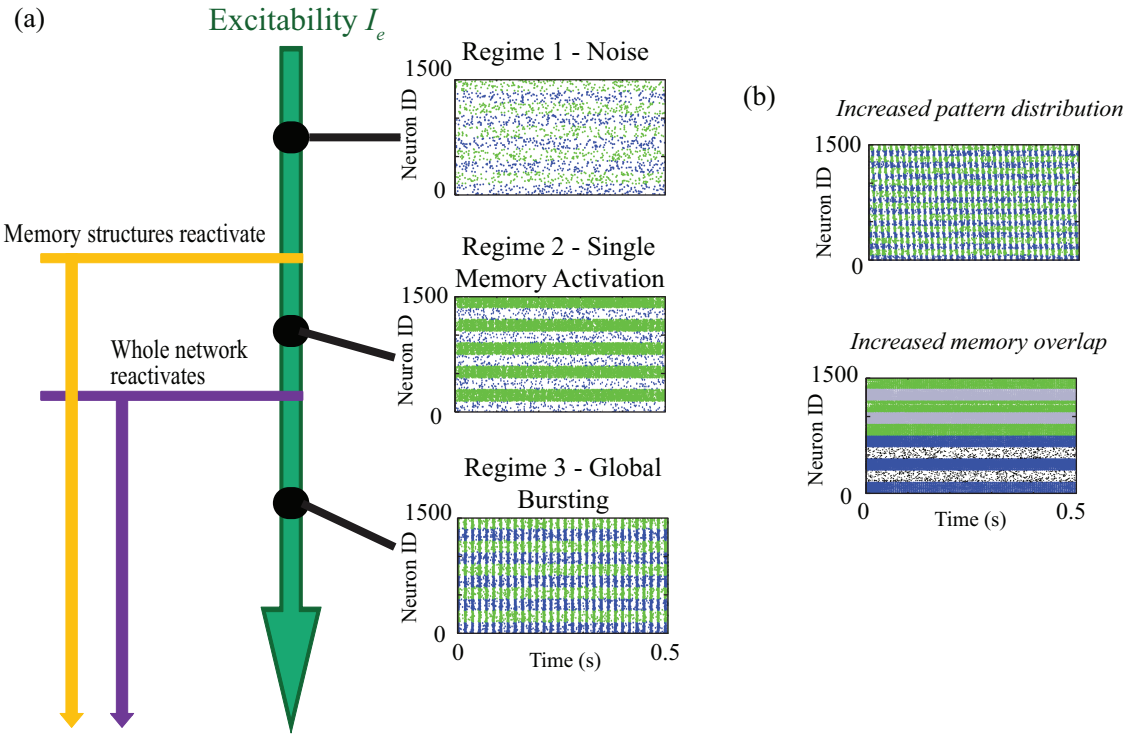

Figure 3.4: Excitability and 3 network regimes. a) Raster plots of the three network regimes – noise (Regime 1), single memory activation (Regime 2), and global bursting (Regime 3) – as a function of increasing excitability I_e. Two memories with $C = 5$ clusters each are embedded in a network with clusters located in alternating fashion for visualization purposes. b) Raster plots of networks for memories stored in $C = 10$ clusters, no overlap (top) and $C = 5$ clusters, $L = 40\%$ overlap (bottom). Green and blue colors represent neurons belonging to memory 1 and memory 2, respectively; gray color represents spiking activity of neurons coding for both patterns. Black dots in raster plot correspond to neurons which aren't encoding either memory.

can be thought of as a single unified concept, at which point activation of both due to stimulation of one could represent the brain's natural ability to recall associated concepts. However, at intermediate levels of overlap, the brain should still be able to distinguish between two concepts and hold one in mind without activating the other. Therefore, a mechanism is needed to suppress activation of the associated memory while allowing full activation of the stimulated memory. Such a mechanism should also help distinguish memories in cases of spontaneous memory reactivation.

In this paper, we implement a simple neural network memory model and explore

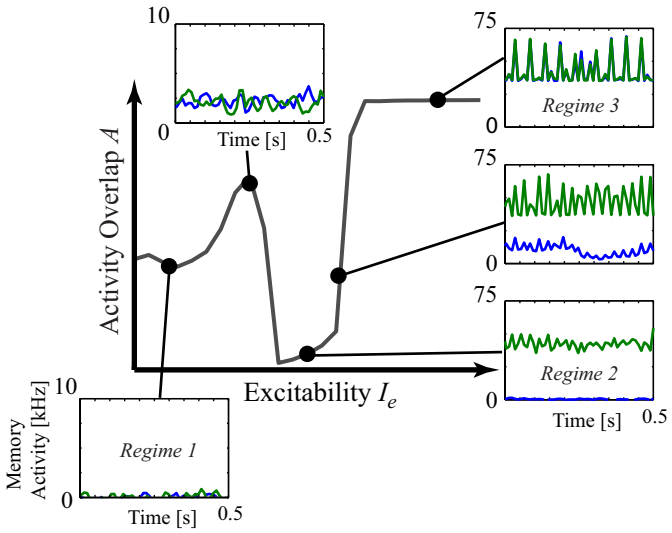

Figure 3.5: Activity overlap displays a characteristic curve as a function of excitability. Insets: Memory activity over time are displayed for characteristic values along the activity overlap curve, showing distinct regimes of activity. Colors correspond to the colors in raster plots.

the limits of the network's ability to manage overlapped and distributed memories (see Figure 3.4b) in both the offline and the active waking state, implementing various inhibitory feedback topologies and examining self-regulating mechanisms to optimize memory reactivation and recognition. We find that the topology of inhibitory feedback is important for maintaining pattern separation and that, further, the network is able to self-regulate its dynamic regime through coarsely monitoring activity. In the waking state, biasing one pattern over another activates inhibitory feedback pathways which suppress the nonstimulated pattern even in cases of higher pattern overlap. In comparison with reactivation, external stimulation of one memory allows for much more robust regime 2 dynamics, as depicted in Figure 3.6. We focused on the case of two memories because it was not the aim of the study to explore capacity but rather how the network can manage increased overlap between pattern representations. We want to understand how the cortex maintains hierarchical knowledge and concepts. Increasing the number of memories to 3 and 4 does not significantly affect the results.

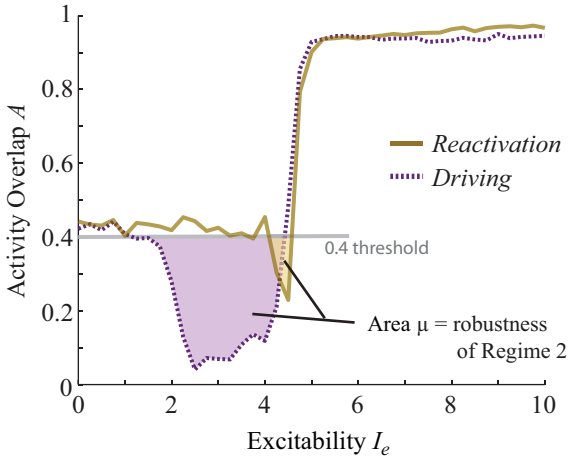

Figure 3.6: Activity overlap for driving and reactivation (no driving). Typical activity overlap curves are shown in the case of reactivation (no external stimulation) and driving of one memory (current $I_d = 2$), with $C = 5$ clusters, overlap $L = 0\%$, and density of inhibitory feedback $S_{ie} = 10\%$. Integrated activity overlap μ quantifies robustness of regime 2 (single memory activation) to variation in excitability I_e.

3.3.1 Interplay between memory storage and inhibitory feedback topology

In characterizing inhibitory feedback topology, we examine various conditions of memory storage, including increased distribution (smaller clusters g or increased number of clusters C) and increased overlap in memory representation (L). Four types of inhibitory feedback are tested: 1) local, modified-Gaussian, 2) random, 3) local combined with random, and 4) local combined with targeted inhibition.

In the case of purely local inhibition, larger clusters tended to promote more single memory activation, as shown in Figure 3.7 in the left column. For very distributed memories ($C = 50$), the activity overlap versus excitability curve displays a prominent rise before descending to the low values of regime 2 dynamics. This is due to a uniform rise in activity level across the whole network (see Figure 3.5) and its inability to fall into an attractor state, or simply remains in a uniform activation attractor state [192]. Such dynamics can be attributed to the diffuse nature of excitatory connections as the number of clusters increases and size of the clusters decreases. As excitatory

connectivity becomes increasingly global due to increased memory distribution, for moderate levels of excitability I_e, current is unable to concentrate within any one discrete area and contributes to a uniform rise in activity, possibility due to the inability of such small clusters to maintain persistent activity [143].

Randomness in inhibitory topology can also induce such dynamics, regardless of the size of clusters (see Figure 3.7, right column). For the random inhibitory feedback case, this peak in activity overlap between regime 1 and regime 2 increases as cluster size decreases, reaffirming the notion that random topology tends to impede the network from falling into global attractor states.

The ability to activate or reactivate a single memory, as quantified by integrated overlap μ, displays different functional relationships with the amount of inhibitory feedback for the two cases, as shown in Figure 3.7c. For local inhibition, as the number of inhibitory connections increases, μ generally increases, representing an increase in robustness of regime 2 (single pattern recovery) dynamics across different levels of excitability. However for highly random topologies, either excitatory ($C = 50$ cell clusters) or inhibitory, as with the random inhibition case, μ begins to fall for higher values of inhibitory-excitatory connectivity, as dynamics are dominated by uniform global increases in activity (see Figure 3.5 for a typical activity time trace) and the range of excitability for which single memories can activate disappears. This effect is especially striking with highly fragmented or distributed memories, $C = 50$, in combination with random inhibitory feedback.

Next we examined the effects of increased overlap between memories in the case of sleep reactivation ($I_d = 0$) and external driving ($I_d = 2$). Without external stimulation, for both local and random inhibition, the network transitions directly from noise to bursting dynamics without displaying single memory activity for all but 0% overlap, as illustrated in Figure 3.8 in the left column. It's clear that as overlap increases, co-activation of stored memories rise sharply, driven by activation of common neurons

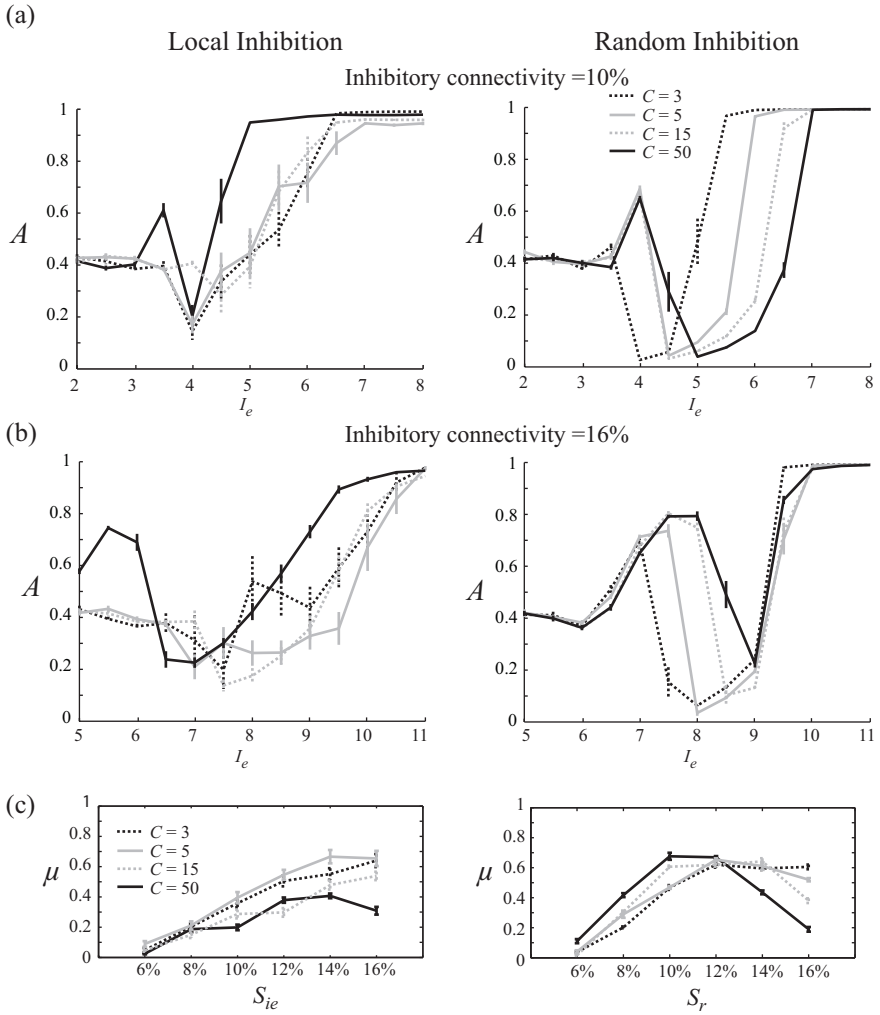

Figure 3.7: Comparison of network performance between local inhibitory-excitatory topology (left) and random, long-range inhibitory-excitatory topology (right). Activity overlap plotted versus excitability for networks with $C = 3$, 5, 15, and 50 clusters in the cases of (a) inhibitory connectivity $S_{ie} = 10\%$ (left), $S_r = 10\%$ (right), and (b) $S_{ie} = 16\%$ (left), $S_r = 16\%$ (right). (c) Plots of integrated activity overlap μ versus S_{ie} and S_r for different C, showing dependence of regime 2 robustness on the strength of inhibition and distribution of patterns stored. Error bars represent standard error of the mean, as for all subsequent figures.

which enervates more than one memory simultaneously. However, with the addition of driving current to one subpopulation of neurons representing stimulation of a single pattern, the network is able to display single memory activation for $L = 20\%$ overlap (see Figure 3.8, right column). In both driven ($I_d = 2$) and nondriven ($I_d = 0$)

cases, as memory patterns become increasingly overlapped, purely random or local inhibitory feedback becomes inadequate to maintain pattern separation, especially in the absence of external driving.

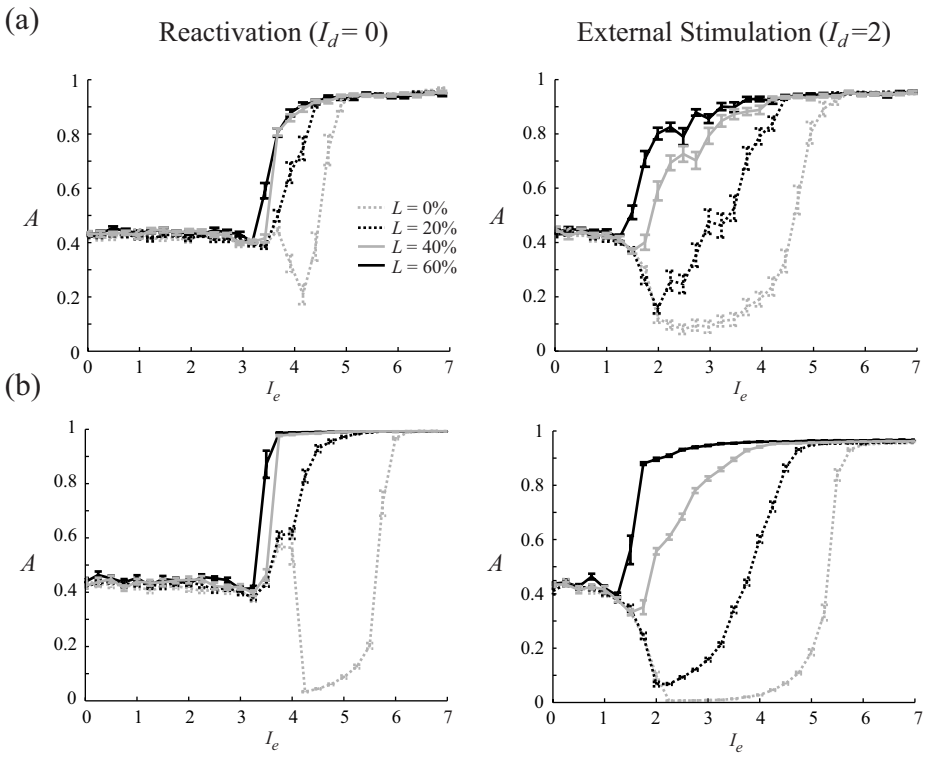

Figure 3.8: Activity overlap plotted versus excitability I_e for different amounts of memory overlap $L = 0\%$, 20%, 40%, and 60% with A) the local inhibitory feedback and B) random inhibitory feedback. Reactivation dynamics are shown in the left column; driving dynamics with $I_d = 2$ shown in the right column. All simulations run with $C = 5$ clusters and inhibitory connectivity $S_{ie/r} = 10\%$.

Therefore we examine more complex connectivities: $S_{ie} = 10\%$ local connectivity combined with $S_r = 6\%$ random, and $S_{ie} = 10\%$ local connectivity combined with $S_a = 6\%$ targeted inhibitory connectivity. As shown in Figure 3.9, targeted inhibition provides the best single memory activation (low A) for all tested ranges of pattern overlap ($L = 0 - 40\%$). In the non-overlapped case, although random inhibition allows for a lower minimum activity overlap A, the large peak between the noise and single memory regime results in a decrease the robustness of regime 2 dynamics. For

the high overlap case, only targeted inhibition combined with baseline local topology is able to recover single memory replay.

Besides the connectivity topology of inhibitory feedback, three other factors determine the range of excitability for which regime 2 dynamics occurs: 1) density of inhibitory feedback connections, 2) amount of overlap between the two memory representations, and 3) amount of external sensory driving. Increased overlap between pattern representations decreases the extent of single memory replay (Figure 3.10a), but increased inhibitory feedback counteracts this effect by creating anti-correlations in memory activation and thus resurrecting or broadening the single memory regime, illustrated in Figure 3.10b. Similarly, increased external driving introduces a bias to one of the memories which allows for more robust single memory activation than during reactivation. However, the ability to separate activation of associated memories is limited in the absence of additional targeted inhibition even with external driving (see Figure 3.10c); a driving current of $I_d = 3$ is required to recover single memory activation with no additional inhibition, but with $S_a = 2\%$ only small driving current is required, while with $S_a = 4\%$ no driving current is needed at all.

3.3.2 Varying size of memories

We next investigated the effect that the size of a memory N_M has on network recall. However, in changing memory size, various other parameters are also affected, such as the fraction of the total network the memory comprises $f = N_M/N_e$ (and subsequently the total size of the excitatory network N_e), the size of individual clusters g, or number of clusters C. Three simulation conditions were run to assess the effects of changing memory size when two parameters are held constant while varying N_M: 1) fraction $f = 0.5$ and cluster size $g = 50$ held constant with varying total network size N_e and cluster number C, 2) $f = 0.5$ and $C = 5$ held constant with varying N_e and g, and 3) $N_e = 2000$ and $g = 50$ held constant with varying f and C. External

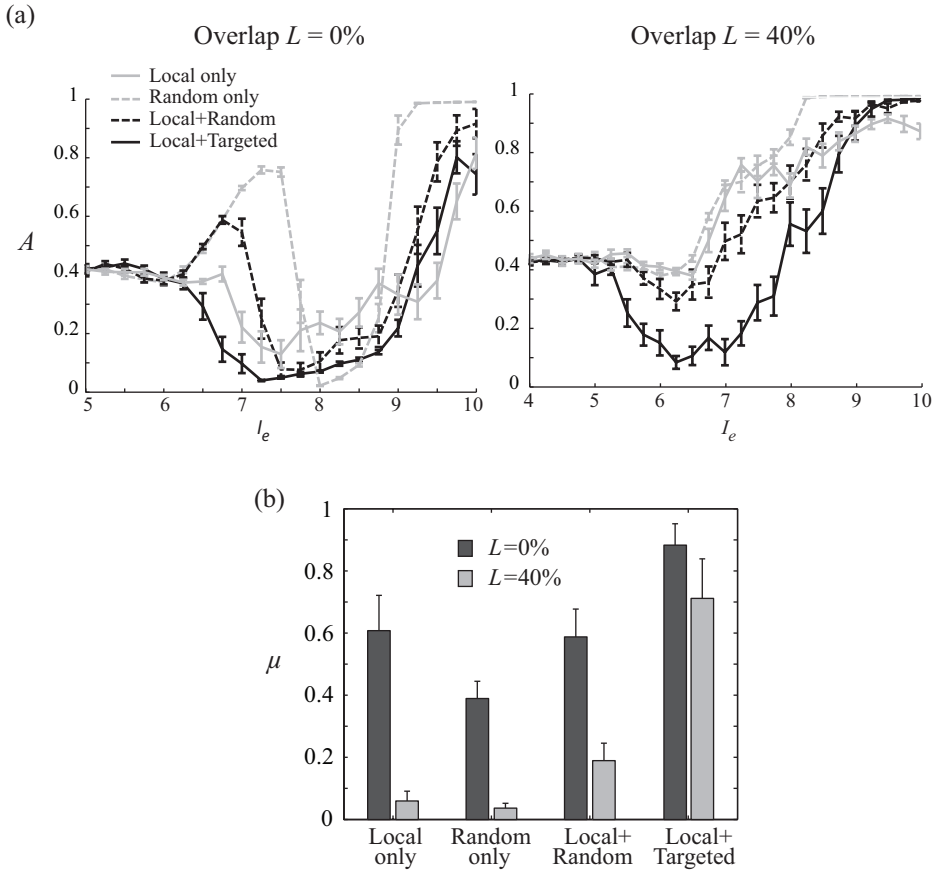

Figure 3.9: (a) Comparison of network performance for four different inhibitory-excitatory connectivity patterns for the reactivation case: 1) local inhibitory connectivity $S_{ie} = 16\%$, 2) random connectivity $S_r = 16\%$, 3) local ($S_{ie} = 10\%$) combined with random ($S_r = 6\%$), and 4) local ($S_{ie} = 10\%$) combined with targeted ($S_a = 6\%$). Left graph is for no overlap, $L = 0\%$, and right graph is with $L = 40\%$ overlap. All four network topologies contain the same number of inhibitory-to-excitatory connections. (b) Integrated activity overlap μ values for each case.

stimulation was held constant for different memory sizes by randomly stimulating 50 neurons in one memory with driving current $I_d = 2$, allowing for the ability to investigate the relative contributions of internally generated activity and external driving on dynamics.

As shown in Figure 3.11a (left), with overlap $L = 0\%$, targeted inhibitory connectivity $S_a = 0\%$, and driving current $I_d = 2$, robustness of single memory activation μ initially decreases with memory size and then rises. This initial decrease is due

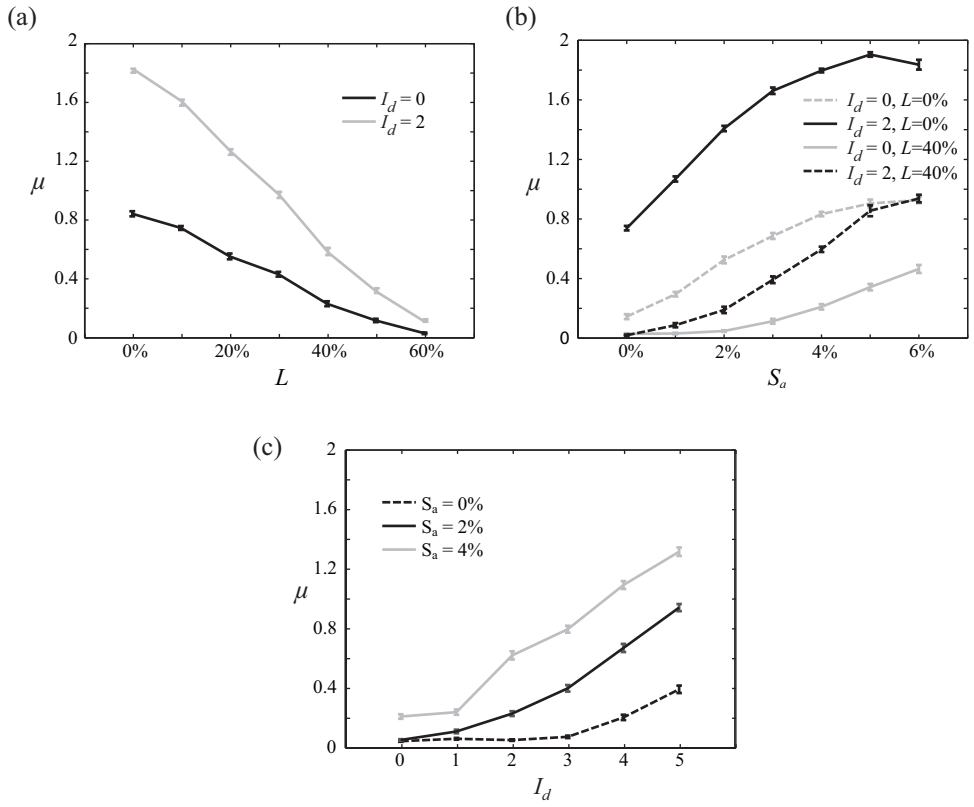

Figure 3.10: Calculation of μ for various parameters to show dependence of regime 2 robustness on (a) overlap L, (b) targeted inhibition S_a, and (c) amount of driving current I_d. Unless being explicitly varied, default parameter values are $S_a = 4\%$, $L = 40\%$, and $C = 10$.

to the fact that for larger memories, the number of stimulated neurons becomes a smaller fraction of the total memory. However, at a certain size, the external stimulation results in generation of self-sustaining internal activity through excitatory feedback loops. This is shown in Figure 3.11a (right), which depicts the mean ratio R of internally generated activity (nondriven neurons) to stimulated activity (driven neurons) when the network is displaying regime 2 dynamics (defined by activity overlap $A < 0.3$). We see that for memories of size $N_M = 500$ and more, all neurons within a memory are able to be activated despite direct stimulation of only a fraction of the memory, signifying pattern completion. For memories of this critical size or larger, the fraction of the network that the memory comprises f significantly affects

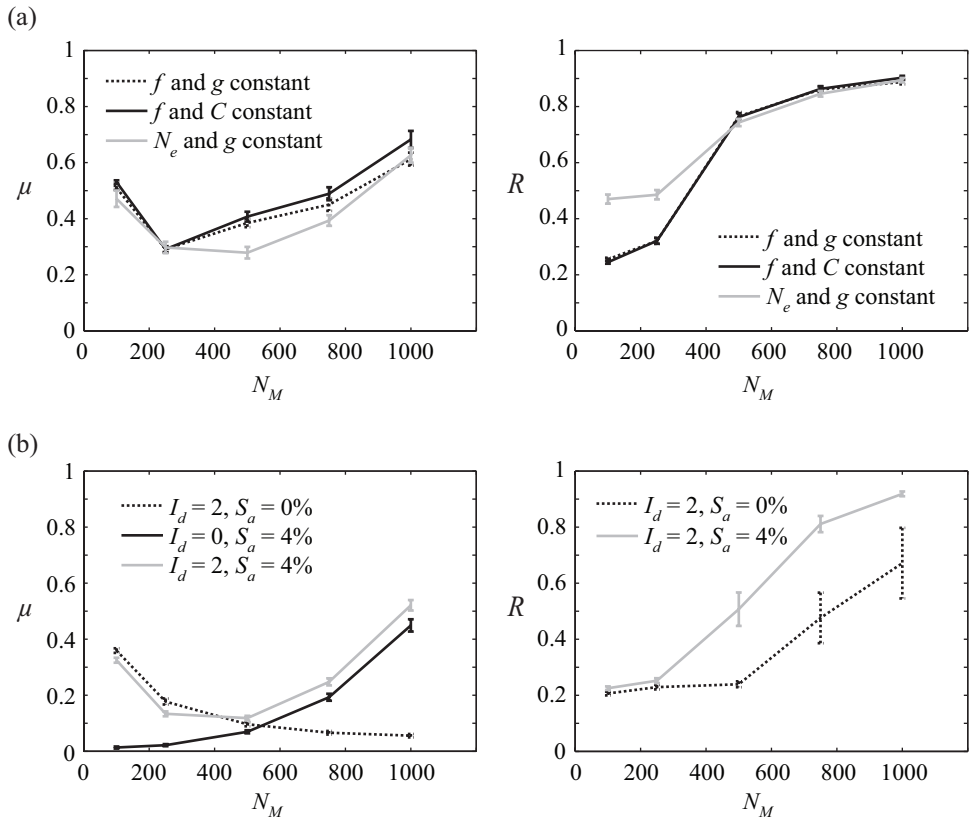

Figure 3.11: Effects of different memory sizes and ratio of memory to total network size on network performance and single memory activation due to partial stimulation. (a) Single memory activation and reactivation as measured by integrated activity overlap μ and ratio of internal activity to stimulated activity R shows different functional dependence on memory size for three cases: constant cluster number $C = 5$ and ratio $f = N_M/N_e = 0.5$, constant cluster size $g = 50$ neurons and $f = 0.5$, and constant $g = 50$ neurons and $N_e = 2000$ neurons. Integrated activity overlap μ (left) and ratio R (right) as a function of memory size N_M for overlap $L = 0\%$, targeted inhibition $S_a = 0\%$, and external current $I_d = 2$. (b) Comparison of effects of external driving and targeted inhibition on μ (left) and R (right) for overlap $L = 40\%$, $f = N_M/N_e = 50\%$, and $g = 50$ neurons per cluster. Driving current is fed to 50 randomly chosen neurons in one memory.

the value of integrated activity overlap μ (light gray solid line versus black solid and dotted lines). Specifically, as the fraction f increases and approaches 0.5, μ rises and approaches the curves corresponding to the constant $f = 0.5$ cases. Low A and high R values correspond to activity where stimulated memories are able to be completed,

but there exists a high degree of coactivation of both memories. For all parameter combinations tested, there is little significant difference between holding the cluster size g constant and holding cluster number C constant, indicating that the overall size of the memory and total network size both contribute more to single memory activation than the distribution or cluster size.

In order to examine the individual effects of external driving and addition of targeted inhibitory connections, we simulated memories overlapped with $L = 40\%$, making up $f = 0.5$ fraction of the excitatory network, and composed of $g = 50$ neurons. As shown in Figure 3.11b, when 50 neurons are driven in the absence of targeted inhibition, single memory activity now decreases as memories get larger (black dotted line) due to coactivation of linked nonstimulated memories. However, in the presence of targeted inhibition but no driving (black solid line), larger memories perform better. When both are combined (light gray solid line), external driving appears to dominate activity for smaller memories, while internally generated activity within a single memory boosted by targeted inhibition is prominent for larger memories (see Figure 3.11b, right). This shows that different mechanisms can contribute to single memory recall or activation, and in varying degrees as a function of memory size and other topological characteristics.

3.3.3 Self-modulated excitability as a mechanism for enhancing single memory replay

Optimal memory recall or replay only occurs for a finite range of excitability values, necessitating a self-regulatory mechanism which the network can employ to quickly achieve single memory activation in a dynamic setting. It is assumed that the network does not know *a priori* which neurons encode for which memories, but is able to coarsely monitor the total number of active neurons and incorporate homeostatic feedback mechanisms to realize a target activity level. These assumptions

are not unreasonable given evidence for the frequency-filtering capabilities of single or small populations of neurons which are able to respond nonlinearly to certain ranges of frequencies [31]. By coupling global excitability I_e to total number of high activity neurons, the network is able to regulate its activity state and recover single memory activation without needing to know beforehand the suitable ranges of excitability. Self-regulation of excitability could represent neuromodulation through various neurotransmitters such as acetylcholine, which has been shown to be responsible for suppressing or enhancing excitatory feedback and thus network responsiveness during memory consolidation processes [72].

Figure 3.12a depicts a single run where the network is able to self-regulate excitability based on total number of high activity cells, and shows quick convergence to single memory activation in the case of $L = 40\%$ overlap and $S_a = 4\%$. Although there exists no *a priori* knowledge of which neurons code for which memories, all neurons of a single memory become activated, corresponding to full pattern recall with suppression of the linked second pattern. For low to moderate ranges of overlap, $0 < L < 40\%$, self-modulation in combination with targeted long-range inhibition is able to recover values of A close to the minimum A values obtained from systematically incrementing excitability (see Figure 3.12b). Similar results are obtained in the presence of external driving (data not shown).

3.4 Discussion

Within a single neural architecture coding for distinct memory representations, increasing levels of commonality and excitatory association between memories leads to increased coactivation. We have highlighted the importance of inhibitory feedback topology in counteracting this coactivation for overlapped and hierarchically stored memory patterns in both cases of sleep reactivation and awake recall. Additionally, we have characterized the impact of memory size on pattern completion as well as

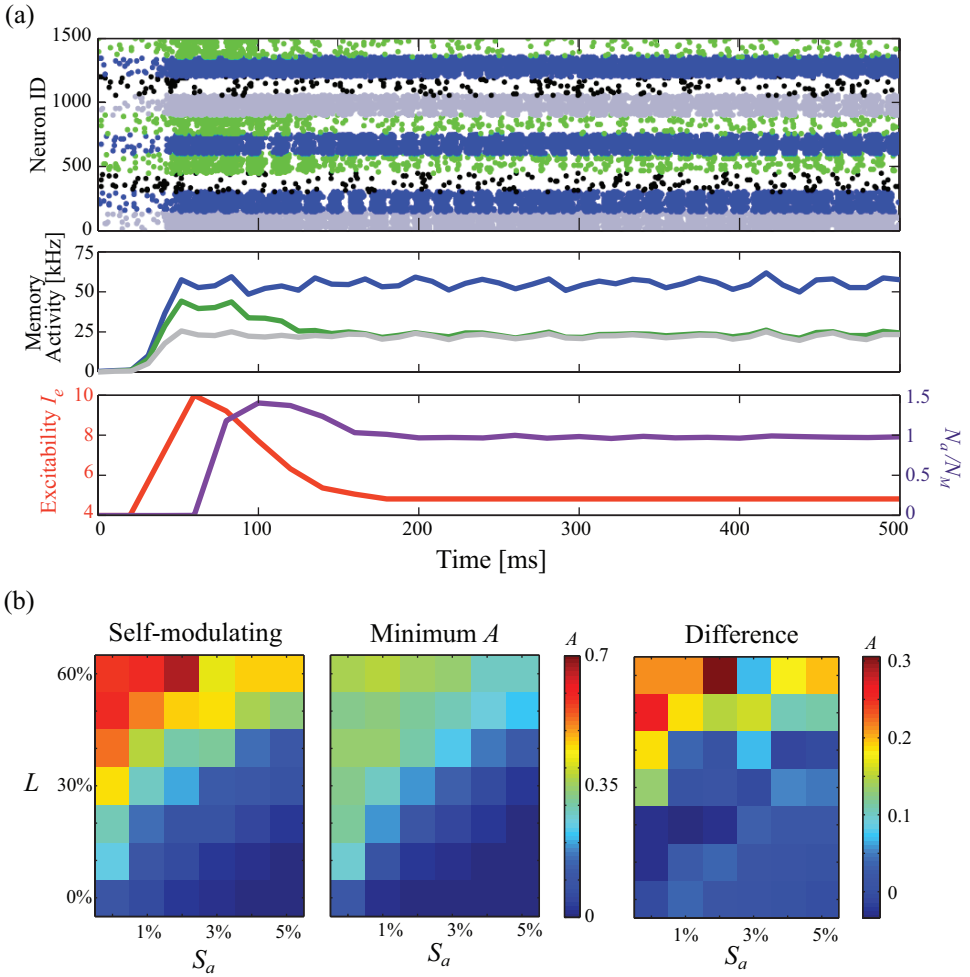

Figure 3.12: Network performance with global self-modulation of excitability. Self-modulation mechanism allows network to tune excitability and dynamically optimize performance. (a) Top: Raster plot showing how self-modulation mechanism brings network into regime 2 state given an arbitrary starting excitability. Middle: Memory activity trace. Color scheme same as in Figure 3.4a. Bottom: Time traces of excitability I_e and the ratio of the number of active neurons N_a to total neurons per memory N_M. $C = 5$, $L = 40\%$, $S_a = 4\%$. (b) Color plots showing activity overlap achieved with the self-modulation mechanism (left) and minimum activity overlap achieved by sweeping through different excitabilities (middle) for various overlap L (0-60%) and targeted inhibitory connectivity S_a (0-5%), $C = 10$. The difference between the two is depicted on the right. All runs are for reactivation ($I_d = 0$).

single memory activation.

We have shown that targeted inhibition is important to maintaining pattern sep-

aration by increasing basins of attraction for single memories, while purely random nontargeted inhibition tends to promote uniform reinjection of current which prevents the network from falling into existing attractor states. We investigated the effects of network architecture on dynamics by studying static states involving memory retrieval independently of subsequent plasticity and information processing. However, it's important to ask how targeted inhibitory connections can be created on the timescale of memory formation in a biological context. The targeted inhibition presented in this paper is simple enough to be implemented via straightforward activity-dependent learning processes because inhibitory feedback is added only between single memories and the rest of the network, with no reference to other existing memories. For instance, upon activation of a subset of neurons due to external sensory stimulation, two simultaneous processes of plasticity are occurring: 1) long-term potentiation of excitatory cells within the active region leading to formation of the memory structure, and 2) potentiation of inhibitory synapses between the active region and the inactive portions of the network, leading to increased mutual inhibition. Structured inhibition is created due to the active memory displaying high frequency mismatch with rest of network, allowing for long-term depression of excitatory cells or potentiation of inhibitory synapses. Through the course of learning multiple memories, preferential strengthening of interneuronal synapses leads to pattern separation of the final embedded memory traces.

We have also observed that external driving results in substantially better single memory activity than with no external input within our model, implying that the existence of bias, whether due to external sensory information or input from other brain regions, is important for accurate and specific memory retrieval. The neocortex tends to store memories in an associated, hierarchical organization, while the hippocampus must be able to maintain distinctions between episodic memories. Does the neocortex play a role in "priming" the hippocampus and leading to increased

pattern separation during replay? Previous findings point to a feedback relationship between the two during sleep [84] and suggest a progression from initial replay of discrete episodes by the hippocampus during slow-wave sleep to more extended replay of distributed memories by the neocortex in REM sleep [90]. Therefore the poorer performance for the "sleep reactivation" condition in our model could be due to the lack of interregional interaction between the hippocampal and cortical areas existent in biological networks.

Network transitions between three dynamical states - 1) noise, 2) single memory replay or activation, and 3) global bursting - are controlled through a global excitability parameter I_e, representing neuromodulatory mechanisms which uniformly affect neurons' probabilities of spiking. The capabilities of a recurrent network to self-regulate its retrieval processes by controlling its network state are studied, using methods of self-inhibition and global monitoring of frequency and rate relationships among subpopulations of neurons. The increased effective excitation introduced into the network due to additional excitatory connections is balanced by additional targeted inhibitory connections. It's postulated that this inhibitory-excitatory balance is important to single memory activation, and the network might institute either global mechanisms of current balance such as with the self-modulated feedback presented in this paper, or more local detailed control through dynamic adjustment of synaptic weights [126]. We only considered global tuning of excitation in the absence of dynamic plasticity in this report. Nevertheless, we are able to observe and characterize complex interactions between both global and spatially patterned sources of excitatory and inhibitory current in the context of pattern recovery. Further studies incorporating learning and plasticity are needed to gain an even fuller understanding of the roles of structure and excitatory-inhibitory current balance in information processing and pattern retrieval.

CHAPTER IV

Network morphology and dynamics in experimental cell cultures

4.1 Introduction

In the previous chapters I've focused on exploring networks theoretically through the use of modeling, showcasing the interrelationships between structural connectivity and the spatiotemporal patterning of neuronal spikes. I next wanted to examine these same relationships in an experimental network. Although it's not possible to recreate an experimental analogue of the learning and memory systems I've discussed so far, it is still possible to characterize certain network properties under different conditions and relate these to a quantification of the dynamics. In this chapter I present work relating the anatomical connectivity found in dissociated cell cultures to the firing dynamics as well as the functional structure which can be inferred from spiking dynamics. Functional structure describes the relationship of temporal correlations in the activity of different dynamic units, which in the field of neuroscience are neurons or brain regions. The pattern of their correlations form a network similar to the underlying anatomical connectivity, but the relationship between the two is far from clear. We therefore aim to explore how gross anatomical properties of *in vitro* hippocampal mixed cultures influence or relate to cell spiking dynamics and

functional network structure.

We examine a reduced system of hippocampal dissociated cell cultures from newborn rats at various time points and in two growth conditions. *In vitro* cultures are artificial in many ways because they're essentially limited to 2-dimensional growth, they're grown in synthetic media, and all preexisting connections are severed before plating. However, cultured neurons still manage to maintain basic neurobiological properties and can sometimes display similar spiking dynamics to *in situ* environments as well as complex spontaneous bursting dynamics [171, 179, 33]. Hippocampal cells are among the most plastic known, and therefore are particularly amenable to culturing and the formation of networks, while still retaining basic biological properties.

The cultures we examine are primary, meaning that the comprising cells come directly from an animal, and mixed, meaning they are a combination of both glial cells and neurons. The hippocampus has two primary types of excitatory neurons, pyramidal and granule, and many types of inhibitory cells, of which the most prevalent are basket cells.

Glial cells are known to support neuronal growth and survival in a variety of ways, including providing nutrients, structural support, neuronal repair, and axonal guidance during development [122]. *In situ*, they are very closely packed with neurons and can interact extensively with them to modulate synaptic transmission and signaling [15, 16, 175]. Due to their close proximity, they are able to uptake or release neurotransmitters within chemical synapses and the extracellular matrix, thereby modulating signal transmission between neurons. The most common type of glial cells are astrocytes, which are capable of displaying sustained and long-range intracellular calcium oscillations which propagate via gap junctions and are sometimes invoked by neuronal activity. These oscillations can in turn elicit calcium changes in neurons, indicating a bidirectional mode of communication with possible repercussions on in-

formation processing [128, 119, 165]. Because calcium is known to be important for LTP and other plasticity processes [99] as well as general neuronal signaling, glial cells are believed to play active roles in computation and self-organization of brain networks.

Because of their vital role in neuronal signaling, we explored the effects of either a high glial growth or a low glial growth condition on neuronal spiking dynamics. We also examined the evolution of morphology and dynamics over time as cultures were allowed to mature. Electrical recordings were conducted by plating and growing cultures on a MEAsetup, with 60 electrode channels which can monitor local electrical activity (see Figure 4.1). Electrodes are spaced 200 μm apart and have a 30 μm diameter, allowing for the detection of action potentials from 1-3 neurons per electrode. Recordings were done at 8, 11, and 13 DIV. Simultaneous cultures from the same animals were plated on gridded dishes and fixed at the same time points for immunocytochemical assay.

We are able to link the morphological evolution of anatomic network structure to changes in spiking dynamics as cultures mature. In particular, we find increasing branching complexity and neuronal process length over DIV, coupled with increasingly global activity and the formation of a single dominant functional cluster. Additionally, changes in glial morphology are also correlated with differences in dynamics. Specifically, low coverage, long, thin, and process-bearing glial cells are linked to more local neuronal communication and fragmented functional clusters, while flat, large glial cells with high coverage of the substrate are linked to global signaling. The results of this chapter have been conducted in collaboration with Sarah Feldt, who conducted the recording and analysis of neuronal dynamics, and submitted for publication with Sarah Feldt, Elizabeth Shtrahman, Rhonda Dzakpasu, Eva Olariu, and Michal Zochowski.

4.2 Experimental methods and protocols

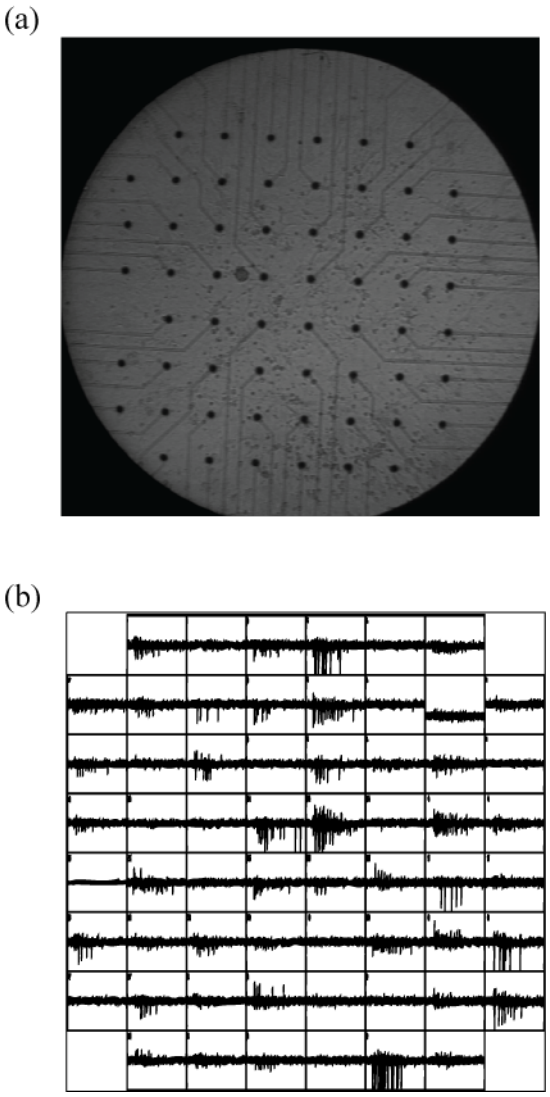

Figure 4.1: Multi-electrode array (MEA) used to record electrical activity of *in vitro* dissociated neuronal cell culture. (a) Example of a culture grown on an MEA showing the spatial layout of the electrodes (black dots). The distance between electrodes is 200 μm. (b) Example of electrical activity recorded on each electrode from a culture displaying bursting dynamics. Each window is 500 ms in length.

4.2.1 Cell culture preparation

Dissociated cell cultures were prepared from neurons (and glia) obtained from the hippocampus of P1 Wistar rats using a protocol modified from [17]. Briefly, hippocampi were first chemically digested in a trypsin solution followed by mechanical titration with a flamed pasteur pipette. Cells were centrifuged and re-suspended in Neurobasal-A Medium supplemented with B-27, 5% heat activated horse serum, 0.5mM L-Glutamine, 0.5mM pen-strep, and 10mM HEPES. The cell density was adjusted by the addition of media such that the density upon plating would be 1400 cells/mm^2.

For electrical recording, the cell suspension was plated on MEAs (Multi Channel Systems, Reutlingen, Germany) which had previously been coated with 0.05% poly-ethylene-imine in borate buffer followed by 20 μg/mL laminin solution in media. Cultures were maintained in a humidified incubator with a 95%O2/5%CO2 saturated atmosphere at 37 °C. For fixation and staining, the cell suspension was plated on culture dishes.

Between 24-36 hours after plating, cultures were split into high and low glial groups. Neurobasal-A media supplemented with horse serum as described above was added to cultures in the high glial group to allow for the proliferation of glial cells, while the media of the low glial group was replaced with Neurobasal-A media that had not been supplemented with horse serum. The sera-free media environment has been shown to inhibit proliferation of glial cells [25]. Following this, half of the media was replaced with the appropriate fresh media once each week.

4.2.2 Cell fixation and fluorescence imaging

Cultures used in staining studies were grown on culture dishes following the same protocol as those used for recordings. The cultures were fixed using 4% paraformalde-hyde in phosphate buffered saline (PBS) for 15 minutes at either 8, 11, or 13 DIV

to correspond to the days of recordings. Crystals of the lipophilic tracer DiI (1,1'-dioctadecyl-3,3,3',3'-tetramethylindocarbocyanine perchlorate, Sigma) were dissolved to a saturated solution in cod liver oil and micro-droplets of the solution were placed on neuronal cell bodies using a picospritzer and micropipette apparatus. The dye was allowed to diffuse through the cell membrane for 5 days, after which the neurons were imaged on an Olympus IX71 inverted fluorescent microscope.

After DiI staining and imaging, cultures were immunolabeled for synapses by standard immunocytochemical techniques. Samples were blocked with blocking solution (5% bovine serum albumin, 5% normal horse serum) for 30 minutes, followed by incubation for 2 hours at room temperature with monoclonal anti-synaptophysin primary antibody (1:200 dilution, Sigma) in blocking solution, and finally incubation for 2 hours at room temperature with fluorescein-conjugated secondary antibody (1:200 dilution, Vector). Colocalization of synapses with neuronal processes was investigated by imaging on a Zeiss LSM 510-META laser-scanning confocal microscope using a 63x water immersion objective.

After imaging, samples were stained for glial cells by permeabilizing (0.3% Triton X-100 in PBS for 20 min) and then blocking (5% BSA, 5% normal goat serum, 0.1% Triton X-100) for 30 minutes, followed by immunolabeling with astrocyte-specific anti-glial fibrillary acidic protein (GFAP) primary antibody (1:100, Sigma) overnight at 4 °C, and finally incubation for 2 hours at room temperature with AMCA-conjugated secondary antibody (1:100, Vector). Cultures were then imaged on a Deltavision-RT fluorescent microscope with a 10x objective.

Immunolabeling of neurons was accomplished by incubation with neuron-specific anti-β-III tubulin antibody (1:200, Millipore) for 2 hours at room temperature, followed by incubation with fluorescein-conjugated secondary antibody (1:200 dilution, Vector) or Cy5-conjugated secondary antibody (1:100, Millipore) for 2 hours at room temperature.

4.2.3 Fluorescent image analysis

To assess process length and complexity, Sholl analysis [152] was performed on the arborization of imaged neurons by counting the number of process crossings with concentric circles of increasing radii centered on the soma. The radius of the circle which encloses half of all crossings (median crossing distance) is then calculated for each neuron. The median crossing distance, total number of crossings, and longest process length was then computed from the distribution of process crossings. For cultures in the high glial group, this analysis was done on N = 9, 11, and 14 neurons for DIV 8, 11, and 13, respectively, and on N = 10, 12, and 13 neurons for DIV 8, 11, and 13, respectively, in the low glial group.

DiI-synaptophysin images were analyzed in ImageJ for synaptic density along neuronal processes. Images were normalized for contrast and each channel was thresholded to distinguish signal from background. The density of synapses was calculated by dividing the number of co-localized areas of synapse and process by the total area encompassed by processes, resulting in the number of synapses per unit area of processes stained by DiI.

GFAP-labeled images were analyzed using ImageJ software to determine the extension of the glial layer over the substrate. Images were thresholded to separate signal from background and the percentage of the image covered in glial cells, P was measured. In order to compare between the different culture conditions, we compute the normalized difference of P between the high and low glial groups denoted as P_H and P_L respectively:

$$D = \frac{[P_H - P_L]}{[P_H + P_L]}. \tag{4.1}$$

4.2.4 MEA recordings and spike detection

Recorded cultures were plated on 60-electrode MEAs which are able to observe local electrical activity due to neuronal spiking. Cultures were recorded at 8, 11, and

13 DIV for N = 5 cultures in the high glial group and N = 4 cultures in the low glial group. For recordings, media was replaced with a recording buffer to maintain the pH of the culture. Cultures were recorded at 25 kHz using a Multi Channel Systems data acquisition card and MC-Rack software. During the recordings, cultures were maintained at 37 °C and each recording lasted 5 minutes.

The local field potential potential recorded from each electrode was assessed for spiking activity and active channels were selected for spike detection. Signals were first filtered through a high pass Butterworth filter at 250 Hz. Spike detection was done using a thresholding method, using 5 standard deviations of the baseline noise as the threshold value. No attempt was made to distinguish between single neurons recorded by the same electrode.

4.2.5 Functional clustering algorithm

Functional clustering was determined from the obtained spike train data using a clustering method developed in our laboratory called the functional clustering algorithm (FCA) [53]. Advantages of using this algorithm include that the clustering is determined directly from the dynamics of the recorded neurons through a comparison to surrogate data, meaning that clustering is based on statistically significant similarities between firing patterns. The use of statistical significance to determine clustering also means that the algorithm has a natural stopping point and no *a priori* knowledge of the number of functional groupings is required. The algorithm is briefly described below; for a complete description of the algorithm, please refer to [53].

The FCA can be summarized in the following 5 steps:

1. Choose a similarity metric and create a matrix of pairwise similarity values between all spike trains.

2. Use surrogate data sets (see below) to calculate 95% confidence intervals for each pairwise similarity. Use this to determine the level of statistical significance for

each pairwise relationship.

3. Choose the pair of trains with the highest significance and group these trains together, recording the significance between the trains. When grouping the two spike trains, create a new train representing the joint activity by merging the spikes into a single train.

4. Remove the trains which were joined from the data set, and recalculate the similarity matrix for the new set of trains. Create new surrogate data sets, and recalculate the pairwise statistical significances.

5. Repeat the joining steps (3 – 4), recording the statistical significance used in each step of the algorithm until no pairwise similarity is statistically significant, indicating that the next joining step is not statistically meaningful. At this point, determine the resultant functional groupings by observing which spike trains have been combined during the algorithm. The results of the clustering algorithm are depicted using a dendrogram where the dashed line denotes the cutoff point of the algorithm.

In order to assess similarities between firing patterns, we used the average minimum distance (AMD) which is a new measure designed to detect synchronous events in discrete event data [53]. To compute the AMD between two spike trains S_i and S_j, we calculate the distance Δt_k^i from each firing event in S_i to the closest firing event in S_j. We then define

$$D_{ij/ji} = \frac{1}{N_{i/j}} \sum_k \Delta t_k^{i/j}, \tag{4.2}$$

where $N_{i/j}$ is the total number of spikes in S_i or S_j, respectively. Finally, we define the AMD to be

$$\Theta_{ij} = \frac{D_{ij} + D_{ji}}{2}. \tag{4.3}$$

Surrogate data sets used in the calculation of significance were created through the addition of jitter to spikes. The jitter is drawn from a uniform distribution over a given window. Here we used a jitter window of 70 ms, centered on each spike. This time scale allows us to examine synchronization at the level of network bursts in the culture.

To asses the level of statistical significance, we used 10,000 surrogate data sets to create cumulative distribution functions (CDF) of AMD values and determine 95% pairwise significance levels. The scaled significance (Figure 4.15) is measured in units defined as the distance from the midpoint of the CDF to the 95% significance cutoff. Thus, a scaled significance greater or equal to 1 is deemed to be statistically significant, while values below 1 are not.

The FCA was applied to the spike train data recorded from cultures in both groups at 8, 11, and 13 DIV. In order to keep the total number of spikes used in the algorithm below 50,000, a 3 minute window of data was used, with the exception of one 13 DIV culture in the low glial group for which a 1 minute time window was used.

4.3 Results

We examine changes in the morphology and dynamics of glial and astrocytic networks over time and in different glial growth conditions. Before a week *in vitro*, there is little spiking activity recorded by electrodes, and after around 14 DIV cultures exhibit globally synchronous bursts interspersed with periods of silence, behavior which does not qualitatively change as cultures get older. In order to examine this transition period from quiescence to spontaneous global bursting, cultures at 8, 11, and 13 DIV are characterized. Changes in neuronal and glial structure are linked to differences in spiking dynamics, and in particular the formation of functional networks and correlated patterning.

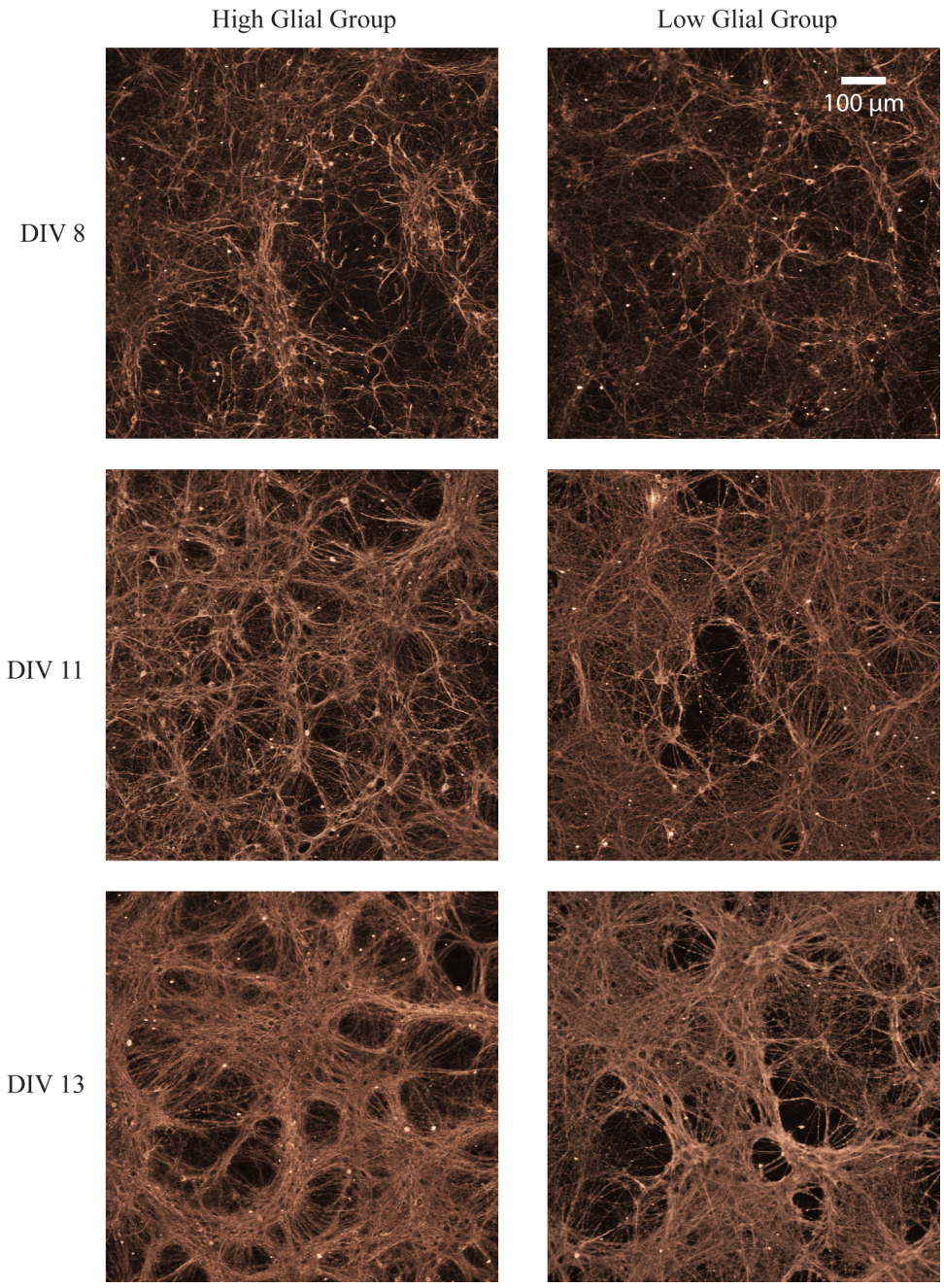

Figure 4.2: Hippocampal neurons in increasing DIV and different glial conditions. Fluorescence image immunolabeled with β-tubulin III primary antibody and fluorescein or cy5 fluorophore.

4.3.1 Global neuronal and glial morphology

Although neurons do not multiply in number over time, they do form extensive processes and connections with other neurons. As shown in Figure 4.2, neurons at

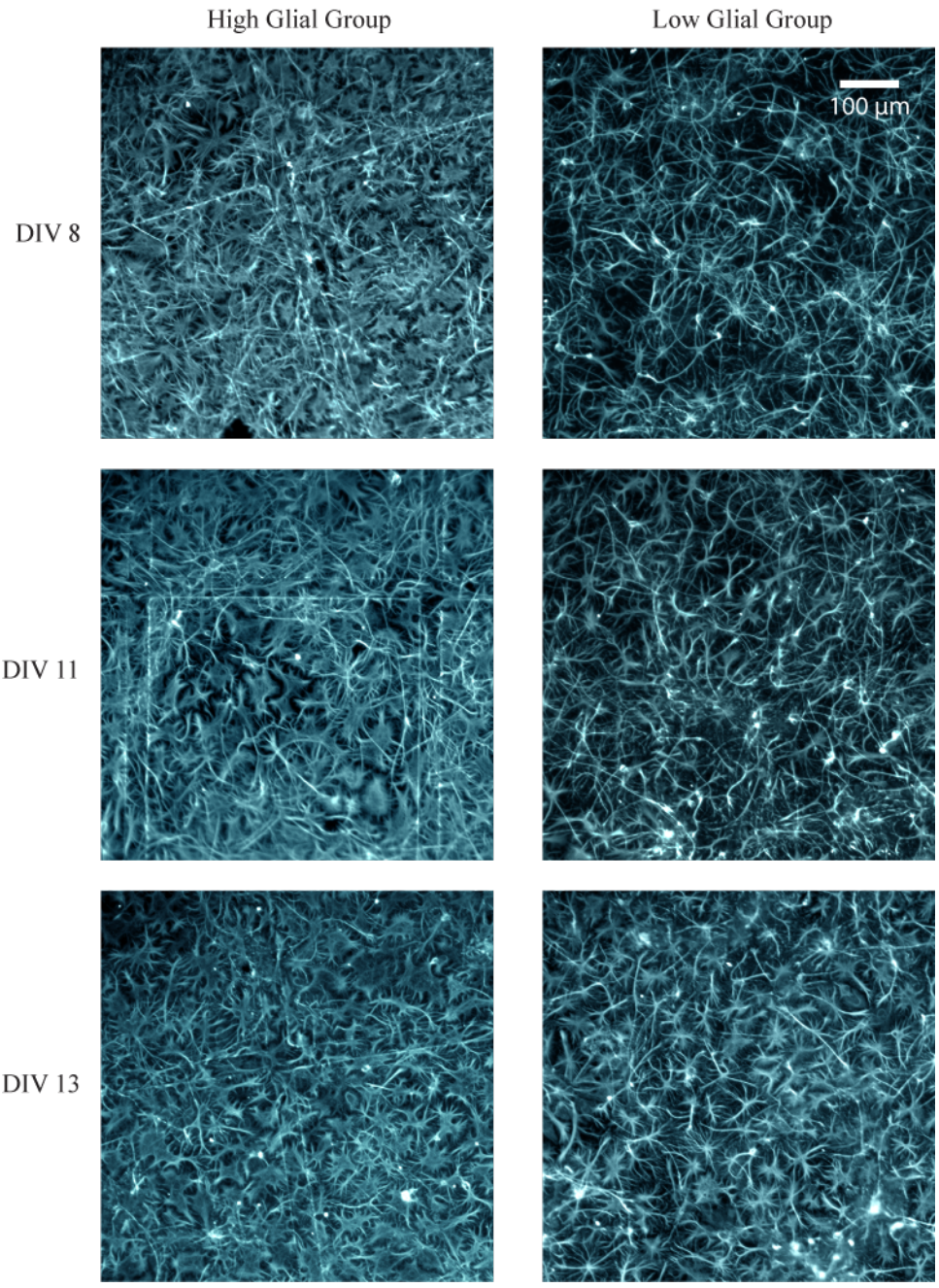

Figure 4.3: Glial cells in increasing DIV and different glial conditions. Fluorescence image immunolabeled with GFAP primary antibody and AMCA fluorophore.

8 DIV display dendritic and axonal processes, but do not appear to be extensively connected with each other. In contrast, by 13 DIV, many processes can be seen, and in fact few neuronal cell bodies can be distinguished due to the thick growth of

processes. There appears to be little difference in neuronal arborization between the two glial growth conditions.

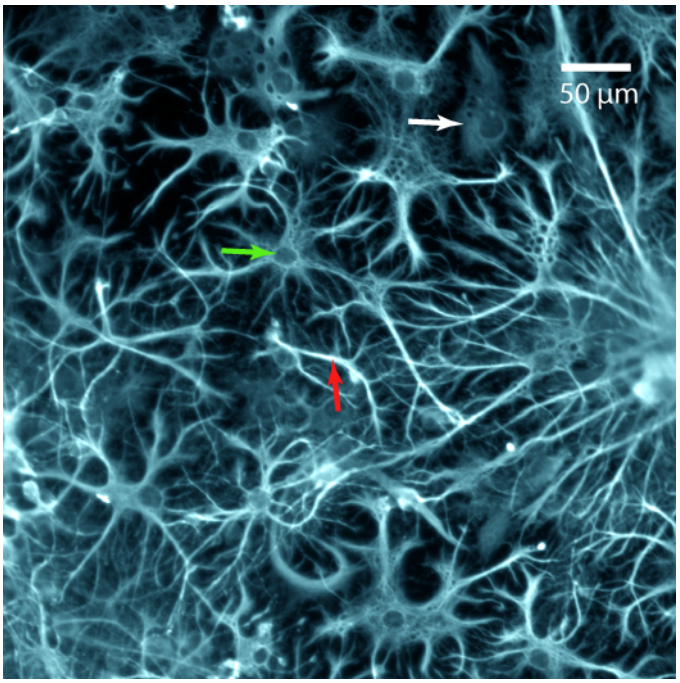

Figure 4.4: Zoomed image of glial cells, in low glial condition. Multiple morphologies of astrocytes are present, including flattened epithelioid cells with few extensive processes (white arrow), glia with a few long, thin processes and distributed in a bipolar arrangement (red arrow), and star-shaped glia with multiple extensive processes (green).

Astrocytes stained with anti-GFAP markers show a marked difference in morphology between the two glial growth conditions, as illustrated in Figure 4.3. It has been shown that neuronal cultures grown in Neurobasal-A medium supplemented with B-27 inhibits the growth and proliferation of glial cells in the absence of supplementary animal serum containing growth factors [25]. The presence of horse serum in the media in the high glial growth condition results in the formation of mostly large, flat cells with no or few short (10-50 μm) processes, typically clearly visible nuclei, and a confluent, very high coverage of the underlying substrate. There is little difference in qualitative morphology of glial cells over the different time points. The low glial group astrocytes, on the other hand, contain mostly thin, long (60-150 μm) processes

which do not cover very much of the substrate for earlier days, but over time appear to either multiply or flatten to cover more of the surface. By day 13, astrocytes in the two growth conditions are qualitatively similar in morphology.

Several different forms of astrocytes can be identified based on overall structure and process features (see Figure 4.4). Flat, large epithelioid astrocytes can be found predominantly in the high glial growth group over all days, while the thin, long processes are characteristic of astrocytes found in young (8 DIV) and low glial growth cultures. A third form midway between the two was also very common, but tended to not be found in younger cultures, consisting of multiple shorter processes and a flatter cell body (see Figure 4.4 green arrow), making them appear star-shaped. This is consistent with that is known biologically, that astrocytes can display many morphological forms and amount of differentiation depending on the presence of various external cues or growth factors [93]. Specifically, the presence of animal serum induces astrocytes within pure glial cultures to take on flat, epithelial shapes with no processes, while removal of this serum causes differentiation of glial cells into multipolar, process-bearing stellate cells which exhibit slow or no proliferation [115, 94].

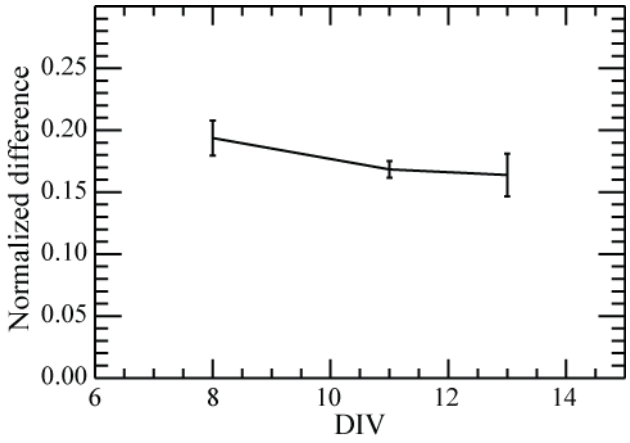

Figure 4.5: Difference in glial cell layer coverage between the high glial group and the low glial group. The fraction of the culture surface covered by astrocytes is calculated for both conditions, and then the difference between HS and SF fractions is divided by the sum to give a normalized difference.

Because of the many overlapping, complex processes, it is difficult to quantify the exact numbers of astrocytes in order to determine if they were in fact more numerous in the high glial growth condition. Nevertheless, a clear difference in morphological structure is evident between the two cases. I quantified this difference by considering the normalized difference in the fraction of the substrate covered by glial cells D (see Methods section). As shown in Figure 4.5, the high glial growth group exhibits more extensive glial cell coverage of the underlying substrate than the low glial group for all time points analyzed, indicating that there are either more glial cells or they are simply larger (or quite possibly a combination of both).

It was also of interest to consider how the neuronal and glial networks were spatially arranged relative to each other. Immunostaining and imaging both glial cells and neurons simultaneously allowed for the visualization of their relative locations. As shown in Figure 4.6(a), while all three morphological forms of glial cells can exist within one culture, their locations are not completely random but affected somewhat by the neuronal network. Larger, flatter epithelioid astrocytes tend to be found where there are fewer neurons, while glia with long, thin processes usually surround clusters of neuronal soma. This is in line with studies which have shown that contact with neurons can determine glial morphology; they remain flat and without processes in absence of neurons, while radial and stellate glial cells predominate in areas with neurons [38]. In addition, Figure 4.6(b) shows that astrocytes and neurons are closely packed when in contact with each other, consistent with what is known about the importance of glial cells to structural support of neuronal networks.

4.3.2 Single neuron structure and connectivity

Due to the high density of neurons and processes, in order to visualize characteristics of dendritic and axonal arborization such as length or branching, it was necessary to selectively label a single, entire neuron separately from those surrounding it. Im-

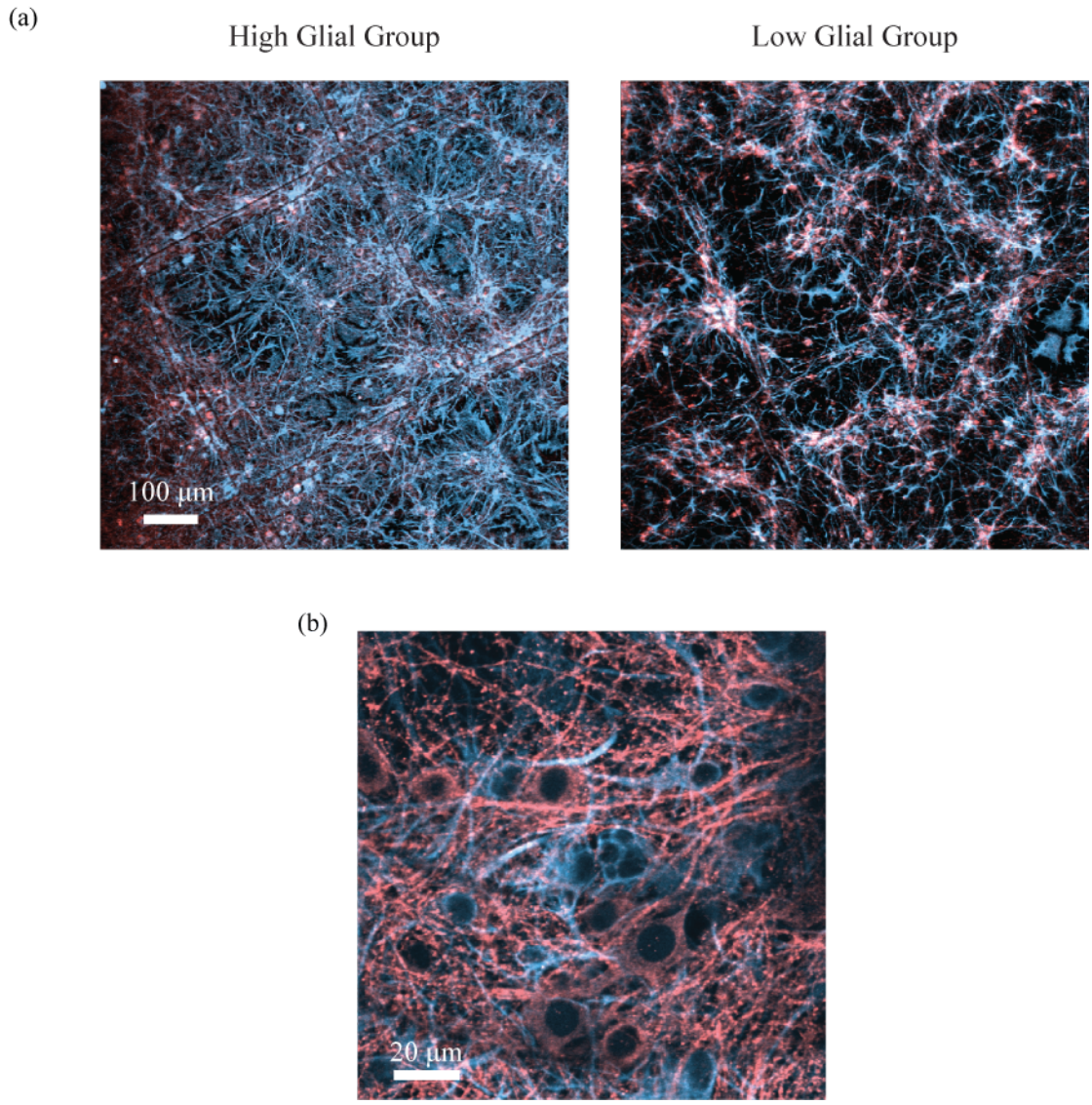

Figure 4.6: Fluorescent overlay of glial and neuronal layers. (a) Glial cells and neurons form a mostly confluent layer for the high glial growth condition, while for the low glial growth condition the glial layer displays low coverage of the underlying substrate. Glial cells not in the vicinity of neurons tend to be flattened and larger than those close to neurons. (b) Confluent layer of neurons and glial cells for the high glial growth condition, zoomed in.

munocytochemical techniques tend to globally label all neurons, so I developed a technique involving the manual application of the lipophilic fluorescent tracer dye DiI to individual soma, which allows the dye to diffuse through the membrane of an entire neuron while leaving surrounding cells unstained. Figure 4.7 depicts a typical

neuron labeled with this process. Large cell bodies (20-50 μm) were picked for labeling under optical microscopy in order to target pyramidal neurons. Cells which displayed processes characteristic of pyramidal neurons were then picked for Sholl analysis, which characterized dendritic and axonal morphology (see Figure 4.7).

Figure 4.8 shows typical DiI-stained neurons over different time points and glial growth conditions. Over time, there is considerably more branching in structure, but no discernible qualitative difference between the high glial and low glial group. A quantification of arborization through Sholl analysis reveals that indeed the two groups do not differ significantly in terms of the complexity of branchings or length of processes, and further that there is a general trend toward longer processes and more branchings as cultures get older (Figure 4.9). However, there is a somewhat significant decrease in process length at 13 DIV for the low glial group, perhaps reflecting a reorganization of dendritic and axonal patterning toward more local connectivity, as opposed to the high glial group which grows more global over time.

Finally, simultaneous imaging of DiI and immunolabeling of synapses allowed for the assessment of synaptic patterning on single neurons through colocalization of the two fluorescence channels. It is found that synapses tend to be relatively uniform in density along the length of processes as well as mostly constant over time (Figure 4.10). This finding, combined with the observation that process complexity increases as cultures mature, indicates that the total number of synapses on a neuron increases over time and in direct proportion with the size of its processes. There is also little difference in synaptic patterning between the two glial groups, although the high glial group tends to exhibit synapses at a slightly higher density at 8 DIV.

4.3.3 Dynamics and functional connectivity

In order to relate the changes in anatomical structure and glial environment with changes in dynamics, the electrical activity recorded at the electrodes at 8, 11, and

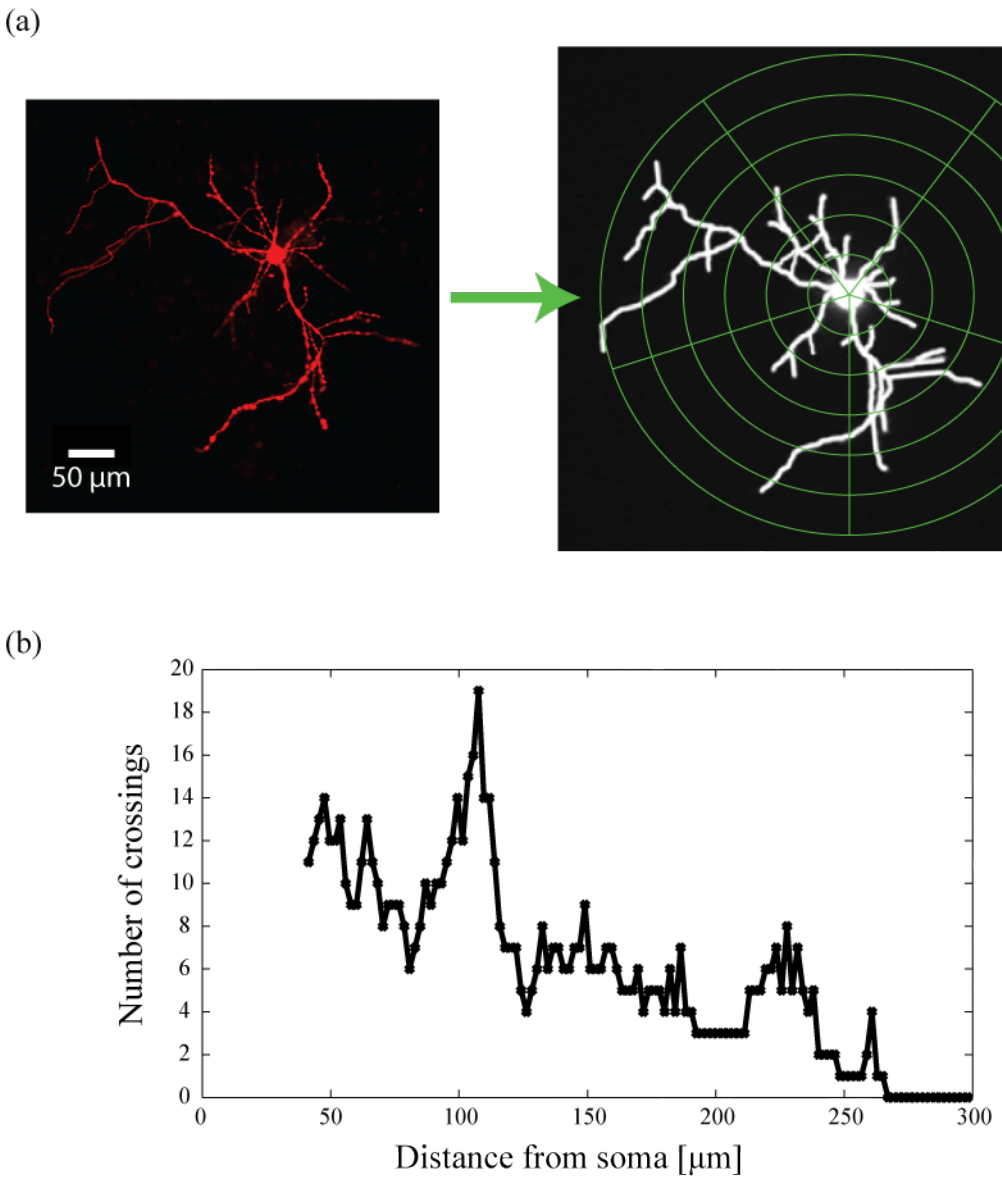

Figure 4.7: Single neuron morphology and Sholl analysis. (a) DiI fluorescence imaging allows visualization of an entire single neuron. Sholl analysis is conducted by drawing concentric rings of increasing size from the center of the soma and counting the number of process crossings at each distance. (b) Plot of the number of process crossings at increasing radial distances from the soma, corresponding to the neuron shown in part (a).

13 DIV for cultures grown on MEAs are analyzed in various ways to determine global and temporal statistics as well as functional connectivity. At 7 DIV, they begin to display spontaneous bursting dynamics characterized by persistent, simultaneous

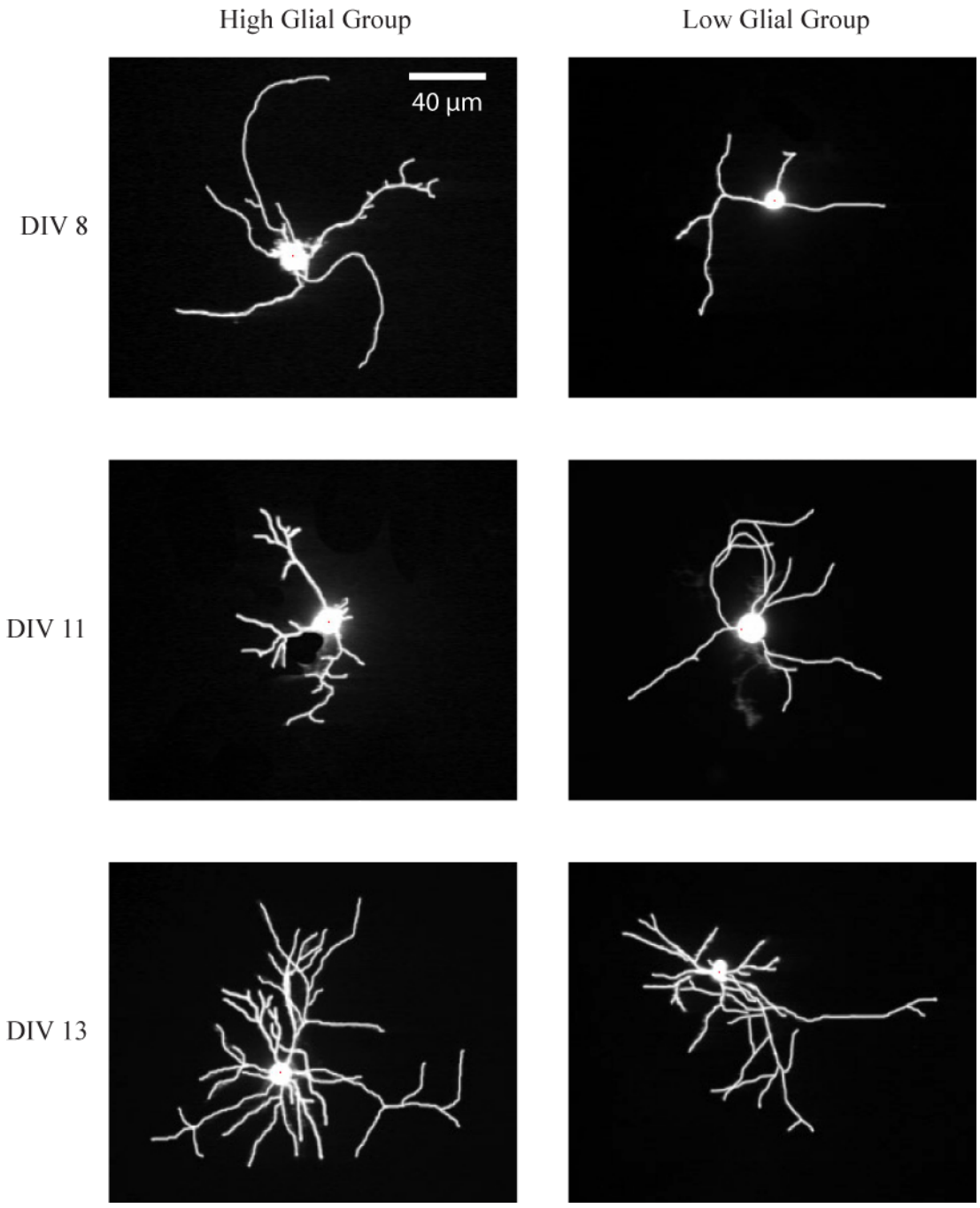

Figure 4.8: Visualization of single neurons in increasing DIV and different glial conditions. Neurons are manually retraced to enhance and normalize contrast for Sholl analysis. The bright spot at the center is not the soma, but rather is a DiI-oil droplet applied to the cell body, which obscures visualization of the soma itself.

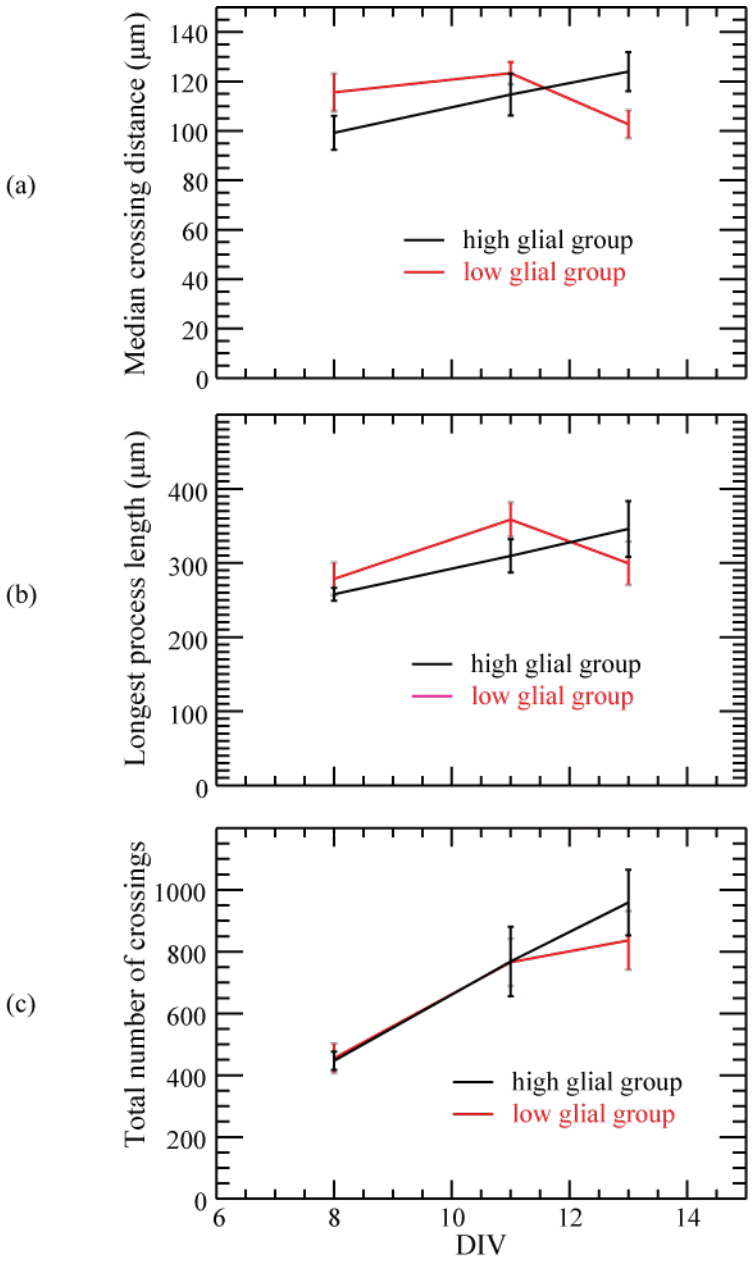

Figure 4.9: Sholl analysis characterizing neuronal process complexity and morphology. Sholl analysis is conducted on DiI-stained neurons by calculating the number of process crossings as a function of radial distance (um) from the soma. (a) The median crossing distance (radius of the circle which encloses half of all crossings), (b) longest process length (radius of the smallest circle which encloses all crossings), and (c)branching complexity (corresponding to the total number of processing crossings) are calculated as a function of DIV.

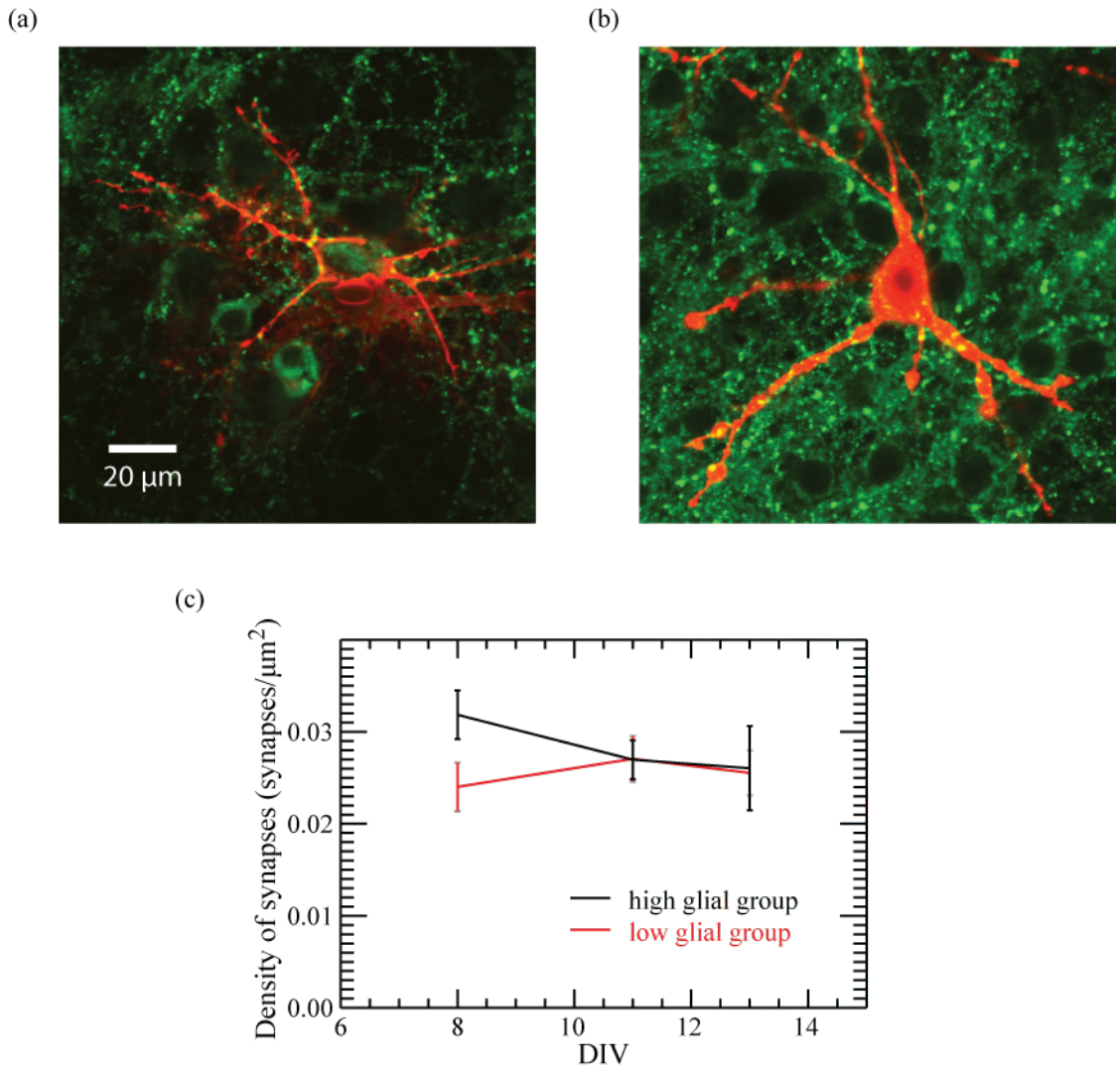

Figure 4.10: Simultaneous imaging of synapses and single neurons to characterize synaptic density. (a, b) Two sample neurons stained with DiI (red) and immunolabeled with synaptophysin-targeted antibody and fluorescein (green). (c) Synaptic density on processes over DIV and for different glial conditions. Synaptic density is calculated by dividing the number of synapses colocalized with DiI-stained neuron and dividing by the total area of the processes.

firing activity over many electrode channels, lasting for hundreds of milliseconds to seconds. Bursting events are interspersed with quiescent periods in which almost all electrodes are inactive (see Figure 4.11(a,b)).

We quantified the evolution of these dynamics by considering the ISI, or time

between spikes, displayed in the different conditions. Cultures grown in the high glial group tended to demonstrate shorter periods of quiescence and therefore a less polarized distribution of ISIs than the low glial group (see Figure 4.11(c)). However, over time, both groups evolved toward markedly different dynamics characterized by changes in their interspike interval distributions. The low glial group especially displayed an increasingly bimodal distribution reflecting global bursts followed by long silent periods.

We next examined the spatial distribution of firing dynamics by considering the number of active electrodes, defined as the number of electrodes from which spikes could be consistently recorded. As shown in Figure 4.12(a), the dynamics of both groups grew increasingly global as cultures matured, indicating the formation of long-range connections and active synapses as processes extended. The high glial group initially bore increased numbers of active electrodes over the low glial group, but the difference became insignificant at 13 DIV. Cultures in both conditions demonstrated increased spiking activity on each active electrode over DIV (Figure 4.12(b)), as is expected as processes grow and networks of synaptic connectivity formed.

The functional connectivity of the cultures was assessed using a clustering algorithm developed in our lab, the functional clustering algorithm [53]. This method specifies a network architecture solely based on correlations in spiking dynamics by clustering electrodes with similar firing patterns. By utilizing comparisons with surrogate data sets, this algorithm is able to functionally separate electrodes into different network clusters with no *a priori* knowledge of the numbers of clusters.

As cultures mature, we see that they become increasingly dominated by a single large functional cluster, although this is much more noticeable with the high glial growth group, corresponding to its primarily global dynamics (Figure 4.13). The dendrograms in Figure 4.13(a, c) are symbolic representations of the steps at which the various electrodes were grouped into one cluster; vertical lines closer to the bottom

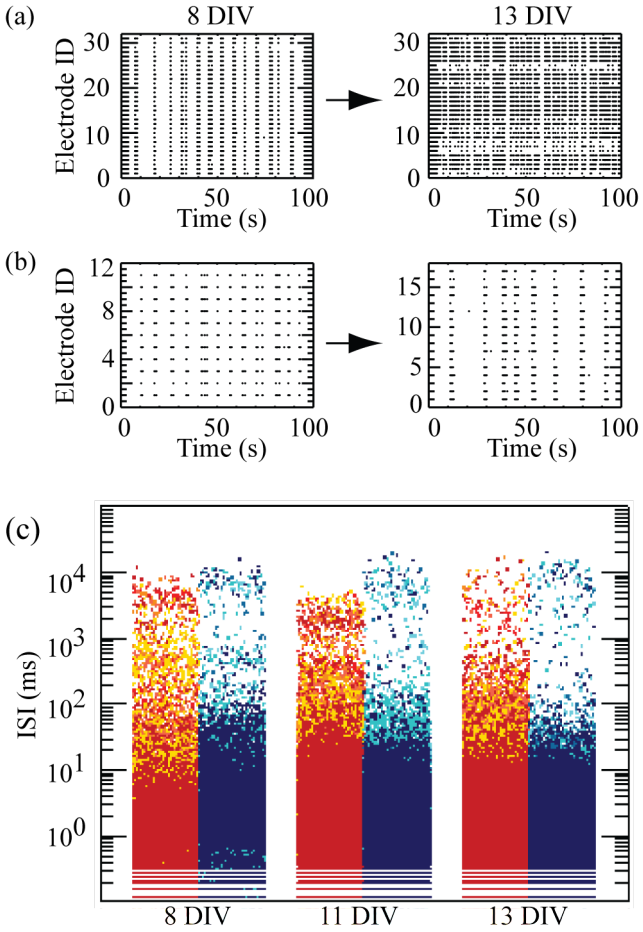

Figure 4.11: Analysis of spiking dynamics over time and glial conditions. (a, b) Example raster plots of spike dynamics over time and in different glial conditions, for the (a) high glial group and (b) low glial group. (c) Histogram of interspike intervals for the high glial group (red shades) and the low glial group (blue shades). Different shades of color represent different trials, and the histograms are smeared horizontally for visualization purposes.

indicate that the electrodes they connect were grouped at an earlier step in the process and are therefore more strongly connected. As shown in Figure 4.14, the largest cluster in both glial groups comprises a significant fraction of the active electrodes, a fraction which increases over time. These results suggest a trend toward increasingly global dynamics as processes extend and connect. However, the low glial group does display more functional clusters over time, suggesting that local organization and dynamics remain important.

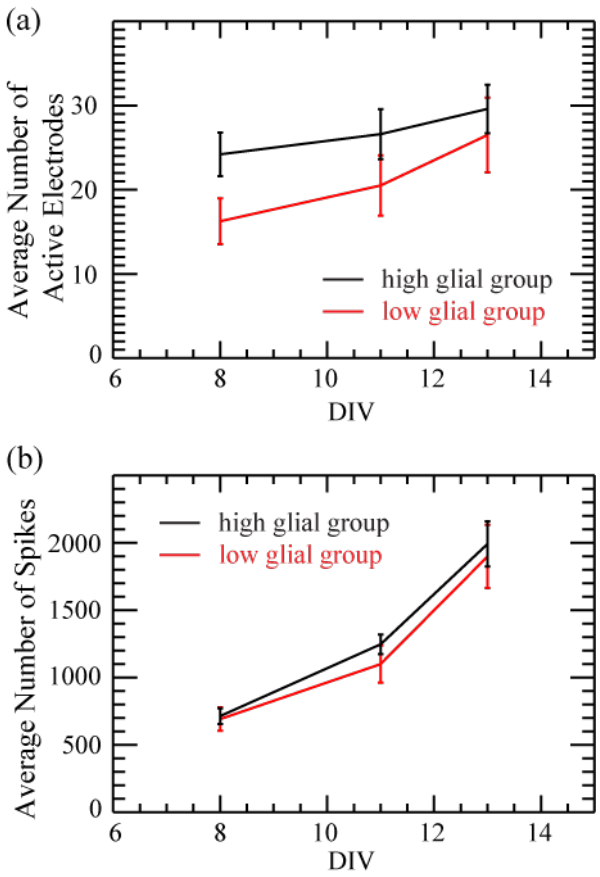

Figure 4.12: Distribution of spiking dynamics over MEA. (a) Average number of active electrodes. (b) Average number of spikes per electrode.

By continuous comparison with a distribution of surrogate data during the joining steps, it was possible to further assess the degree of synchronization between the firing dynamics of various electrodes by examining the scaled significance value (see Section 4.2.5). As shown in Figure 4.15(a), the scaled significance declines as significantly correlated electrodes are joined into functional clusters at each step of the algorithm. Joining stops when the scaled significance falls below a value of 1 (dashed horizontal line). The average of the scaled significance over significant joining steps gives an estimate of the overall level of synchronization within the detected functional clusters. This value increases as cultures age, indicating more synchronized firing dynamics as networks develop and connectivity increases (see Figure 4.15(b)). For later days, the

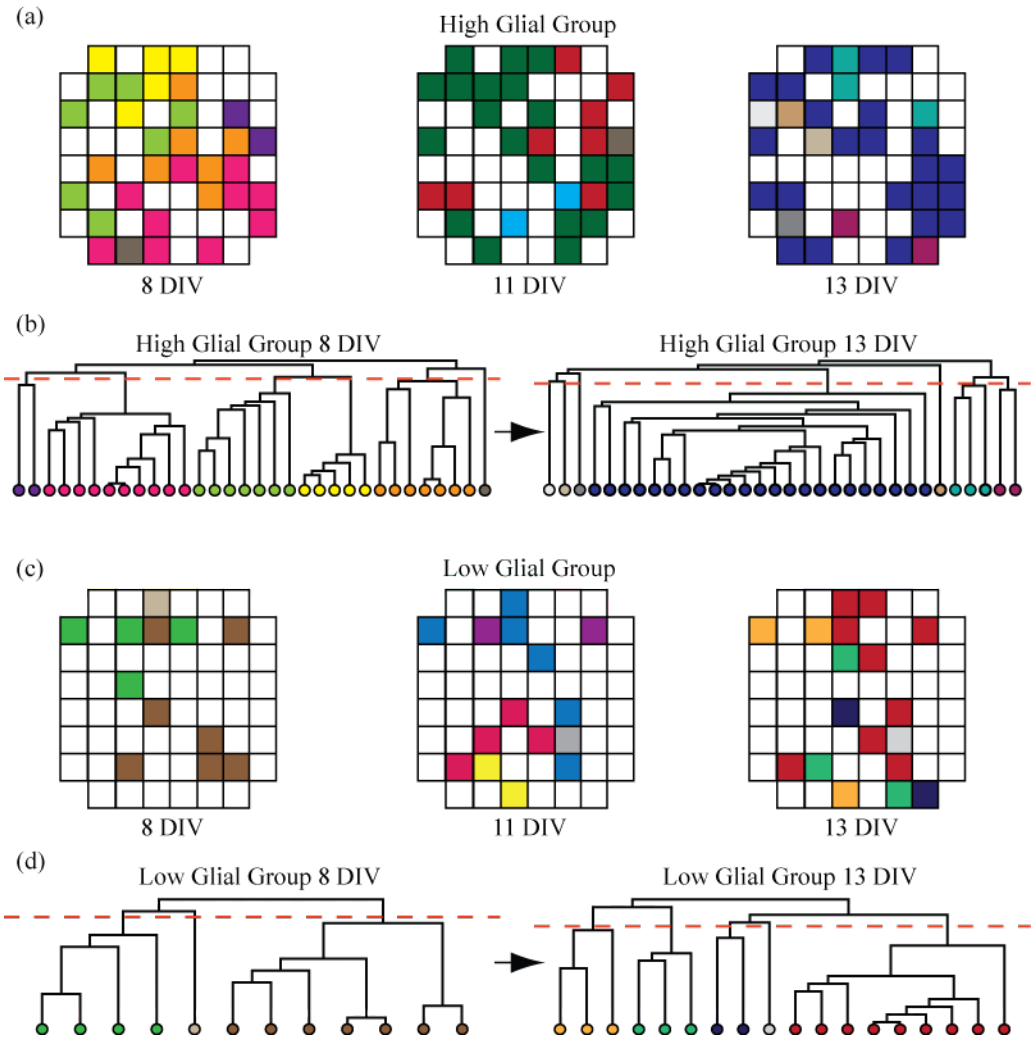

Figure 4.13: Examples of functional groupings obtained from the application of the FCA to culture data. (a,c) Spatial representation of functional clusters. Colored squares indicate active electrodes and squares of the same color belong to the same functional group. (a) High glial group. (c) Low glial group. The clustering becomes increasingly global over time for both glial conditions, but is much more pronounced for the high glial growth group. (b,d) Examples of the dendrogram corresponding to the spatial maps in (a) and (c) at 8 DIV and 13 DIV.

high glial growth cultures display significantly higher average scaled significance than the low glial growth cultures, possibly reflecting the higher level of global signaling implied in the anatomical analyses.

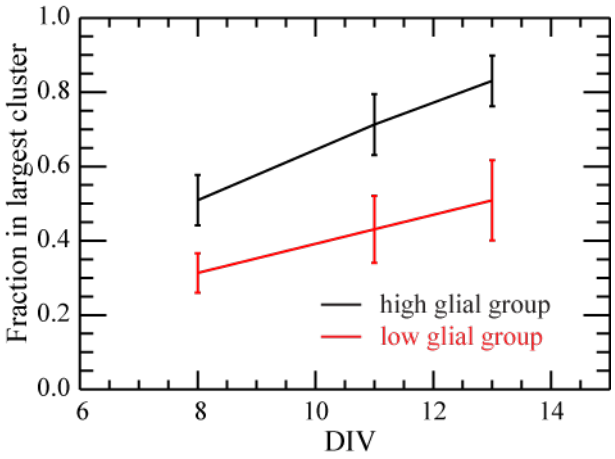

Figure 4.14: Percentage of electrodes participating in the largest functional cluster as a function of DIV. The percentage increases over time for the high glial group indicating the spread of global synchronization. Although we also see an increase in this number for cultures in the the low glial group, the percentage remains smaller, as these groupings remain more fragmented.

4.4 Discussion

We have examined through a reduced experimental neural system how anatomical connectivity is reflected in the functional network structure and spiking dynamics. Although many studies have been conducted examining the spatiotemporal dynamics [146, 171, 179, 33] or morphological structure [32, 130] of *in vitro* neuronal cultures, few have quantified the exact effects of anatomical network structure on firing dynamics. We attempted to elucidate the functional consequences of certain network characteristics and connectivity on spiking behavior, and further have linked the astrocytic network to neuronal dynamics. Beyond being important for neuronal survival, glial cells are known to actively modulate neurotransmission and participate in the creation and propagation of calcium waves [128, 119, 165]. It is evident from our results that changes in the glial network is linked to differences in neuronal signaling.

Morphological characterization of the glial and neuronal networks of dissociated mixed hippocampal cultures indicate a progressive shift toward increased connectivity

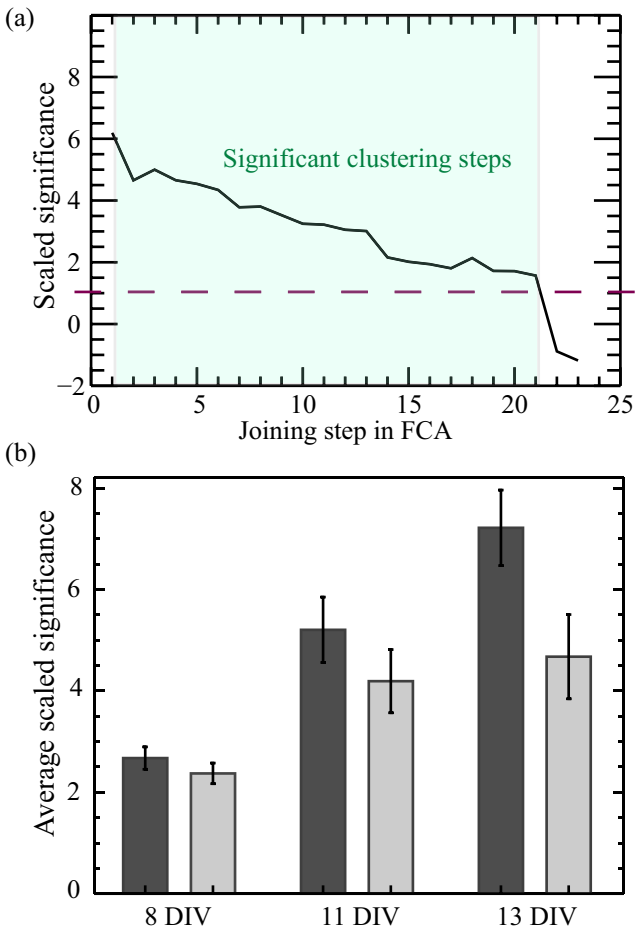

Figure 4.15: Scaled significance during joining steps of the FCA. (a) Example of the scaled significance calculated over joining steps in the FCA, for day 11 cultures from the high glial growth group. (b) The average of the scaled significance over significant joining steps for different DIV and glial growth conditions.

as cultures mature, although local signaling appears to be more prevalent over time for the low glial growth group and global signaling for the high glial growth group. This is paired with findings of functional connectivity which shows the formation of global functional clusters over time, although the low glial group still demonstrates significant fragmentation of dynamics, indicating that networks have self-organized local activity in addition to global structure.

We further find that among the functional clusters, synchronization of firing dynamics increases as cultures age and is generally higher for the high glial growth

condition. Therefore, these networks appear to self-organize over time to form functional clusters which both spatially increase in size to include more electrodes as well as exhibit more coherence in bursting dynamics. This self-organization appears to be aided by more extensive coverage and proliferation of the glial network.

This suggests that changes in the glial network are able to affect neuronal network dynamics. In particular, the existence of large, flat, epithelioid astrocytes promotes global synchronization of activity, while thin, process-bearing astrocytes with slow proliferation is correlated with the formation of localized clusters of activity. Increased localization of activity could explain the longer quiescent periods observed in between bursts, as a decrease in long-range signaling would reduce the occurrence of global spontaneous activity. It is also possible that the difference in culture media (with horse serum versus without) between the two glial conditions directly and fully accounts for the disparities observed in neuronal dynamics. However, while Sholl analysis of single neuronal arborizations showed some differences in process length between the two groups, these differences are not as great as is seen in the glial network. Further, given the established neuromodulatory effect of glial cells on neurotransmission, it's reasonable to assume that changes in both cell groups affect and result in the observed dynamics. Further work will need to be done to assess the exact contributions from each population to shaping firing activity.

CHAPTER V

Summary and significance

With the brain being the most complex structure known, it's not immediately clear exactly what "understanding" it entails. Cataloging every physiological property of every neuron hardly amounts to a deep comprehension of the brain any more than sequencing every gene in the human genome offers complete insight into how the human body functions. This is due to the nontrivial interactions within and between multiple spatiotemporal scales – from the physical workings of ion channels and neurotransmitters which guide the detailed dynamics of single neurons, to the intricate circuitry of neural connections which underlie information processing and learning, and to the highest level inter-regional interactions thought to be responsible for cognition and consciousness. Comprehension at each scale necessitates careful and deliberate methods of simplification and approximation, geared toward condensing the system down to key points of function which contribute to understanding the system as a whole.

In order to understand cognitive processes, which are widely believed to be due to network effects and interactions, I have aimed to investigate the brain at the network level, utilizing computational simulation and reduced experimental preparations as well as network analysis techniques. Due to the dynamic and temporally-evolving nature of neuronal systems, it is possible and enlightening to define a functional

connectivity dependent on the spatiotemporal patterning of activity as well as an anatomical network. How functional structure arises from and is related to anatomical structure is nontrivial and could prove imperative to decoding the language of the brain. This relation is at least in part dependent on global or local neuromodulation which defines different brain states and functional modes. Further, it is bidirectional in that network dynamics can give rise to changes in anatomical connectivity through plasticity mechanisms.

All of these relationships are considered in Chapter II in a simplified two-network model of memory consolidation within the hippocampus and neocortex. Anatomical structure in the form of localized increases in excitatory connectivity density are reflected in the functional connectivity within finite ranges of network excitability, a global modulatory parameter controlling the probability of neuronal firing. These localized heterogeneities, which can be thought of as memory stored due to plasticity, underlie the persistent activation of neurons associated with the memory. When coupled with inhibitory neocortical feedback and two different timescales of plasticity in the hippocampal and neocortical networks, structural heterogeneities can mediate two cognitive roles depending on the excitability regime: 1) familiarity or novelty detection in the presence of direct stimuli in the low excitability regime, and 2) memory consolidation or forgetting in the high excitability regime. Such findings are supported by experimental data which show a shift in input dominance from hippocampal to neocortical drives as familiarity increases [134]. These results predict that both an increasing inhibitory contribution from long-term cortical memory systems as well as distinctly different timescales of plasticity underlie this shift.

I more closely examine the role that heterogeneities play in optimizing memory storage and recall by also considering structured inhibitory feedback topologies in Chapter III. Memories which are overlapped when encoded are able to competitively inhibit each other upon reactivation when excitatory heterogeneities are balanced with

matching structural heterogeneities in the inhibitory feedback connectivity. This detailed balance between excitatory and inhibitory current increases the dynamic range of global excitability levels at which semantic memories and concepts can be recovered, hence improving the robustness of network functioning to different modulatory states. In addition, the network is able to self-regulate this memory recovery state by coupling global neuronal activity patterns to global excitability. The link between anatomical and functional structure is therefore intimately and profoundly influenced by neuromodulatory effects and excitatory-inhibitory current balance.

These same explorations of functional structure are continued in a reduced biological system: *in vitro* dissociated hippocampal cell cultures, discussed in Chapter IV. Although these cultures cannot be said to realistically represent real brain networks, they do retain the same ratios of cells and other neurobiological characteristics of the hippocampus *in vivo*. Most importantly, cells are able to grow processes and connect together to form networks which can be easily visualized and recorded. In this way, morphological parameters and the physical anatomical network structure can be compared to functional connectivity derived from spiking data. It is found that network development and reorganization over time is reflected in spiking dynamics and thus the functional structure. Specifically, as the cultures mature and develop extended processes, bursting dynamics grow more coherent and global. Different glial network conditions additionally modulate functional groupings, with more extensive glial morphology associated with global neuronal signaling and higher synchronization in firing dynamics.

As a whole, these studies aim to understand brain systems from a network perspective, in particular considering the interactions between functional and anatomical connectivity. The research discussed in this dissertation highlights the complex dynamics which can arise as a result of interactions across multiple spatiotemporal scales. Cognitive concepts such as learning and memory are considered in the contexts

of information processing, storage, and recall within simplified neuronal networks. I have illustrated how network dynamics can be modulated by global input or network parameters as well as how network structure can in turn be modified as a result of dynamics through plasticity. Combining these network analytical tools with neurobiological experiment and knowledge could provide new insights into the intricate complexities of brain dynamics and, ultimately, a better understanding of cognitive functioning.

BIBLIOGRAPHY

BIBLIOGRAPHY

[1] L. F. Abbott and S. B. Nelson. Synaptic plasticity: taming the beast. *Nat Neurosci*, 3 Suppl:1178–83, 2000.

[2] S. Achard, R. Salvador, B. Whitcher, J. Suckling, and E. Bullmore. A resilient, low-frequency, small-world human brain functional network with highly connected association cortical hubs. *J Neurosci*, 26(1):63–72, 2006.

[3] H. Adesnik and M. Scanziani. Lateral competition for cortical space by layer-specific horizontal circuits. *Nature*, 464(7292):1155–60, 2010.

[4] P. Alvarez and L. R. Squire. Memory consolidation and the medial temporal lobe: A simple network model. *Proc Natl Acad Sci U S A*, 91(15):7041, 1994.

[5] D. J. Amit and N. Brunel. Model of global spontaneous activity and local structured activity during delay periods in the cerebral cortex. *Cereb Cortex*, 7(3):237–252, 1997.

[6] P. Andersen, R. Morris, D. Amaral, T. Bliss, and J. O'Keefe. *The hippocampus book*. Oxford University Press, Oxford, 2007.

[7] A. Araque, V. Parpura, R. P. Sanzgiri, and P. G. Haydon. Tripartite synapses: glia, the unacknowledged partner. *Trends Neurosci*, 22(5):208–15, 1999.

[8] B. V. Atallah and M. Scanziani. Instantaneous modulation of gamma oscillation frequency by balancing excitation with inhibition. *Neuron*, 62(4):566–577, 2009.

[9] N. Axmacher, M. M. Henseler, O. Jensen, I. Weinreich, C. E. Elger, and J. Fell. Cross-frequency coupling supports multi-item working memory in the human hippocampus. *Proc Natl Acad Sci U S A*, 107(7):3228–33.

[10] C. Babiloni, F. Vecchio, G. Mirabella, M. Buttiglione, F. Sebastiano, A. Picardi, G. Di Gennaro, P. P. Quarato, L. G. Grammaldo, P. Buffo, V. Esposito, M. Manfredi, G. Cantore, and F. Eusebi. Hippocampal, amygdala, and neocortical synchronization of theta rhythms is related to an immediate recall during rey auditory verbal learning test. *Hum Brain Mapp*, 30(7):2077–89, 2009.

[11] A.-L. Barabsi. *Linked : the new science of networks*. Perseus Pub., Cambridge, Mass., 2002.

[12] M. Barahona and L. M. Pecora. Synchronization in small-world systems. *Phys Rev Lett*, 89(5):054101, 2002.

[13] C. C. Bell, V. Z. Han, Y. Sugawara, and K. Grant. Synaptic plasticity in cerebellum-like structure depends on temporal order. *Nature*, 387(6630):278–281, 1997.

[14] F. M. Benes and S. Berretta. Gabaergic interneurons: implications for understanding schizophrenia and bipolar disorder. *Neuropsychopharmacology*, 25(1):1–27, 2001.

[15] P. Bezzi, M. Domercq, S. Vesce, and A. Volterra. Neuron-astrocyte cross-talk during synaptic transmission: physiological and neuropathological implications. *Prog Brain Res*, 132:255–65, 2001.

[16] P. Bezzi and A. Volterra. A neuron-glia signalling network in the active brain. *Curr Opin Neurobiol*, 11(3):387–94, 2001.

[17] G. Q. Bi and M. M. Poo. Synaptic modifications in cultured hippocampal neurons: dependence on spike timing, synaptic strength, and postsynaptic cell type. *J Neurosci*, 18(24):10464–72, 1998.

[18] C. Blakemore and E. A. Tobin. Lateral inhibition between orientation detectors in the cat's visual cortex. *Exp Brain Res*, 15(4):439–40, 1972.

[19] T. V. Bliss and G. L. Collingridge. A synaptic model of memory: long-term potentiation in the hippocampus. *Nature*, 361(6407):31–9, 1993.

[20] T. V. Bliss and T. Lomo. Long-lasting potentiation of synaptic transmission in the dentate area of the anaesthetized rabbit following stimulation of the perforant path. *J Physiol*, 232(2):331–56, 1973.

[21] S. Boccaletti, V. Latora, Y. Moreno, M. Chavez, and D. U. Hwang. Complex networks: Structure and dynamics. *Physics Reports-Review Section of Physics Letters*, 424(4-5):175–308, 2006.

[22] V. Booth and G. R. Poe. Input source and strength influences overall firing phase of model hippocampal ca1 pyramidal cells during theta: Relevance to rem sleep reactivation and memory consolidation. *Hippocampus*, 16(2):161, 2006.

[23] S. L. Bressler. Large-scale cortical networks and cognition. *Brain Res Rev*, 20(3):288–304, 1995.

[24] S. L. Bressler and V. Menon. Large-scale brain networks in cognition: emerging methods and principles. *Trends Cogn Sci.*

[25] G. J. Brewer, J. R. Torricelli, E. K. Evege, and P. J. Price. Optimized survival of hippocampal neurons in b27-supplemented neurobasal, a new serum-free medium combination. *J Neurosci Res*, 35(5):567–76, 1993.

[26] V. H. Brun, K. Ytterbo, R. G. Morris, M. B. Moser, and E. I. Moser. Retrograde amnesia for spatial memory induced by nmda receptor-mediated long-term potentiation. *J Neurosci*, 21(1):356–62, 2001.

[27] N. Brunel and X. J. Wang. Effects of neuromodulation in a cortical network model of object working memory dominated by recurrent inhibition. *J Comput Neurosci*, 11(1):63–85, 2001.

[28] E. Bullmore and O. Sporns. Complex brain networks: graph theoretical analysis of structural and functional systems. *Nat Rev Neurosci*, 10(3):186–98, 2009.

[29] D. V. Buonomano. A learning rule for the emergence of stable dynamics and timing in recurrent networks. *J Neurophysiol*, 94(4):2275–83, 2005.

[30] H. Burianova and C. L. Grady. Common and unique neural activations in autobiographical, episodic, and semantic retrieval. *J Cogn Neurosci*, 19(9):1520–34, 2007.

[31] G. Buzsaki. *Rhythms of the Brain*. Oxford University Press, Oxford, 2006.

[32] A. Caceres, G. A. Banker, and L. Binder. Immunocytochemical localization of tubulin and microtubule-associated protein 2 during the development of hippocampal neurons in culture. *J Neurosci*, 6(3):714–22, 1986.

[33] M. Chiappalone, M. Bove, A. Vato, M. Tedesco, and S. Martinoia. Dissociated cortical networks show spontaneously correlated activity patterns during in vitro development. *Brain Res*, 1093(1):41–53, 2006.

[34] A. Compte. Computational and in vitro studies of persistent activity: Edging towards cellular and synaptic mechanisms of working memory. *Neuroscience*, 139(1):135–51, 2006.

[35] A. Compte, N. Brunel, P. S. Goldman-Rakic, and X.-J. Wang. Synaptic mechanisms and network dynamics underying spatial working memory in a cortical network model. *Cereb Cortex*, 10(9):910–923, 2000.

[36] C. Constantinidis and X. J. Wang. A neural circuit basis for spatial working memory. *Neuroscientist*, 10(6):553–65, 2004.

[37] N. Cowan. *Attention and Memory: An Integrated Framework*. Oxford psychology series. Oxford University Press, New York City, 1995.

[38] S. M. Culican, N. L. Baumrind, M. Yamamoto, and A. L. Pearlman. Cortical radial glia: identification in tissue culture and evidence for their transformation to astrocytes. *J Neurosci*, 10(2):684–92, 1990.

[39] C. D. Davis, F. L. Jones, and B. E. Derrick. Novel environments enhance the induction and maintenance of long-term potentiation in the dentate gyrus. *J Neurosci*, 24(29):6497–6506, 2004.

[40] W. E. DeCoteau, C. Thorn, D. J. Gibson, R. Courtemanche, P. Mitra, Y. Kubota, and A. M. Graybiel. Learning-related coordination of striatal and hippocampal theta rhythms during acquisition of a procedural maze task. *Proc Natl Acad Sci U S A*, 104(13):5644–9, 2007.

[41] L. Descarries and D. Umbriaco. Ultrastructural basis of monoamine and acetylcholine function in cns. *Semin Neurosci*, 7(5):309–318, 1995.

[42] S. Diekelmann, I. Wilhelm, and J. Born. The whats and whens of sleep-dependent memory consolidation. *Sleep Med Rev*, 13(5):309–21, 2009.

[43] J. Dubnau, A. S. Chiang, and T. Tully. Neural substrates of memory: from synapse to system. *J Neurobiol*, 54(1):238–53, 2003.

[44] D. Durstewitz and J. K. Seamans. Beyond bistability: biophysics and temporal dynamics of working memory. *Neuroscience*, 139(1):119–33, 2006.

[45] D. Durstewitz, J. K. Seamans, and T. J. Sejnowski. Neurocomputational models of working memory. *Nat Neurosci*, 3 Suppl:1184–91, 2000.

[46] H. Dvorak-Carbone and E. M. Schuman. Long-term depression of temporoammonic-ca1 hippocampal synaptic transmission. *J Neurophysiol*, 81(3):1036–1044, 1999.

[47] V. M. Eguiluz, D. R. Chialvo, G. A. Cecchi, M. Baliki, and A. V. Apkarian. Scale-free brain functional networks. *Phys Rev Lett*, 94(1):–, 2005.

[48] H. Eichenbaum. Hippocampus: cognitive processes and neural representations that underlie declarative memory. *Neuron*, 44(1):109–20, 2004.

[49] H. Eichenbaum, G. Schoenbaum, B. Young, and M. Bunsey. Functional organization of the hippocampal memory system. *Proc Natl Acad Sci U S A*, 93(24):13500, 1996.

[50] A. D. Ekstrom, J. Meltzer, B. L. McNaughton, and C. A. Barnes. Nmda receptor antagonism blocks experience-dependent expansion of hippocampal "place fields". *Neuron*, 31(4):631–638, 2001.

[51] J. Epsztein, M. Milh, R. I. Bihi, I. Jorquera, Y. Ben-Ari, A. Represa, and V. Crepel. Ongoing epileptiform activity in the post-ischemic hippocampus is associated with a permanent shift of the excitatory-inhibitory synaptic balance in ca3 pyramidal neurons. *J Neurosci*, 26(26):7082–92, 2006.

[52] D. E. Feldman. Timing-based ltp and ltd at vertical inputs to layer ii/iii pyramidal cells in rat barrel cortex. *Neuron*, 27(1):45–56, 2000.

[53] S. Feldt, J. Waddell, V. L. Hetrick, J. D. Berke, and M. Zochowski. Functional clustering algorithm for the analysis of dynamic network data. *Phys Rev E*, 79(5 Pt 2):056104, 2009.

[54] R. Fitzhugh. Impulses and physiological states in theoretical models of nerve membrane. *Biophys J*, 1(6):445–66, 1961.

[55] N. J. Fortin, K. L. Agster, and H. B. Eichenbaum. Critical role of the hippocampus in memory for sequences of events. *Nat Neurosci*, 5(5):458–62, 2002.

[56] L. Fortuna, M. Frasca, M. La Rosa, and A. Spata. Dynamics of neuron populations in noisy environments. *Chaos*, 15(1):14102, 2005.

[57] P. W. Frankland and B. Bontempi. The organization of recent and remote memories. *Nat Rev Neurosci*, 6(2):119–130, 2005.

[58] U. Frey and R. G. Morris. Synaptic tagging and long-term potentiation. *Nature*, 385(6616):533–6, 1997.

[59] W. N. Frost, G. A. Clark, and E. R. Kandel. Parallel processing of short-term memory for sensitization in aplysia. *J Neurobiol*, 19(4):297–334, 1988.

[60] S. Funahashi, C. J. Bruce, and P. S. Goldman-Rakic. Mnemonic coding of visual space in the monkeys dorsolateral prefrontal cortex. *J Neurophysiol*, 61(2):331–349, 1989.

[61] J. M. Fuster. Behavioral electrophysiology of the prefrontal cortex of the primate. *Prog Brain Res*, 85:313–324, 1990.

[62] S. Gais and J. Born. Low acetylcholine during slow-wave sleep is critical for declarative memory consolidation. *Proc Natl Acad Sci U S A*, 101(7):2140–2144, 2004.

[63] S. Gais, B. Lucas, and J. Born. Sleep after learning aids memory recall. *Learn Mem*, 13(3):259–262, 2006.

[64] E. M. Galloway, N. H. Woo, and B. Lu. Persistent neural activity in the prefrontal cortex: A mechanism by which bdnf regulates working memory? *Prog Brain Res*, 169:251–266, 2008.

[65] M. Garagnani, Y. Shtyrov, and F. Pulvermller. Effects of attention on what is known and what is not: Meg evidence for functionally discrete memory circuits. *Front Hum Neurosci*, 3(10):1–12, 2009.

[66] P. S. Goldman-Rakic. Cellular basis of working memory. *Neuron*, 14(3):477–85, 1995.

[67] T. T. Hahn, B. Sakmann, and M. R. Mehta. Phase-locking of hippocampal interneurons' membrane potential to neocortical up-down states. *Nat Neurosci*, 9(11):1359–61, 2006.

[68] B. Haider and D. A. McCormick. Rapid neocortical dynamics: cellular and network mechanisms. *Neuron*, 62(2):171–189, 2009.

[69] K. D. Harris. Neural signatures of cell assembly organization. *Nat Rev Neurosci*, 6(5):399–407, 2005.

[70] R. M. Harris-Warrick and E. Marder. Modulation of neural networks for behavior. *Annu Rev Neurosci*, 14:39–57, 1991.

[71] M. E. Hasselmo. Neuromodulation and cortical function: modeling the physiological basis of behavior. *Behav Brain Res*, 67(1):1–27, 1995.

[72] M. E. Hasselmo. Neuromodulation: Acetylcholine and memory consolidation. *Trends Cogn Sci*, 3(9):351–359, 1999.

[73] M. E. Hasselmo and J. M. Bower. Cholinergic suppression specific to intrinsic not afferent fiber synapses in rat piriform (olfactory) cortex. *J Neurophysiol*, 67(5):1222–1238, 1992.

[74] M. E. Hasselmo, M. P. Brandon, M. Yoshida, L. M. Giocomo, J. G. Heys, E. Fransen, E. L. Newman, and E. A. Zilli. A phase code for memory could arise from circuit mechanisms in entorhinal cortex. *Neural Netw*, 22(8):1129–38, 2009.

[75] M. E. Hasselmo, E. Schnell, and E. Barkai. Dynamics of learning and recall at excitatory recurrent synapses and cholinergic modulation in rat hippocampal region ca3. *J Neurosci*, 15(7 Pt 2):5249–62, 1995.

[76] M. E. Hasselmo, B. P. Wyble, and G. V. Wallenstein. Encoding and retrieval of episodic memories: role of cholinergic and gabaergic modulation in the hippocampus. *Hippocampus*, 6(6):693–708, 1996.

[77] D. O. Hebb. *The Organization of Behavior*. Wiley, New York, 1949.

[78] J. L. Hindmarsh and R. M. Rose. A model of neuronal bursting using three coupled first order differential equations. *Proc R Soc Lond B Biol Sci*, 221(1222):87–102, 1984.

[79] A. L. Hodgkin and A. F. Huxley. A quantitative description of membrane current and its application to conduction and excitation in nerve. *J Physiol*, 117(4):500–44, 1952.

[80] J. J. Hopfield. Neural networks and physical systems with emergent collective computational abilities. *Proc Natl Acad Sci U S A*, 79(8):2554–8, 1982.

[81] R. J. Hussain and D. O. Carpenter. Development of synaptic responses and plasticity at the sc-ca1 and mf-ca3 synapses in rat hippocampus. *Cell Mol Neurobiol*, 21(4):357–368, 2001.

[82] J. T. R. Isaac, R. A. Nicoll, and R. C. Malenka. Evidence for silent synapses: Implications for the expression of ltp. *Neuron*, 15(2):427–434, 1995.

[83] P. Jablonski, G. R. Poe, and M. Zochowski. Structural network heterogeneities and network dynamics: A possible dynamical mechanism for hippocampal memory reactivation. *Phys Rev E*, 75(1):011912, 2007.

[84] D. Ji and M. A. Wilson. Coordinated memory replay in the visual cortex and hippocampus during sleep. *Nat Neurosci*, 10(1):100–107, 2007.

[85] A. Kamondi, L. Acsady, X. J. Wang, and G. Buzsaki. Theta oscillations in somata and dendrites of hippocampal pyramidal cells in vivo: activity-dependent phase-precession of action potentials. *Hippocampus*, 8(3):244–61, 1998.

[86] E. R. Kandel, J. H. Schwartz, and T. M. Jessell. *Princles of Neural Science*. McGraw-Hill, 4 edition, 2000.

[87] M. P. Kilgard and M. M. Merzenich. Cortical map reorganization enabled by nucleus basalis activity. *Science*, 279(5357):1714–8, 1998.

[88] J. J. Kim and M. S. Fanselow. Modality-specific retrograde amnesia of fear. *Science*, 256(5057):675–677, 1992.

[89] P. Lavenex and D. G. Amaral. Hippocampal-neocortical interaction: a hierarchy of associativity. *Hippocampus*, 10(4):420–430, 2000.

[90] A. K. Lee and M. A. Wilson. Memory of sequential experience in the hippocampus during slow wave sleep. *Neuron*, 36(6):1183–1194, 2002.

[91] M. Lengyel, J. Kwang, O. Paulsen, and P. Dayan. Matching storage and recall: hippocampal spike timing-dependent plasticity and phase response curves. *Nat Neurosci*, 8(12):1677–1683, 2005.

[92] J. K. Leutgeb, S. Leutgeb, M.-B. Moser, and E. I. Moser. Pattern separation in the dentate gyrus and ca3 of the hippocampus. *Science*, 315(5814):961–966, 2007.

[93] R. Lim, K. Mitsunobu, and W. K. Li. Maturation-stimulation effect of brain extract and dibutyryl cyclic amp on dissociated embryonic brain cells in culture. *Exp Cell Res*, 79(1):243–6, 1973.

[94] R. M. Lindsay, P. C. Barber, M. R. Sherwood, J. Zimmer, and G. Raisman. Astrocyte cultures from adult rat brain. derivation, characterization and neurotrophic properties of pure astroglial cells from corpus callosum. *Brain Res*, 243(2):329–43, 1982.

[95] G. Liu. Local structural balance and functional interaction of excitatory and inhibitory synapses in hippocampal dendrites. *Nat Neurosci*, 7(4):373–9, 2004.

[96] K. Louie and M. A. Wilson. Temporally structured replay of awake hippocampal ensemble activity during rapid eye movement sleep. *Neuron*, 29(1):145–156, 2001.

[97] V. M. Luna and D. L. Pettit. Asymmetric rostro-caudal inhibition in the primary olfactory cortex. *Nat Neurosci*, 13(5):533–5, 2010.

[98] G. Maccaferri and C. J. McBain. Passive propagation of ltd to stratum oriens-alveus inhibitory neurons modulates the temporoammonic input to the hippocampal ca1 region. *Neuron*, 15(1):137–145, 1995.

[99] R. C. Malenka and M. F. Bear. Ltp and ltd: an embarrassment of riches. *Neuron*, 44(1):5–21, 2004.

[100] E. Marder and V. Thirumalai. Cellular, synaptic and network effects of neuromodulation. *Neural Netw*, 15(4-6):479–93, 2002.

[101] H. Markram, J. Lbke, M. Frotscher, and B. Sakmann. Regulation of synaptic efcacy by coincidence of postsynaptic aps and epsps. *Science*, 275(5297):213–215, 1997.

[102] D. Marr. Simple memory: A theory for archicortex. *Phil Trans R Soc B*, 262(841):23–81, 1971.

[103] M. Masahiro, B. H. Ghwiler, and U. Gerber. Recruitment of an inhibitory hippocampal network after bursting in a single granule cell. *Proc Natl Acad Sci U S A*, 104(18):7640–7645, 2007.

[104] J. L. McClelland. Category learning. learning the general but not the specific. *Curr Biol*, 4(4):357–8, 1994.

[105] J. L. McClelland. The organization of memory. a parallel distributed processing perspective. *Rev Neurol (Paris)*, 150(8-9):570–9, 1994.

[106] J. L. McClelland, B. L. McNaughton, and R. C. O'Reilly. Why there are complementary learning systems in the hippocampus and neocortex: Insights from the successes and failures of connectionist models of learning and memory. *Psychol Rev*, 102(3):419, 1995.

[107] A. R. McIntosh. Towards a network theory of cognition. *Neural Netw*, 13(8-9):861–70, 2000.

[108] M. G. McKernan and P. Shinnick-Gallagher. Fear conditioning induces a lasting potentiation of synaptic currents in vitro. *Nature*, 390(6660):607–11, 1997.

[109] M. R. Mehta, C. A. Barnes, and B. L. McNaughton. Experience-dependent, asymmetric expansion of hippocampal place fields. *Proc Natl Acad Sci U S A*, 94(16):8918–8921, 1997.

[110] R. Metherate and N. M. Weinberger. Cholinergic modulation of responses to single tones produces tone-specific receptive field alterations in cat auditory cortex. *Synapse*, 6(2):133–45, 1990.

[111] S. Micheloyannis, M. Vourkas, V. Tsirka, E. Karakonstantaki, K. Kanatsouli, and C. J. Stam. The influence of ageing on complex brain networks: a graph theoretical analysis. *Hum Brain Mapp*, 30(1):200–8, 2009.

[112] G. A. Miller. The magical number seven plus or minus two: some limits on our capacity for processing information. *Psychol Rev*, 63(2):81–97, 1956.

[113] P. M. Milner. A cell assembly theory of hippocampal amnesia. *Neuropsychologia*, 27(1):23–30, 1989.

[114] G. Mongillo, O. Barak, and M. Tsodyks. Synaptic theory of working memory. *Science*, 319(5869):1543–1546, 2008.

[115] G. Moonen, Y. Cam, M. Sensenbrenner, and P. Mandel. Variability of the effects of serum-free medium, dibutyryl-cyclic amp or theophylline on the morphology of cultured new-born rat astroblasts. *Cell Tissue Res*, 163(3):365–72, 1975.

[116] N. G. Muller, M. Mollenhauer, A. Rosler, and A. Kleinschmidt. The attentional field has a mexican hat distribution. *Vision Res*, 45(9):1129–37, 2005.

[117] C. E. Myers and H. E. Scharfman. A role for hilar cells in pattern separation in the dentate gyrus: A computational approach. *Hippocampus*, 19(4):321–337, 2009.

[118] K. Nakazawa, M. C. Quirk, R. A. Chitwood, M. Watanabe, M. F. Yeckel, L. D. Sun, A. Kato, C. A. Carr, D. Johnston, M. A. Wilson, and S. Tonegawa. Requirement for hippocampal ca3 nmda receptors in associative memory recall. *Science*, 297(5579):211–8, 2002.

[119] W. J. Nett, S. H. Oloff, and K. D. McCarthy. Hippocampal astrocytes in situ exhibit calcium oscillations that occur independent of neuronal activity. *J Neurophysiol*, 87(1):528–37, 2002.

[120] E. A. Newman. New roles for astrocytes: regulation of synaptic transmission. *Trends Neurosci*, 26(10):536–42, 2003.

[121] M. E. J. Newman. *Networks: An Introduction*. Oxford University Press, Oxford, 2010.

[122] J. G. Nicholls, R. A. Martin, B. G. Wallace, and P. A. Fuchs. *From Neuron to Brain*. Sinauer Associates, Inc., Sunderland, 4 edition, 2001.

[123] T. Nishikawa, A. E. Motter, Y. C. Lai, and F. C. Hoppensteadt. Heterogeneity in oscillator networks: are smaller worlds easier to synchronize? *Phys Rev Lett*, 91(1):014101, 2003.

[124] D. A. Nitz and B. L. McNaughton. Differential modulation of ca1 and dentate gyrus interneurons during exploration of novel environments. *J Neurophysiol*, 91(2):863–872, 2004.

[125] R. J. O'Brien, S. Kamboj, M. D. Ehlers, K. R. Rosen, G. D. Fischbach, and R. L. Huganir. Activity-dependent modulation of synaptic ampa receptor accumulation. *Neuron*, 21(5):1067–78, 1998.

[126] R. C. O'Reilly and J. L. McClelland. Hippocampal conjunctive encoding, storage, and recall: avoiding a trade-off. *Hippocampus*, 4(6):661–682, 1994.

[127] E. Pastalkova, P. Serrano, D. Pinkhasova, E. Wallace, A. A. Fenton, and T. C. Sacktor. Storage of spatial information by the maintenance mechanism of ltp. *Science*, 313(5790):1141–4, 2006.

[128] L. Pasti, A. Volterra, T. Pozzan, and G. Carmignoto. Intracellular calcium oscillations in astrocytes: a highly plastic, bidirectional form of communication between neurons and astrocytes in situ. *J Neurosci*, 17(20):7817–30, 1997.

[129] C. Pavlides and J. Winson. Influences of hippocampal place cell firing in the awake state on the activity of these cells during subsequent sleep episodes. *J Neurosci*, 9(8):2907–2918, 1989.

[130] J. H. Peacock, D. F. Rush, and L. H. Mathers. Morphology of dissociated hippocampal cultures from fetal mice. *Brain Res*, 169(2):231–46, 1979.

[131] G. Perea, M. Navarrete, and A. Araque. Tripartite synapses: astrocytes process and control synaptic information. *Trends Neurosci*, 32(8):421–31, 2009.

[132] T. A. Pitler and B. E. Alger. Cholinergic excitation of gabaergic interneurons in the rat hippocampal slice. *J Physiol*, 450:127–142, 1992.

[133] G. R. Poe, B. L. McNaughton, C. A. Barnes, M. S. Suster, K. L. Weaver, and J. L. Gerrard. Place cell theta phase firing profile differences from maze running to rem sleep: Familiar vs. novel place fields. *Society for Neuroscience Abstract*, 22:1871, 1996.

[134] G. R. Poe, D. A. Nitz, B. L. McNaughton, and C. A. Barnes. Experience-dependent phase-reversal of hippocampal neuron firing during rem sleep. *Brain Res*, 855(1):176–180, 2000.

[135] Y. L. Qin, B. L. McNaughton, W. E. Skaggs, and C. A. Barnes. Memory reprocessing in corticocortical and hippocampocortical neuronal ensembles. *Phil Trans R Soc B*, 352(1360):1525–1533, 1997.

[136] M. N. Rajah and A. R. McIntosh. Overlap in the functional neural systems involved in semantic and episodic memory retrieval. *J Cogn Neurosci*, 17(3):470–82, 2005.

[137] M. Remondes and E. M. Schuman. Direct cortical input modulates plasticity and spiking in ca1 pyramidal neurons. *Nature*, 416(6882):736–740, 2002.

[138] M. Remondes and E. M. Schuman. Molecular mechanisms contributing to long-lasting synaptic plasticity at the temporoammonic-ca1 synapse. *Learn Mem*, 10(4):247–252, 2003.

[139] M. Remondes and E. M. Schuman. Role for a cortical input to hippocampal area ca1 in the consolidation of a long-term memory. *Nature*, 431(7009):699–703, 2004.

[140] A. Renart, P. Song, and X. J. Wang. Robust spatial working memory through homeostatic synaptic scaling in heterogeneous cortical networks. *Neuron*, 38(3):473–85, 2003.

[141] S. Ribeiro, V. Goyal, C. V. Mello, and C. Pavlides. Brain gene expression during rem sleep depends on prior waking experience. *Learn Mem*, 6(5):500–508, 1999.

[142] S. Ribeiro, C. V. Mello, T. Velho, T. J. Gardner, E. D. Jarvis, and C. Pavlides. Induction of hippocampal long-term potentiation during waking leads to increased extrahippocampal zif-268 expression during ensuing rapid-eye-movement sleep. *J Neurosci*, 22(24):10914–10923, 2002.

[143] H. Riecke, A. Roxin, S. Madruga, and S. A. Solla. Multiple attractors, long chaotic transients, and failure in small-world networks of excitable neurons. *Chaos*, 17(2):026110, 2007.

[144] E. T. Rolls. A theory of hippocampal function in memory. *Hippocampus*, 6:601–620, 1996.

[145] E. T. Rolls. An attractor network in the hippocampus: theory and neurophysiology. *Learn Mem*, 14(11):714–31, 2007.

[146] J. D. Rolston, D. A. Wagenaar, and S. M. Potter. Precisely timed spatiotemporal patterns of neural activity in dissociated cortical cultures. *Neuroscience*, 148(1):294–303, 2007.

[147] S. Romani, D. J. Amit, and G. Mongillo. Mean-field analysis of selective persistent activity in presence of short-term synaptic depression. *J Comput Neurosci*, 20(2):201–217, 2006.

[148] A. Roxin, H. Riecke, and S. A. Solla. Self-sustained activity in a small-world network of excitable neurons. *Phys Rev Lett*, 92(19):198101, 2004.

[149] R. Salvador, J. Suckling, M. R. Coleman, J. D. Pickard, D. Menon, and E. Bullmore. Neurophysiological architecture of functional magnetic resonance images of human brain. *Cereb Cortex*, 15(9):1332–42, 2005.

[150] W. B. Scoville and B. Milner. Loss of recent memory after bilateral hippocampal lesions. *J Neurol Neurosurg Psychiatry*, 20(1):11–21, 1957.

[151] O. Shefi, I. Golding, R. Segev, E. Ben-Jacob, and A. Ayali. Morphological characterization of in vitro neuronal networks. *Phys Rev E*, 66(2):021905, 2002.

[152] D. A. Sholl. Dendritic organization in the neurons of the visual and motor cortices of the cat. *J Anat*, 87(4):387–406, 1953.

[153] S. Song, K. D. Miller, and L. F. Abbott. Competitive hebbian learning through spike-timing-dependent synaptic plasticity. *Nat Neurosci*, 3(9):919–26, 2000.

[154] O. Sporns and J. D. Zwi. The small world of the cerebral cortex. *Neuroinformatics*, 2(2):145–162, 2004.

[155] L. R. Squire. Memory and the hippocampus: a synthesis from findings with rats, monkeys, and humans. *Psychol Rev*, 99(2):195–231, 1992.

[156] L. R. Squire. The anatomy of amnesia: Neurohistological analysis of three new cases. *Learn Mem*, 13:699–710, 2006.

[157] L. R. Squire. Rapid consolidation. *Science*, 316(5821):57–58, 2007.

[158] L. R. Squire and P. J. Bayley. The neuroscience of remote memory. *Curr Opin Neurobiol*, 17(2):185–196, 2007a.

[159] C. J. Stam and J. C. Reijneveld. Graph theoretical analysis of complex networks in the brain. *Nonlinear Biomed Phys*, 1(1):3, 2007.

[160] R. Stickgold. Sleep: off-line memory reprocessing. *Trends Cogn Sci*, 2(12):484–492, 1998.

[161] R. Stickgold. Sleep-dependent memory consolidation. *Nature*, 437(7063):1272–8, 2005.

[162] R. Stickgold and M. P. Walker. Sleep-dependent memory consolidation and reconsolidation. *Sleep Med*, 8(4):331–43, 2007.

[163] B. Tahvildari, A. A. Alonso, and C. W. Bourque. Ionic basis of on and off persistent activity in layer iii lateral entorhinal cortical principal neurons. *J Neurophysiol*, 99(4):2006–2011, 2008.

[164] B. Tahvildari, E. Fransn, A. A. Alonso, and M. E. Hasselmo. Switching between "on" and "off" states of persistent activity in lateral entorhinal layer iii neurons. *Hippocampus*, 17(4):257–263, 2007.

[165] Y. Takayama, H. Moriguchi, K. Kotani, and Y. Jimbo. Spontaneous calcium transients in cultured cortical networks during development. *IEEE Trans Biomed Eng*, 56(12):2949–56, 2009.

[166] C. Tallon-Baudry, O. Bertrand, F. Peronnet, and J. Pernier. Induced gamma-band activity during the delay of a visual short-term memory task in humans. *J Neurosci*, 18(11):4244–54, 1998.

[167] A. Treves and E. T. Rolls. Computational analysis of the role of the hippocampus in memory. *Hippocampus*, 4(3):374, 1994.

[168] D. Tse, R. F. Langston, M. Kakeyama, I. Bethus, P. A. Spooner, E. R. Wood, M. P. Witter, and R. G. Morris. Schemas and memory consolidation. *Science*, 316(5821):76–82, 2007.

[169] G. G. Turrigiano. Homeostatic plasticity in neuronal networks: the more things change, the more they stay the same. *Trends Neurosci*, 22(5):221–227, 1999.

[170] G. G. Turrigiano and S. B. Nelson. Homeostatic plasticity in the developing nervous system. *Nat Rev Neurosci*, 5:97–107, 2004.

[171] J. van Pelt, P. S. Wolters, M. A. Corner, W. L. Rutten, and G. J. Ramakers. Long-term characterization of firing dynamics of spontaneous bursts in cultured neural networks. *IEEE Trans Biomed Eng*, 51(11):2051–62, 2004.

[172] M. C. van Rossum, G. Q. Bi, and G. G. Turrigiano. Stable hebbian learning from spike timing-dependent plasticity. *J Neurosci*, 20(23):8812–21, 2000.

[173] F. Varela, J. P. Lachaux, E. Rodriguez, and J. Martinerie. The brainweb: phase synchronization and large-scale integration. *Nat Rev Neurosci*, 2(4):229–39, 2001.

[174] R. P. Vertes. Hippocampal theta rhythm: a tag for short-term memory. *Hippocampus*, 15(7):923–35, 2005.

[175] S. Vesce, P. Bezzi, and A. Volterra. Synaptic transmission with the glia. *News Physiol Sci*, 16:178–84, 2001.

[176] O. S. Vinogradova. Hippocampus as comparator: role of the two input and two output systems of the hippocampus in selection and registration of information. *Hippocampus*, 11(5):578–98, 2001.

[177] T. P. Vogels and L. F. Abbott. Gating multiple signals through detailed balance of excitation and inhibition in spiking networks. *Nat Neurosci*, 12(4):483–491, 2009.

[178] V. Volman, R. Gerkin, P.-M. Lau, E. Ben-Jacob, and G.-Q. Bi. Calcium and synaptic dynamics underlying reverberatory activity in neuronal networks. *Phys Biol*, 4(2):91–103, 2007.

[179] D. A. Wagenaar, J. Pine, and S. M. Potter. An extremely rich repertoire of bursting patterns during the development of cortical cultures. *BMC Neurosci*, 7(1):1–11, 2006.

[180] J. J. Wagner, L. R. Etemad, and A. M. Thompson. Opioid-mediated facilitation of long-term depression in rat hippocampus. *J Pharmacol Exp Ther*, 296(3):776–781, 2001.

[181] P. E. Wais, J. T. Wixted, R. O. Hopkins, and L. R. Squire. The hippocampus supports both the recollection and the familiarity components of recognition memory. *Neuron*, 49(3):459–466, 2006.

[182] M. P. Walker and R. Stickgold. Sleep-dependent learning and memory consolidation. *Neuron*, 44(1):121–33, 2004.

[183] J. X. Wang, G. R. Poe, and M. Zochowski. From network heterogeneities to familiarity detection and hippocampal memory management. *Phys Rev E*, 78(4):041905–041914, 2008.

[184] X. J. Wang. Synaptic basis of cortical persistent activity: the importance of nmda receptors to working memory. *J Neurosci*, 19(21):9587–603, 1999.

[185] X. J. Wang. Synaptic reverberation underlying mnemonic persistent activity. *Trends Neurosci*, 24(8):455–63, 2001.

[186] X.-J. Wang, J. Tegner, C. Constantinidis, and P. S. Goldman-Rakic. Division of labor among distinct subtypes of inhibitory neurons in a cortical microcircuit of working memory. *Proc Natl Acad Sci U S A*, 101(5):1368–1373, 2004.

[187] Y. Wang, H. Markram, P. H. Goodman, T. K. Berger, J. Ma, and P. S. Goldman-Rakic. Heterogeneity in the pyramidal network of the medial prefrontal cortex. *Nat Neurosci*, 9(4):534–542, 2006.

[188] D. J. Watts. *Small worlds : the dynamics of networks between order and randomness*. Princeton studies in complexity. Princeton University Press, Princeton, N.J., 1999.

[189] D. J. Watts and S. H. Strogatz. Collective dynamics of "small-world" networks. *Nature*, 393(6684):440–442, 1998.

[190] M. Wehr and A. M. Zador. Balanced inhibition underlies tuning and sharpens spike timing in auditory cortex. *Nature*, 426(6965):442–6, 2003.

[191] M. A. Wilson and B. L. McNaughton. Reactivation of hippocampal ensemble memories during sleep. *Science*, 265(5172):676–679, 1994.

[192] K.-F. Wong and X.-J. Wang. A recurrent network mechanism of time integration in perceptual decisions. *J Neurosci*, 26(4):1314–1328, 2006.

[193] A. J. Yu and P. Dayan. Uncertainty, neuromodulation, and attention. *Neuron*, 46(4):681–92, 2005.